Journal of Air Pollution and Health (Winter 2023); 8(1): 1-12

Original Article

Available online at http://japh.tums.ac.ir

Monitoring and mapping noise levels of university campus in central part of India

Vishal Kumar*, Ajay Vikram Ahirwar, A. D. Prasad

Civil Engineering Department, National Institute of Technology Raipur, Raipur, India

ARTICLE INFORMATION

Article Chronology:
Received 12 October 2022
Revised 09 November 2022
Accepted 20 February 2023
Published 29 March 2023

Keywords:
Noise mapping; Inverse distance weighted (IDW); Hot spot; Educational institute; India

CORRESPONDING AUTHOR:

rprvishal@gmail.com
Tel : (+91 771) 2255920
Fax : (+91 771) 2255920

ABSTRACT

Introduction: Each one of us is directly or indirectly exposed to noise pollution in our daily life. Noise has chronic effect on the human but many of us are not aware. In our modern research platform very few studies are available for monitoring and mitigating of noise pollution compared to other environmental pollution.

Materials and methods: This study has been designed to monitor, map the noise pollution in educational institute and find out the sources of noise followed by identification of hot spot. In this regards National Institute of Technology Raipur, Chhattisgarh, India was selected as study area. Noise levels measurements were carried out at 15 locations within the study area at time intervals of forenoon (9:30 – 10:30 AM), noon (12:30-1:30 PM) and afternoon (4:30-5:30 PM) for 5 days of the week (working days). Using GIS tool observed noise levels were interpolated by Inverse Distance Weighted (IDW) method and graphical plots were prepared for different time intervals.

Results: Noise Levels were found to be between 46 dBA to 72.08 dBA during our study. Sources contributing to higher levels of noise in the premises were traffic, honking of trains followed by students themselves. On comparing the finding with Central Pollution Control Board, New Delhi, India (CPCB) standards all the locations recorded higher noise levels than the prescribed limits.

Conclusion: Based on our finding, mitigating approaches like: plantation of trees, construction of noise barriers, proper parking area, restricting high speed of vehicles etc. were suggested for making a healthy learning environment.

Introduction

Unwanted sound generated in the environment causing discomfort to the ear is categorised as noise. From the Latin word “nausea” meaning sensation of discomfort or seasickness word “noise” has been derived. Noise comprises those occurring sound which are not acceptable in our environment. Noise is serious problem in many of the urban areas throughout the world however very less attention are paid regarding its monitoring and mitigating approaches [1-2]. Noise pollution is assessed by measuring the levels of noise in the environment from

Please cite this article as: Kumar V, Ahirwar AV, Prasad A. D. Monitoring and mapping noise levels of university campus in central part of India. Journal of Air Pollution and Health. 2023;8(1): 1-12.

Copyright © 2023 Tehran University of Medical Sciences. Published by Tehran University of Medical Sciences.
This work is licensed under a Creative Commons Attribution-NonCommercial 4.0 International license (https://creativecommons.org/licenses/by-nc/4.0/). Noncommercial uses of the work are permitted, provided the original work is properly cited.

the different sources in the surroundings. When human beings are exposed to higher levels of noise for long duration it leads to psychological and physical illness [3-4]. Based on the magnitude and length of occurrence noise pollution effects are differentiated into four categories - (i) physical effects (hearing problem) (ii) psychological effect (anxiety, late night sleep, sleeplessness and bad temper) (iii) physiological effects (rise in blood pressure and heart beat abnormality) (iv) effects on efficiency [5]. To the modern world noise pollution causes series of health issues and mitigating of noise pollution can help in controlling these health effects: sleep disturbance, cardiovascular disease, learning impairment, loss of hearing, speech interference and many more [6-8].World Health Organization (WHO) also reported 7 categories of impact of noise on humans in 2011. The health effect described above falls under these categories. The higher level noise exposures are generally made by different sources which are classified as natural and manmade. Natural consists of noise from insects, birds, barking of dogs, thunderstorm, wind whereas for manmade traffic, industry, construction work, loudspeaker on festival eve, railway, firecrackers are the major contributor to the noise in our environment [9-12].

Noise pollution mapping is one of the modern techniques of showing noise levels of different locations on a single map [6, 9]. Noise map represents noise levels of geographical area at particular time and are useful in acoustic urban planning [13]. It helps in identifying the hotspot for noise pollution in an area. Noise mapping helps in evaluating noise pollution as well as it helps in mitigating noise pollution in an area [14]. In order to make noise map the digital information of area are required along with Geographic Information System (GIS) [5].

Hospitals, schools, universities, library, colleges have been categorised under silence zone [15]. In most of the cities across the world these areas are surrounded by the road and rail. The location in heart of the city also makes this area prone to higher levels of noise thus making such areas exposed to higher level of noise. Students learning capability and academic performances are affected when they are exposed to the higher level of noise in school or colleges [16]. In silence zone people exposed to higher levels of noise faces common problem of interference in communication [17]. While the lecture is going on students find difficult in hearing the voice of teachers and discussion in classrooms and other activities. Students can perform better in silence condition rather than noisy environment [18]. Students learning outcomes are directly affected by the learning environment. The background noise in the class can affect the learning's of students and hamper the class environment [19].

Many studies have been carried out for monitoring and mapping of noise pollution at different zones of the city but there is lack of study in context with educational zone. In order to provide a healthy learning environment in campus such studies are necessary. Noise pollution in the NITRR campus can be seen as it is situated in the heart of city surrounded by highway and busy railway line. Thus there is need for monitoring and mapping of noise pollution in the campus. Noise pollution monitoring has not been carried out for the campus neither noise map is available therefore this study has been set to find out the noise levels at different location of the campus with following objectives:

- To prepare noise map by measuring noise levels within NITRR campus.
- To identify the hot spot and main causes for noise pollution within campus.

• To suggest mitigating approaches for control of higher noise level in Campus.

Materials and methods

Study area

For carrying out this study National Institute of Technology, Raipur campus was selected. NITRR began as a campus of Government Engineering College in September, 1956 and is spread over an area of 100 acres at 21.2497° N, 81.6050° E coordinates. Campus front side is located on Great Eastern Road whereas its back side is situated on Mumbai- Howrah main rail line. This rail line is one of the busy lines in central India. The permanent site of NITRR consists of academic blocks, staff quarter, girl's hostel, boy's hostel, relaxation park, dispensary and playing area. Inside the campus the main sources contributing to noise are; vehicular traffic, honking of trains, generators, noise from students waiting for lectures and from students who finished their lecture. Study area is shown in Fig. 1. Methodology has been shown in Fig. 2.

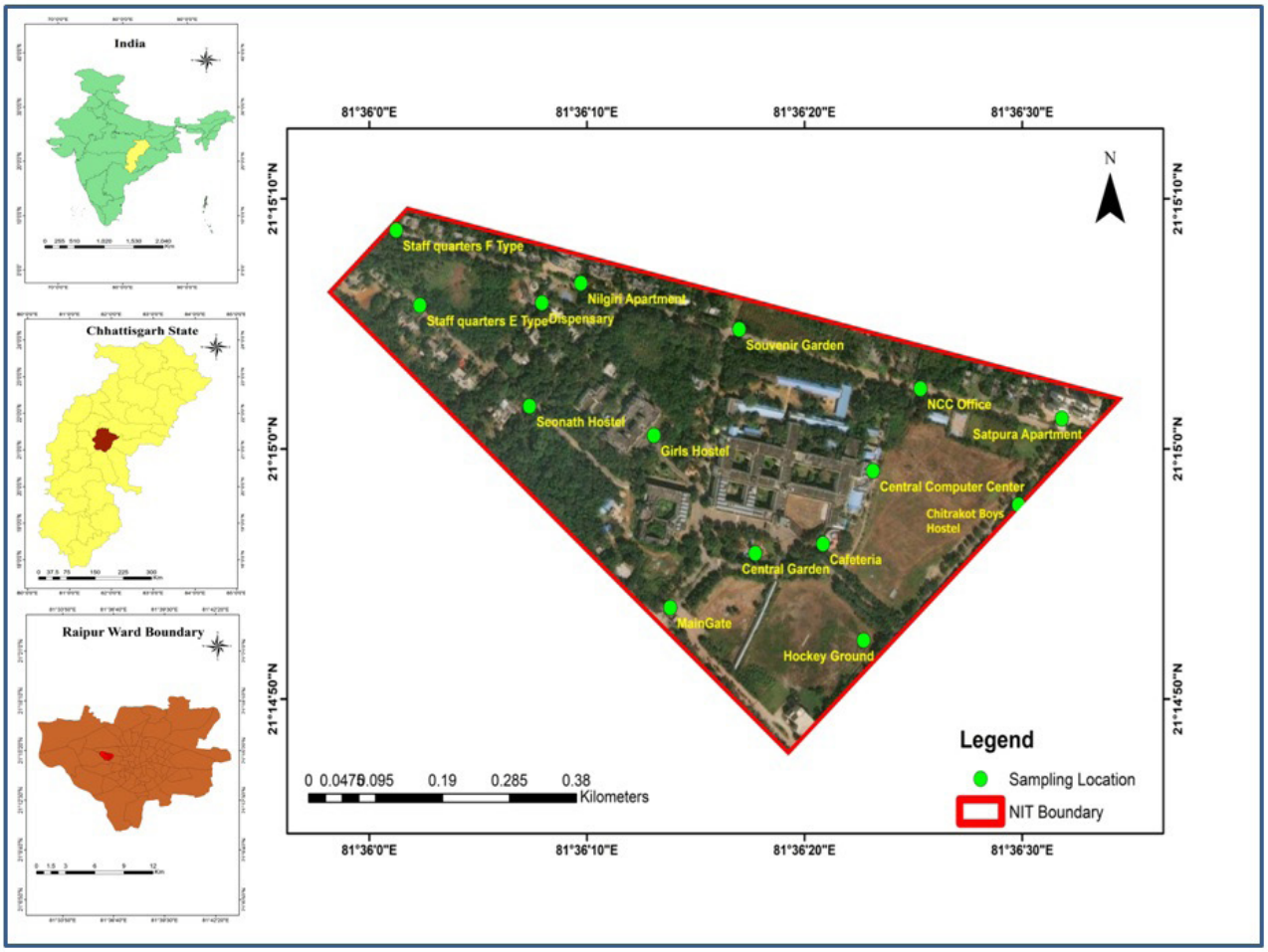

Fig. 1. Study area showing selected point for monitoring of noise within the campus

Sampling technique and data collection

Sampling stations were selected according to land uses in the campus for monitoring and mapping of noise pollution levels. The locations are shown in Table 1. Academic block (lecture hall, library, labs etc.), residential area (hostel and staff quarters), dispensary (health), recreational and commercial (gardens, playing area and cafeteria) were identified and selected for the study purpose respectively. Readings of noise levels were taken in forenoon 9:30 to 10:30 am, at noon from 12:30-1:30 pm and afternoon 4:30-5:30 pm (Monday to Friday) from 23rd May to 27th May 2022 in the academic year 2022-2023. Selection of this dates were made to cover all the working days in a week of the institute.

All the readings were taken by the help of field assistants across selected stations. Readings were taken by the using sound level meter (Extech-SL 400). Calibration of instruments was done before going to the sampling. Noise levels at 15 locations (Table 2) were taken using sound level meter. Microphone was placed 1.5 m above the ground surface and values displayed on the screen were recorded and mean values for each location were taken out. After collecting the data noise parameter LNP (Noise Pollution Level) was found out by using the equation given below (Eq. 1).

$LNP = L_{eq} \times 2.56\ \partial$ ..... (1)

Where LNP= Noise pollution level, L_{eq}= equivalent noise level, ∂ = standard deviation [20]

OR

$LNP = LA_{eq.} + (L10 - L90)$ .....(2)

OR

$LNP = LA_{eq.} + KS$ .....(3)

Where K= 2.56 and S= standard deviation of A weighted noise level [21]

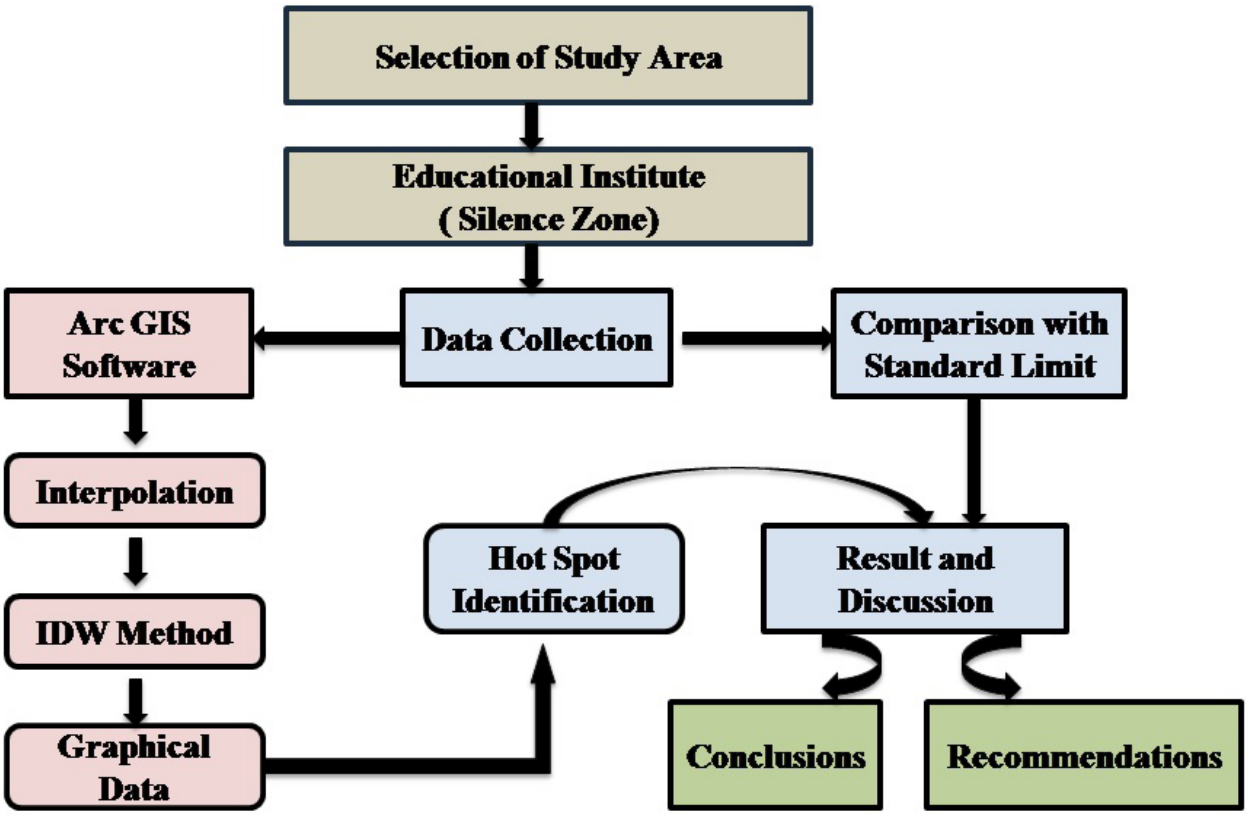

Fig. 2. Methodology of the study

Table 1. Selected points for noise monitoring

S. No.	Monitoring Station	Land Use	Station point
1	Dispensary	Health	S1
2	Staff quarters F Type		S2
3	Nilgiri Apartment		S3
4	Girls Hostel		S4
5	Seonath Hostel	Residential	S5
6	Staff quarters E Type		S6
7	Satpura Apartment		S7
8	Chitrakot Boys Hostel		S8
9	Central Computer Center	Academics	S9
10	Cafeteria		S10
11	Central Garden	Recreational and Playing	S11
12	Souvenir Garden		S12
13	Hockey Ground		S13
14	Main Gate	Commercial	S14
15	NCC Office		S15

Table 2. Central pollution control board, Delhi prescribed standards

Types of Area	Environmental Noise Standards (L_{eq}) in dBA	
	Day Time	Night Time
Industrial Area	75	70
Commercial Area	65	55
Residential Area	55	45
Silence Area	50	40

Source: C.P.C.B. New Delhi

Instrument, software, and techniques for data analysis

In order to carry out the mapping and monitoring of noise levels the instrument used along with software and techniques is combinations of the following;

- *Sound level meter:* In order to perform the noise pollution monitoring this instrument is used to find out the noise levels in the ambient environment. Calibration of SLM is done in dB(A) and dB(C). A weight is used while measuring the noise levels by SLM as it copies exactly the response of human ear to noise. The unit of measurement taken during the sampling are denoted as dB(A). After reading are taken stop button is pressed in order to save the readings in the inbuilt memory of instrument. Later on the readings are retrieved by connecting the instrument to the computer.

- *ArcGIS:* Utilization of this tool was done for data analysis and mapping. This software was used for performing the interpolation and generation of noise map. Study area map by plotting the coordinates reading of the study area was also prepared by using this software. For preparation of noise map IDW (Inverse Distance Weighted) technique was employed.

- *Microsoft excel:* To prepare the tables, computation of figures, chart plotting and converting data for exporting to ArcGIS workable conditions this software was used. Also retrieving of data from the SLM was done in this software.

- *GPS (Global Positioning System):* In order to get the coordinates reading of the study point this devise was used.

- *Microsoft Word:* For presenting the research work and formatting this software was used.

Results and discussion

Noise levels at 15 locations were observed and recorded in the selected study area. The results of the study are presented using numeric table and maps (graphical plots). The observations for the study period are presented in Table 3. For the forenoon, noon and afternoon during the study ranges of L_{eq} was found to be between 46 dBA to 72.08 dBA and for the L_{np} the ranges observed was between 50.13 dBA to 80.63 dBA respectively.Result in the table shows that for the silence zone S1, noise level is on elevated side compared to the CPCB standards (50dBA). Consequently in the residential zone S2 – S8 levels of noise is greater than 55dBA except for few locations in the noon when compared with the standards. The recorded noise levels for locations S9-S15 were also found to be on the higher side. Noise from railway is the major contributor of high levels of noise in the residential area of the campus. Thus from the obtained results of noise levels at all locations it is revealed that most of the locations are exposed to higher levels of noise within the campus.

Table 3. Leq(noise equivalent levels) and Lnp(noise pollution levels) for the study area

S. No.	Monitoring Station	Time	Average Leq(dBA)	Standard Deviation	Lnp
1	S1	Forenoon	53.41	0.87	55.63
		Noon	50.69	1.87	55.47
		Afternoon	51.78	1.28	55.06
2	S2	Forenoon	55.50	2.71	62.44
		Noon	50.53	0.70	52.32
		Afternoon	61.19	4.96	73.88
3	S3	Forenoon	57.21	1.87	61.99
		Noon	51.20	0.82	53.31
		Afternoon	57.78	1.67	62.05
4	S4	Forenoon	56.32	2.10	61.70
		Noon	50.27	2.14	55.75
		Afternoon	55.78	3.84	65.61
5	S5	Forenoon	53.69	1.38	57.23
		Noon	52.01	0.82	54.11
		Afternoon	53.76	0.98	56.27
6	S6	Forenoon	57.65	5.34	71.32
		Noon	62.15	7.22	80.63
		Afternoon	49.97	1.83	54.65
7	S7	Forenoon	51.55	0.94	53.96
		Noon	46.00	1.69	50.34
		Afternoon	48.71	0.55	50.13
8	S8	Forenoon	60.44	3.34	68.99
		Noon	59.54	4.14	70.15
		Afternoon	50.27	4.32	61.33
9	S9	Forenoon	53.66	1.37	57.17
		Noon	53.93	2.28	59.77
		Afternoon	56.11	3.43	64.89
10	S10	Forenoon	59.32	1.67	63.60
		Noon	60.33	0.89	62.61
		Afternoon	55.76	3.79	65.46
11	S11	Forenoon	63.87	1.55	67.84
		Noon	61.74	1.72	66.13
		Afternoon	61.69	2.21	67.35
12	S12	Forenoon	72.08	2.57	78.66
		Noon	55.43	5.06	68.39
		Afternoon	63.17	2.47	69.49
13	S13	Forenoon	56.70	1.19	59.75
		Noon	57.77	0.96	60.23
		Afternoon	54.87	1.96	59.90
14	S14	Forenoon	57.74	1.64	61.94
		Noon	50.73	0.90	53.04
		Afternoon	56.45	3.57	65.59
15	S15	Forenoon	54.45	2.90	61.87
		Noon	48.62	1.11	51.46
		Afternoon	56.23	1.34	59.65

Observed noise levels in the forenoon at the study area

Form the observations made at different locations noise maps was prepared for the forenoon noise levels as shown in Fig. 3. From the Table 3 ranges of noise levels in the forenoon is between 51.55 to 72.08 dBA.A highest noise level in the forenoon was 72.08 dBA at station S12. Also the L_{np} of 78.66 dBA at S12 was recorded as highest. As this station is situated nearer to the railway line and does not have any noise barrier. A lowest noise level of 51.55 dBA was recorded at station S7. The reason for low noise level is its location. Station S12 is situated at the end of the campus boundary in north east direction, very less vehicles moves in this area. From Fig. 3, it is found that stations S10, S11, S12, S13 and S14 recorded higher noise levels than other stations. The reason is because of its location from the main road of the city which is about 100 m. All vehicles enter to the campus from station S14 and thus lead to the generation of high noise levels. Work carried out by researchers reveals that in and around the educational institution noise levels should range between 40dBA to 50dBA [18]. On comparing our result we can say that at all the stations of our study area showed higher noise levels in the forenoon.

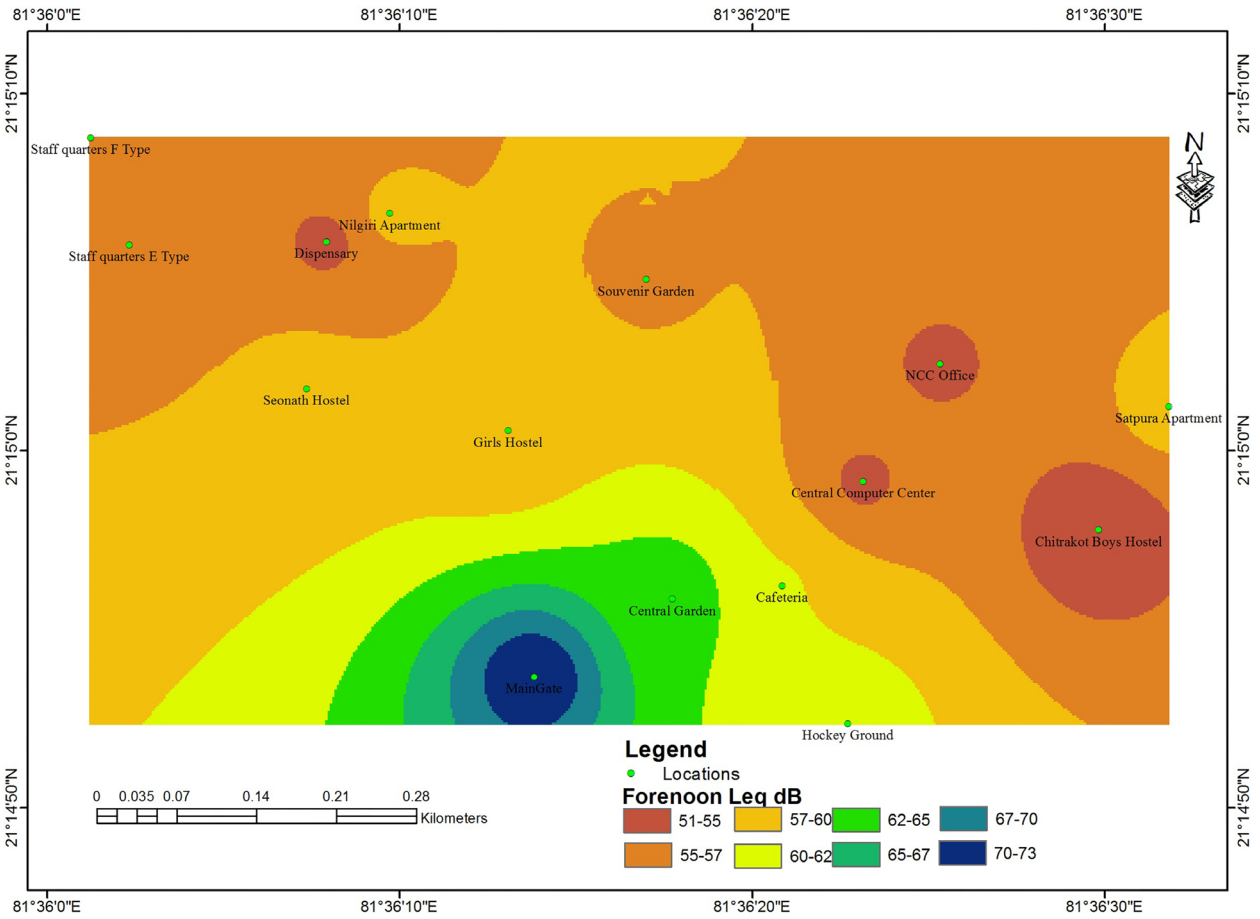

Fig. 3. Forenoon noise levels distribution in the study area

Observed noise levels in the noon at the study area

From the Table 3 ranges of Leq noise level for the noon is between 46 to 62.15 dBA while the L_{np} ranges between 50.34 to 80.63 dBA respectively. Highest level at station S10 and S11 were recorded i.e. above 60dBA. Most of the students take their lunch in cafeteria and garden in the noon time due to this reason the increase in levels of noise at both the locations were observed. Noise levels near to 50dBA were recorded for most of stations in the noon time which is lower than the forenoon noise levels. From Fig. 4 it is observed that stations S1 to S8 recorded lower noise levels compared to other stations. The reason for this is because the stations are surrounded by trees, thus the trees act as noise barrier for these locations as a result of which lower noise levels are observed. In a study, researchers concluded that major source for noise in the educational institute is vehicles (46%) and students (40%) [18].

Observed noise levels in the afternoon at the study area

From Table 3 the ranges of L_{eq} in the afternoon are found to be between 48.71 to 63.17 dBA. The maximum noise levels at station S12 is observed. The ranges of L_{np} are found to be between 50.13 to 73.88 dBA. At most of the stations noise levels are exceeding the CPCB standards shown in Table 2. From the Fig. 5, it is seen that noise levels in the afternoon are higher than the noon. The change in the levels is because of the movement of vehicles in the afternoon. After the ending of classes and working hour of the institute the vehicles start leaving the institute hence causing increase in noise levels in the premises.

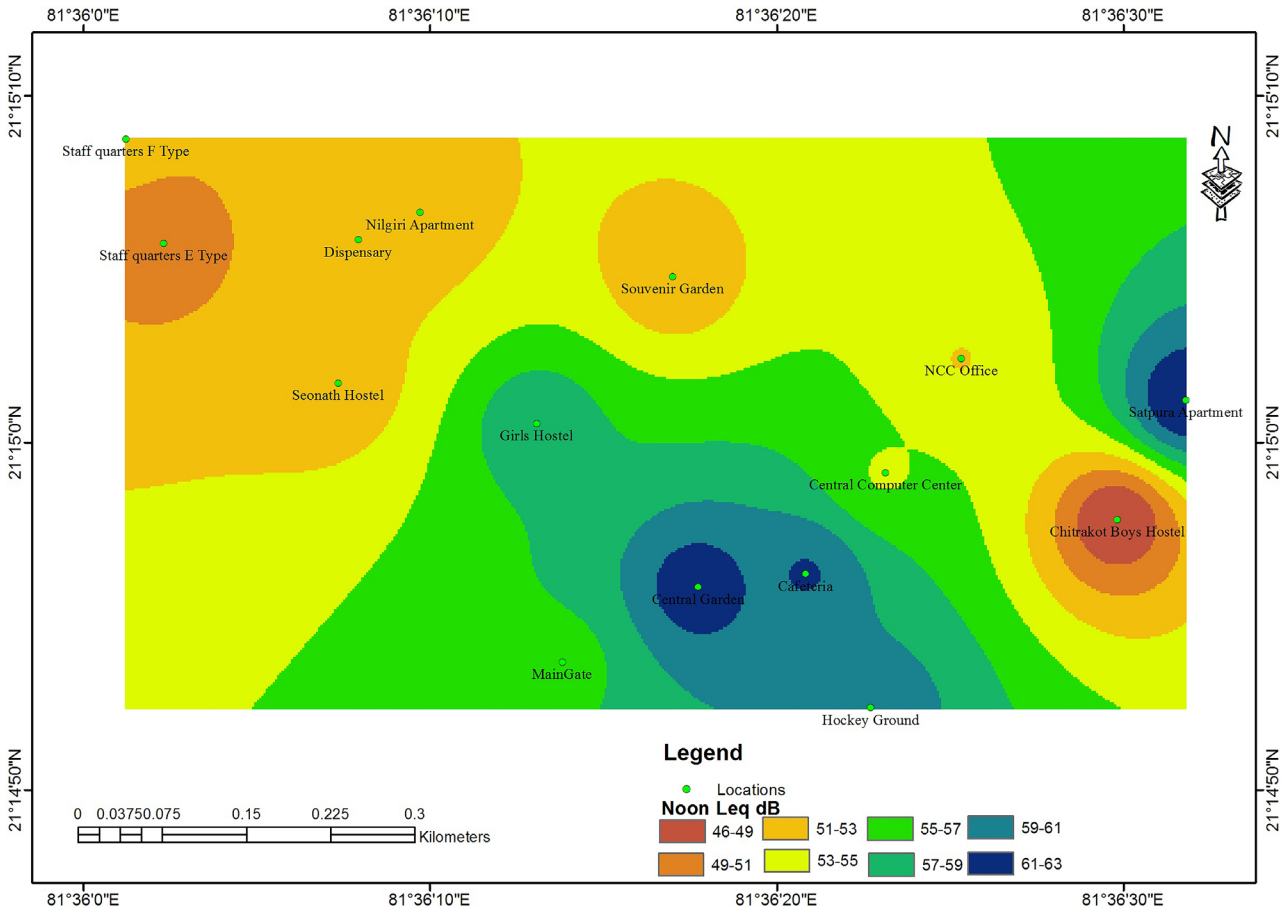

Fig. 4. Noon noise levels distribution in the study area

Hot spot identification, causes and sources of noise in the study area

Graphical plot prepared after the observations are compared and based on the three maps hot spot is identified. Among all the three maps common station S11 (central garden) and S14 (main gate) are showing high levels of noise in all the three intervals (forenoon, noon, afternoon) of observation. Hence from our finding it is concluded that both this station are hot spot for our study area. The main sources of noise in this are traffic and students itself. Our finding was corroborated by a study which was reported that, the educational institute lying beside the railway station and/or national highways have advantage but at the same time they contribute to higher noise levels in the premises of institute [15]. Our finding also aligns with a study in Nagaon, Assam India, where was concluded that main sources for higher noise levels in educational area was traffic as all the institutes were laying beside the busy road of the city [18]. Frequent honking of trains and noise from wheels of passing train also contribute to the high levels of noise in our study area.

Recommendations

Our finding shows that a higher noise level in the study area exists. Hence to reduce the noise to acceptable level following measures may be taken in the institute:

- Planting of more tress and vegetations near to the buildings and beside the service roads of the institute will help in absorbing the noise levels.
- Applying speed limit for the vehicles inside the campus and near to the main gate of institute will help in reducing high levels of noise.
- Making strict law on using of horns within the institute will mitigate noise pollution.
- Making public, teachers and students aware about harmfull effects of noise on health.
- Installing noise barriers near the railway and roadway will help in reducing noise pollution within the campus.
- Restricting outside vehicles movement within the premises and making parking area near to the entrance will help in reducing noise pollution.

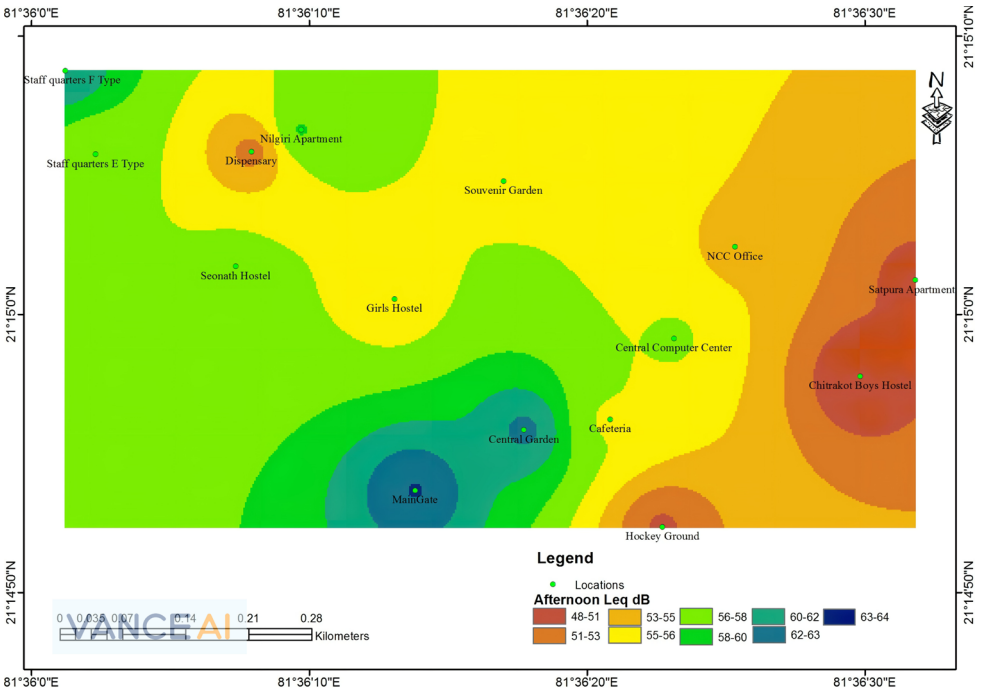

Fig. 5. Afternoon noise levels distribution in the study area

Conclusion

Based on the study it is concluded that noise generated by honking and movement of trains nearby, movement of vehicles inside the campus followed by students themselves are the major source of noise pollution. The range of noise levels for forenoon, noon and afternoon are found to be 51.55 to 72.08 dBA, 46 to 62.15 dBA and 48.71 to 63.17 dBA respectively. From the graphical plots it is concluded that noise levels in noon time is lower than forenoon and afternoon noise levels. Based on comparison of graphical plot stations S11 (central garden) and S14 (main gate) are identified as hot spot of the institute. On comparing the observed noise levels with the CPCB standards it is revealed that almost all stations have higher noise levels. The institute authorities must reassign the vehicle parking area so that the noise from honking and movement of vehicles does not interfere with the learning activities of the students. In order to make a healthy environment for students and staff suggested mitigating approaches must be incorporated. During the study it is found that, stations surrounded by trees recorded lower noise levels compared to other stations. Hence special events must be organized for plantation of trees and vegetation within the campus.

Financial supports

This research did not receive any financial support.

Competing interests

The authors declare that there is not any conflict of interests regarding the publication of this manuscript.

Acknowledgements

The authors would like to thank all those who contributed to this research.

Ethical considerations

"Ethical issues (Including plagiarism, Informed Consent, misconduct, data fabrication and/ or falsification, double publication and/ or submission, redundancy, etc) have been completely ob-served by the authors."

References

1. Prascevic MR, Mihajlov DI, Cvetkovic DS. Measurement and evaluation of the environmental noise levels in the urban areas of the city of Nis (Serbia). Environmental monitoring and assessment. 2014 Feb;186(2):1157-65.

2. Al-Taai SH. Noise and its impact on environmental pollution. Materials Today: Proceedings. 2021 May 19.

3. Leong ST, Laortanakul P. Monitoring and assessment of daily exposure of roadside workers to traffic noise levels in an Asian city: a case study of Bangkok streets. Environmental monitoring and assessment. 2003 Jun;85(1):69-85.

4. Andersson EM, Ögren M, Molnár P, Segersson D, Rosengren A, Stockfelt L. Road traffic noise, air pollution and cardiovascular events in a Swedish cohort. Environmental research. 2020 Jun 1;185:109446.

5. Das N. Mapping and assessing vulnerability in meso level urban environment of Eastern India, Sustain. Cities Soc.(46):101416.

6. Kumar R, Mukherjee A, Singh VP. Traffic noise mapping of Indian roads through smartphone user community participation. Environmental monitoring and assessment. 2017 Jan;189(1):1-4.

7. Tabraiz S, Ahmad S, Shehzadi I, Asif MB. Study of physio-psychological effects on traffic wardens due to traffic noise pollution; exposure-effect relation. Journal of environmental health science and engineering. 2015 Dec;13(1):1-8.

8. Stansfeld S, Clark C. Health effects of noise

exposure in children. Current environmental health reports. 2015 Jun;2(2):171-8. doi: 10.1007/s40572-015-0044-1.

9. Cai M, Zou J, Xie J, Ma X. Road traffic noise mapping in Guangzhou using GIS and GPS. Applied Acoustics. 2015 Jan 1;87:94-102.

10. Trombetta Zannin PH, Bunn F. Noise annoyance through railway traffic-a case study. Journal of Environmental Health Science and Engineering. 2014 Dec;12(1):1-2.

11. Yang W, He J, He C, Cai M. Evaluation of urban traffic noise pollution based on noise maps. Transportation Research Part D: Transport and Environment. 2020 Oct 1;87:102516.

12. Kalawapudi K, Singh T, Dey J, Vijay R, Kumar R. Noise pollution in Mumbai Metropolitan Region (MMR): An emerging environmental threat. Environmental monitoring and assessment. 2020 Feb;192(2):1-20.

13. Mishra RK, Nair K, Kumar K, Shukla A. Dynamic noise mapping of road traffic in an urban city. Arabian Journal of Geosciences. 2021 Jan;14(2):1-1.

14. Tsai KT, Lin MD, Chen YH. Noise mapping in urban environments: A Taiwan study. Applied Acoustics. 2009 Jul 1;70(7):964-72.

15. Thattai D, Sudarsan JS, Sathyanathan R, Ramasamy V. Analysis of noise pollution level in a University campus in South India. InIOP Conference Series: Earth and Environmental Science 2017 Jul 1 (Vol. 80, No. 1, p. 012053). IOP Publishing.

16. Ochiabuto OM, Abonyi IC, Ofili RN, Obiagwu OS, Ede AO, Okeke M, Eze PM. Assessment of Noise Levels in Primary and Secondary Schools in Nnewi, Anambra State. European Journal of Environment and Public Health. 2021;5(1).

17. Chowdhury RB, Dey R, Alam MS, Chakraborty P. Extent of traffic induced noise in the noise sensitive institutions of Chittagong city, Bangladesh. Noise & Vibration Worldwide. 2010 Jan;41(1):28-36.

18. Debnath D, Nath SK, Barthakur NK. Environmental noise pollution in educational institutes of Nagaon Town, Assam, India. Global Journal of Science Frontier Research Enviornment & Earth Sciences. 2012;12(1):1-5.

19. Gilavand A, Jamshidnezhad A. The effect of noise in educational institutions on learning and academic achievement of elementary students in Ahvaz, South-West of Iran. 2016: 1453-1463.

20. Joshi AN, Joshi NC, Rane PP. Noise mapping in Mumbai city, India. International Journal of Innovative Science, Engineering & Technology. 2015 Mar;2(3):2348-7968.

21. Owojori AA. Assessment of noise level and its effects on teaching and learning process in primary and secondary schools in Zaria metropolis, Nigeria (Doctoral dissertation, M. Sc. Dissertation, Ahmadu Bello University).

22. Central Pollution Control Board, (CPCB), New Delhi, India .https://cpcb.nic.in/noise-pollution/(Retrieved on 22-06-2022)

Journal of Air Pollution and Health (Winter 2023); 8(1): 13-22

Original Article

Available online at http://japh.tums.ac.ir

Carbon dioxide capture from combustion gases in residential building by microalgae cultivation

Ramazan Ali Dianati Tilaki[1,*], *Morteza Jafarsalehi*[2]

[1] Department of Environmental Health, Faculty of Health, Mazandaran University of Medical Sciences, Sari, Iran
[2] Department of Environmental Health, Faculty of Health, Kashan University of Medical Sciences, Kashan, Iran

ARTICLE INFORMATION

Article Chronology:
Received 19 April 2022
Revised 28 January 2023
Accepted 20 February 2023
Published 29 March 2023

Keywords:
Carbon dioxide (CO_2); Capture; Combustion gas; Microalgae

CORRESPONDING AUTHOR:

dianatitilaki@gmail.com
Tel: (+98 11) 33543081
Fax: (+98 11) 33542473

ABSTRACT

Introduction: Global warming and the need to reduce greenhouse gas emissions from various emission sectors are not hidden from anyone. The aim of this study was to determine Carbon dioxide (CO_2)capture from combustion gases of methane for cultivation of microalgae spirulina platensis.

Materials and methods: Microalgae culture medium was added in two photobioreactor. Air and combustion gas was injected into control and test reactors respectively. Artificial light with 10 Klux intensity was used and operated in continuous and intermittent (14 h ON and 8 h OFF) modes. Inlet concentration of carbon dioxide in to the test photobiorector was set in the range of 2000 to 6000 ppm and was measured in the inlet and outlet of photo-bioreactor by ND-IR CO_2 analyzer.

Results: In the control photo-bioreactor, the average removal of CO_2 from the air was 42%. In the test reactor with an inlet CO_2 concentration of 4100 ppm, the average removal of CO_2 from the combustion gas was 23%. After 9 days of cultivation, the amount of carbon dioxide stabilized by microalgae was 0.528 and 1.14 g/L (dry weight) in the control and experimental photo-bioreactors respectively. The CO_2 bio-fixation rate was in the range of 2.2% and 4.0% at different runs. After 9.0 days of cultivation concentration of microalgae was 0.25 and 1.0 g/L in the control and test reactors respectively. Algae productivity with intermittent light was 35% less than continuous light exposure.

Conclusion: It is possible to use CO_2 capture from combustion gases of commercial heater for cultivation of microalgae spirulina.

Introduction

The increase of Greenhouse Gases (GHGs) emissions has led to global warming and climate change. Concentration of Carbon dioxide (CO_2)in atmosphere has increased from the preindustrial level of 280 ppm to 418 ppm in 2022 [1] and even 421 ppm in some regional atmosphere [2] and increase

Please cite this article as: Dianati Tilaki RA, Jafarsalehi M. Carbon dioxide capture from combustion gases in residential building by microalgae cultivation. Journal of Air Pollution and Health. 2023;8(1): 13-22.

Copyright © 2023 Tehran University of Medical Sciences. Published by Tehran University of Medical Sciences.
This work is licensed under a Creative Commons Attribution-NonCommercial 4.0 International license (https://creativecommons.org/licenses/by-nc/4.0/). Noncommercial uses of the work are permitted, provided the original work is properly cited.

in the average temperature of 1°C above the preindustrial level, and if this trend continues, it is projected to rise 1.5 °C by 2050 [3]. Human activities including fossil fuels combustion in various sectors such as transportation, power generation, industries, residential, commercial, and agricultural, along with deforestation, land use change, and solid waste burning are the main reasons for increased CO_2 concentrations in the atmosphere [4, 5]. In addition to solutions such as using renewable energy resource, recycling materials, and changing lifestyles, methods for decrease CO_2 concentration in atmosphere are categorized into two main categories. The first category is CO_2 Capture and Storage (CCS) from flue gases of major point sources such as power plants, cement factory, and so on. The second category is CO_2 Removal (CDR) methods including Bio-Energy with Carbon Capture and Storage (BECCS), Direct Air Capture (DAC) by physicochemical or biological methods, bio char production, enhanced weathering, and ocean fertilization [6, 7]. Among the different methods, CO_2 capture by microalgae cultivation is a promising technology. Microalgae cultivation is generally carried out in outdoor ponds and also in controlled photo-bioreactors. In a photo-bioreactor, CO_2 is captured during photosynthesis, microalgae grow and biomass is produced [8]. One type of microalgae that has attracted much attention is Spirulina platensis. It is a genus of cyanobacteria (blue-green algae) that can grow in both fresh and salt water. Each 100 g of dried spirulina contains 23.9 g carbohydrate, 7.72 g fat, 57.47g of 18 types of proteins, 15 types of vitamins, and eight types of minerals. Spirulina is used in different countries in cosmetics, medication, aquaculture, and animal and poultry farms. This ingredient is widely used as a supplement for certain foods. The optimum growth condition is alkaline condition and temperatures above 25°C [9]. One of the major CO_2 emission sources is residential sector. Natural gas and kerosene are used for heating and hot water production of buildings in many countries and considerable direct emissions of CO_2 are from heating in buildings [10].

Totally, 40% of energy consumption is in building sector. Moreover, building sector contributes about 30 percent of total annual greenhouse gas emissions, which is expected to double in the next 20 years [11]. According to Iran's third national communication to UNFCCC, CO_2 emission by residential building subsector in 2000 and 2010 was 69 and 107 million tons respectively , and it is expected to be 152 million tons in 2020 [12]. National Iranian oil products distribution company reported that annual consumption of kerosene and natural gas in the residential-commercial sector was 3400 million L and 2 billion m^3 respectively in 2018 [13] . The CO_2 biofixation by microalgae cultivation is a promising, eco-friendly, and cost-effective technique to reduce CO_2 emission. Numerous studies have been conducted to cultivate different microalgae by using CO_2 [14]. Several studies have been conducted for microalgae cultivation by CO_2 capture from industrial flue gas [15-17]. Capture of CO_2 from power plant desulfured flue gas [18], CO_2 capture from flue gas of steel plant by cultivation of Chlorella sp [19], Cultivation of Chlorella , Synechocystis and Tetraselmis in photo-bioreactor by industrial combustion gases of methane [20], using flue gas of a coal-fired power plant for microalgae cultivation and biofuel production [21], utilization of biogas as CO_2 provider for Spirulina platensis cultivation [22], using flue gas of industrial heater to growth of Euglena grasilis [23]

and microalgae production from kerosene combustion [24] have been examined for microalgae cultivation using industrial flue gases.

In all of the above-mentioned studies, high concentrations of CO_2 have been examined. Industrial flue gas has high concentrations of CO_2 (4-14% v/v or more) along with toxic gases such as SO_2, NO_x, and heavy metals with high temperatures [25, 26]. High concentrations of CO_2 inhibit the growth of microalgae [27]. Sulfur dioxide (SO_2) in flue gas in excess of 100 ppm inhibits algae growth [28]. Moreover, the presence of Nitrogen Oxides (NO_x) gases in excess of 300 ppm has a negative effect on the growth of algae [29]. Due to the high volumes of industrial flue gases and presence of toxic gases, industrial flue gas needs pre-treatment in order to grow algae, which increases the cost [30].

In a review article, the use of microalgae photo bioreactors in the architecture and facades as well as types of PBR for integration with buildings and their technical requirements were described [31]. An article outlining the types of intelligent buildings, refers to a building in the Hamburg- Germany with a facade made of PBR used for microalgae cultivation [32].

According to literature review, there is no study on using residential combustion gases for microalgae cultivation, the aim of this study was to capture carbon dioxide from house chimney gases for cultivation of microalgae spirulina.

Materials and methods

Spirulina platensis seed culture was obtained from caspian institute of ecology and fisheries in Sari, Iran. In order to prepare stock microalgae, 50.0 mL of seed culture was inoculated into 5.0 L of Zarrouk culture medium in a glass vessel. Composition of modified (carbon free) Zarrouk medium was: $NaNO_3$ 2.5g/L, NaCl 1.0g/L, K_2SO_4 1.0 g/L, K_2HPO_4 0.5g/L , $MgSO_4.7H_2O$ 0.2g/L, $FeSO_4$ 0.01g/L, $CaCl_2.2H_2O$ 0.08g/L, EDTA 0.08g/L and pH=9.5 by adding NaOH 1.0N [25]. Aeration of growth medium was performed by an aquarium air pump. Four white fluorescent lamps (each 20W) were used for light illumination of culture medium. Modified Zarrouk medium containing above mentioned composition without $NaHCO_3$ (or carbon free) was used for microalgae cultivation in our experiments. 50 mL of stock microalgae was inoculated in photo-bioreactor containing 3.0 L of modified zarrouk medium. Microalgae spirulina was grown in the air aerated stock culture vessel containing modified Zarrouk medium. Spirulina cultivation was performed by air injection in two neutral and alkaline medium separately. Initial pH of the growth medium was adjusted to 9.5 by adding a few milliliter of NaOH 1.0N [26]. Concentration of algal biomass at the beginning of each test run was 20 mg/L. In order to determine algal biomass concentration, light absorbance of microalgae medium was measured at 689 nm by spectrophotometer (HACK, DR2800). Carbon percentage in spirulina biomass was measured by the CHNS analyzer (Perkin-Elmer,2400,USA).

The photo-bioreactor used in this study was fabricated by plexiglass with total volume of 5.6 L containing 3.0 L of growth medium. In order to supply combustion gases, commercial gas heater was used. Combustion gases of methane (the sole carbon source for microalgae cultivation) were injected into photo-bioreactor after passing through a condenser to remove water vapor (Fig. 1). Air was injected in control photo-bioreactor.

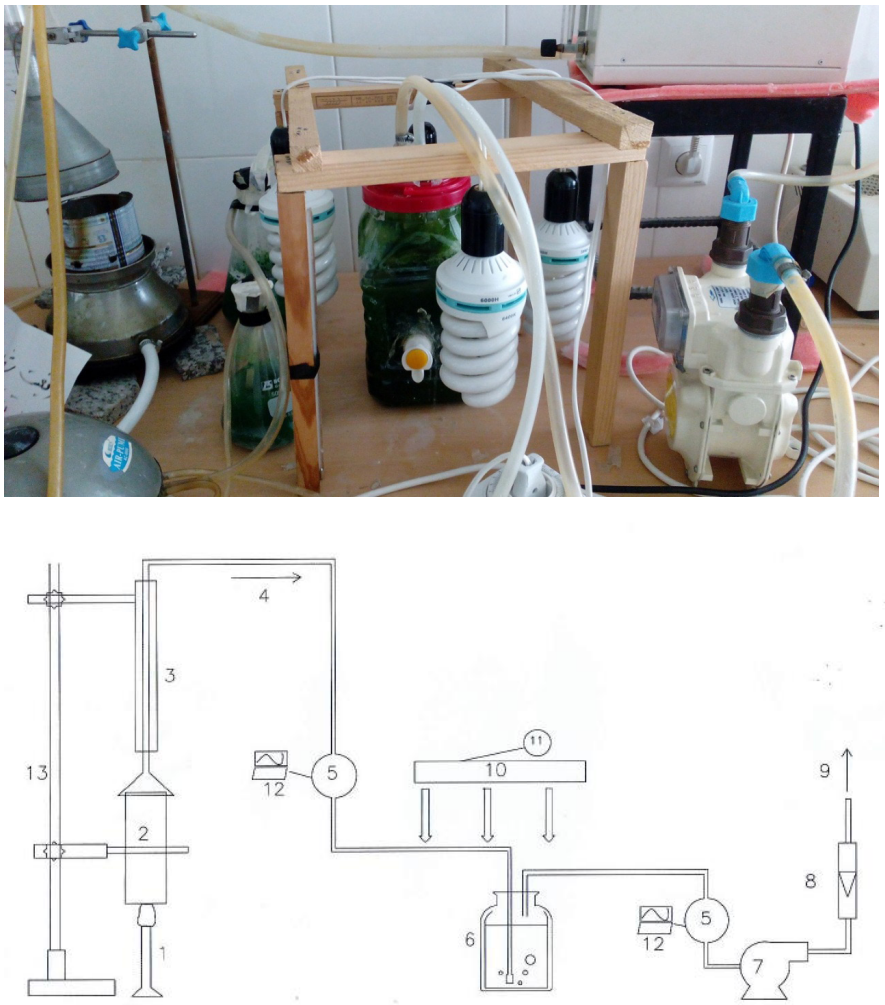

Fig. 1. Schematic and photo of experimental setup - 1:gas heater 2:funnel 3:condenser; 4:connection tube; 5: CO_2 analyzer; 6:photo-bioreactor; 7:air suction pump; 8:rotameter; 9:out let pipe; 10:fluorescent lamp; 11: timer; 12:computer; 13:holder stand

Light exposure with the intensity of 10 Klux was in intermittent (14 h on / 10 h off) and continuous mode [26]. Flow rate of combustion gas into the photo-bioreactor was set at 1.5 L/min. In order to prevent the heating of the culture medium, due to the small size of the photobioreactor, part of the flue gas was separated and injected into the medium. The initial concentration of carbon dioxide was in the range of 2000 to 6000 ppm and measured in the inlet and outlet of photo-bioreactor by ND-IR CO_2 analyzer. Daily sampling of culture medium was performed to measure optical density and mass of microalgae. Plot of algal biomass concentration (g/L) versus optical density was used as calibration curve. Duration of each test run was 9.0 days and each daily sample from pho-bioreactor was filtered by using GF/A filter and biomass of microalgae was measured by analytic balance (0.0001g) after 12 h drying at 80°C. The maximum microalgae productivity was calculated using Eq. 1.

$$P_{max} = X_t\text{-}X_0 / t_x\text{-}t_0 \quad (1)$$

Where P_{max}, is the maximum algae production (g/L.d) during cultivation period (t_x-t_0), X_t is

concentration (g/L of algae in the final day and X_0 is initial concentration (g/L) of microalgae. The stabilized CO_2 in the bioreactor is derived from Eq. 2.

$$F = (X_t - X_0)\ M \times V \times \left(\frac{44}{12}\right) \quad (2)$$

Where F is stabilized CO_2 (g), X_t is algae concentration (g/L) at t (d), X_0 is algae concentration at inoculation (t_0), M is a fraction of carbon in algae determined by CHNS analyzer (g/g of algae), V is volume of culture medium (L). The percentage of carbon stabilized in algae was calculated by dividing the amount of carbon in algae by the total carbon injected into the reactor (27).

Results and discussion

Effect of pH on the growth of microalgae in control photo-bioreactor which was operated by injecting air containing 600 ppm of carbon dioxide, is shown in Figure 2.When the pH of the culture medium was increased from 7 to 9, the concentration of algal biomass increased daily and reached to 0.48 g/L after 9 days. The initial pH of the culture medium was 9.5 and gradually reached to 8.5 at the end of experiment (9th days). Due to the formation of bicarbonate, the pH of culture medium was always higher than 8 and the alkaline conditions was suitable for microalgae growth. A study showed that there was a direct relationship between algae production and pH [28] .

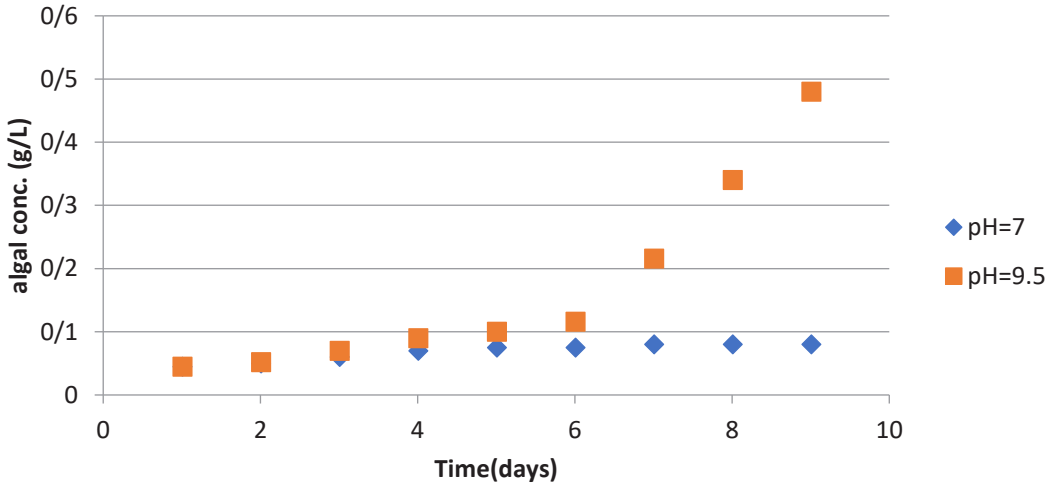

Fig. 2. Effect of pH on growth of microalgae

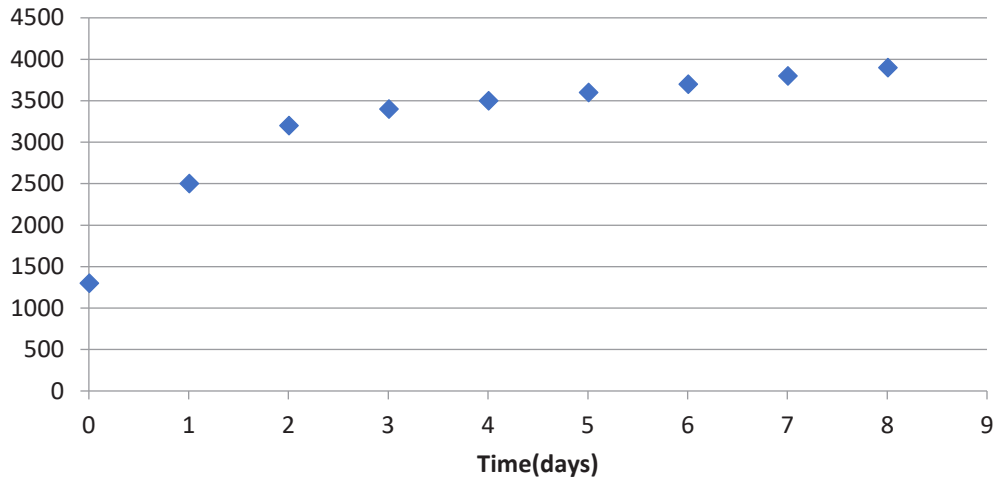

Fig. 3. Effect of contact time on concentration of CO_2 in the outlet of photo-bioreactor

Fig. 3 shows the change in CO_2 concentration in the outlet of photobioreactor with the inlet CO_2 concentration of 4000 ppm. As can be seen in the Fig. 3 , the maximum absorption of carbon dioxide occurred immediately after the injection of combustion gas in the culture medium and after 9.0 days of cultivation the outlet concentration was reached to 4000 ppm. In a study power plant flue gas was used for microalgae cultivation in a pilot plant photo-bioreactor that results showed 2,234 kg CO_2 per year was absorbed [18]. In another study flue gas of steel factory was used for CO_2 capture and microalgae cultivation in a 50.0 L photo-bioreactor and after six days, concentration of algal microalgae was increased from 0.75 to 2.87 g/L [19]. In a study algal bloom was occurred in the CO_2 concentration of 4,000 to 6,000 ppm at the fourth or fifth days using combustion gases of methane [29]. In another study, the effects of different concentration of CO_2 on growth rate of three types of microalgae was investigated, and when concentration of CO_2 was in the range of 50,000 to 60,000 ppm, growth rate of alga was low because high concentrations of CO_2 had an inhibitory effect on algal growth. In a study, by changing the concentration of CO_2 and measuring the growth rate of algae, the best CO_2 concentration for optimal growth of algae was in the range of 1,000 to 6,000 ppm [20]. In one study flue gas of coal burning power plant was used for microalgae Scenedesmus cultivation. Diluted combustion gas containing 10,000 to 40,000 ppm CO_2 was injected in Scenedesmus cultivation pond and results showed that highest growth rate of microalgae was in CO_2 concentration of 20,000 ppm [21].

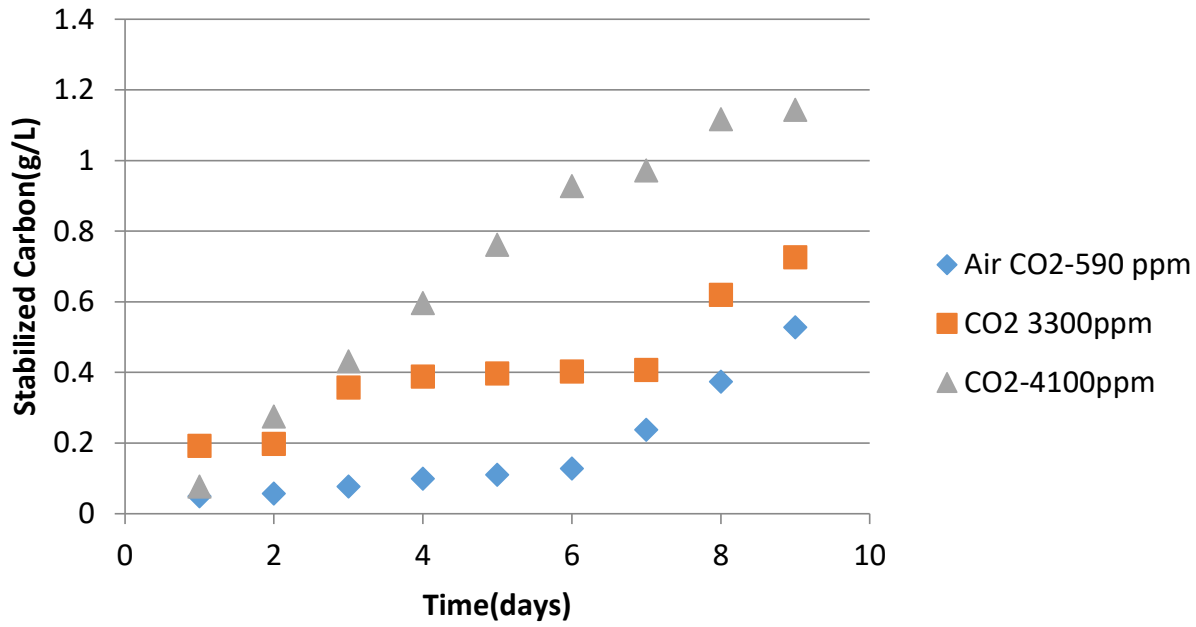

Fig. 4. Diurnal stabilized CO_2 in photo-bioreactor in different inlet concentration

Fig. 4 shows the diurnal stabilized CO_2 in control and test photo-bioreactor at different concentration of inlet CO_2. As it can be seen from Fig. 5 the stabilized CO_2 was increased by increasing the contact time and inlet CO_2 concentration. In one study biogas was supplied as CO_2 source in microalgae spirulina cultivation with the initial pH of 9.0 and the results showed that with injection of air, algal growth was continued but with injection of biogas, the microalgae concentration was decreased sharply [22]. Carbon dioxide capture from combustion gas of methane was studied by three species of microalgae by increasing concentration of CO_2 from 1,000 to 10,000 ppm, and results showed that the algal biomass was increased, however when the concentration of carbon dioxide reached above 10,000 ppm, the amount of algae production decreased [20] .In one study it was shown that increased CO_2 emissions from coal combustion up to 20,000 ppm had led to an increase in the production of Chlorella and Scenedesmus and the inhibitory effects on the growth of algae appeared at 40,000 ppm of CO_2 [21]. In another study the combustion gas was passed from an alkaline medium (lime solution) and then injected into photo-bioreactor [20]. In another similar study after 12 days of aeration, the maximum concentration of Spirulina algae reached to 1.02 g/L [30] . Simulated combustion gas containing NO_x, SO_2, and CO_2 with concentration of 60, 100 and 120,000 ppm respectively was used to produce Spirulina and the results showed that maximum algae concentration was 1.42 g/L, the algae production rate was 0.1 g/Ld, and the fixation of CO_2 was 0.14 g/Ld [25]. In another research cultivation of microalgae Euglena grasilis by using combustion gases of kerosene was studied [23]. Cultivation of Chlorella by using 20,000 ppm of CO_2 was studied and 2.6 g/L biomass was produced [30]. In the present study by using intermittent light and combustion gas of methane with CO_2 concentration of 2100 and 5500 ppm, the algal biomass was 0.66 and 1.04 g/L respectively, which is comparable reported by other researchers 1.2 g/L [21] and 1.02 g/L [30].

Carbon dioxide stabilized in two light exposure (continuous and intermittent) by using combustion gases of methane was shown in Fig. 5. As it can be seen, microalgae concentration in continuous light exposure was more than intermittent light and the difference between the two modes was statistically significant ($p<0.05$).

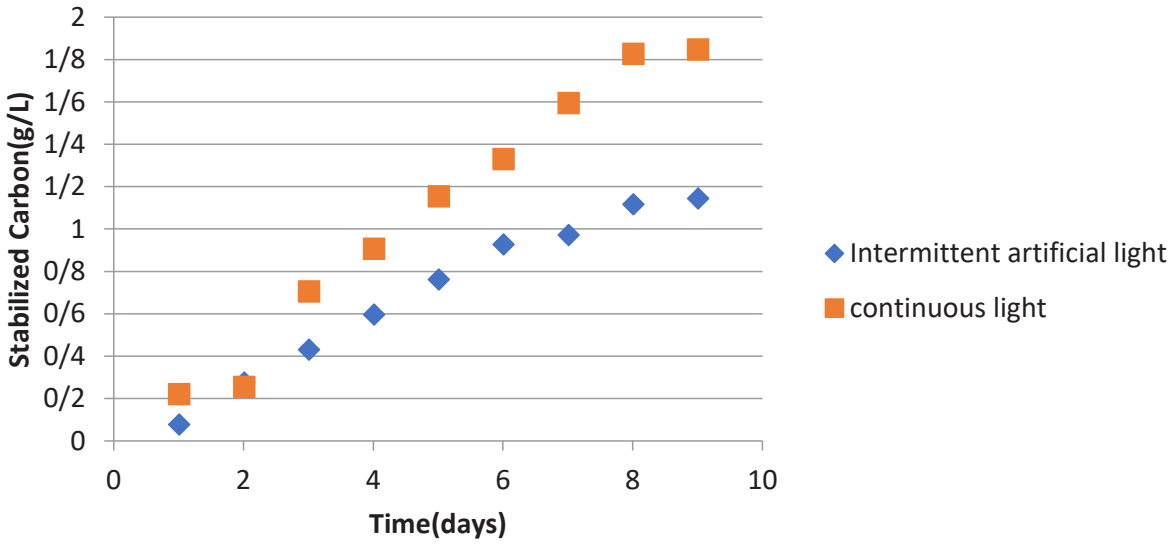

Fig. 5. Concentration of microalgae with time by using combustion gases of methane (CO_2 5500 ppm)

There is a study that shows the microalgae production in intermittent light is 25% less than continuous light [29]. In a study the growth of Clamydomonas was measured and results showed that the specific growth rate in intermittent light was 31% lower than continuous light due to consumption of biomass during respiration reaction at the dark hours [33]. Capture of CO_2 in a photo-bioreactor is carried out in two forms including absorption in culture medium and uptake by microalgae. Due to the lack of carbon source in the culture medium, photosynthesis in algae was performed only by uptake of CO_2 from combustion gas.

Conclusion

One of the important sources of greenhouse gas emission of carbon dioxide is the residential and commercial sector. Microalgae can be produced by using the combustion gases of heating devices in the buildings. In this study microalgae spirulina was produced by injection of combustion gas of methane as sole carbon source into photo-bioreactor containing the culture medium and carbon dioxide was removed from combustion gases.

Financial supports

This study was financially supported by research deputy of Mazandaran University of Medical Sciences.

Competing interests

The authors declare that there are no competing interests.

Acknowledgements

We would like to thank Dr. Reza Safari for providing microalgae spirulina platensis from Caspian institute of ecology and fisheries in Sari-Iran

Ethical considerations

"Ethical issues (Including plagiarism, Informed Consent, misconduct, data fabrication and/ or falsification, double publication and/ or submission, redundancy, etc.) have been completely observed by the authors."

References

1. Mousavi SM, Dinan NM, Ansarifard S, Sonnentag O. Analyzing spatio-temporal patterns in atmospheric carbon dioxide concentration across Iran from 2003 to 2020. Atmospheric Environment: X. 2022;14:100163.
2. Lindsey R. DE. Climate Change: Atmospheric Carbon Dioxide: EPA; 2022 [Available from: https://www.climate.gov.
3. Allen M, Antwi-Agyei P, Aragon-Durand F, Babiker M, Bertoldi P, Bind M, et al. Technical Summary: Global warming of 1.5 C. An IPCC Special Report on the impacts of global warming of 1.5 C above pre-industrial levels and related global greenhouse gas emission pathways, in the context of strengthening the global response to the threat of climate change, sustainable development, and efforts to eradicate poverty. 2019.
4. IPCC. IPCC. Fifth Assessment Report 2014 [Available from: https://www.ipcc.ch/pdf/assessment/report/ar5/syr/SYR_AR5_Final_Full__Cover.pdf.
5. Tilaki RA, Norouzi F. Carbon dioxide removal from exhaust gases of methane combustion by amine modified MCM-41. Journal of Air Pollution and Health. 2017;2(2):109-18.
6. Bhatia SK, Bhatia RK, Jeon J-M, Kumar G, Yang Y-H. Carbon dioxide capture and bioenergy production using biological system–A review. Renewable and sustainable energy reviews. 2019;110:143-58.
7. Breyer C, Fasihi M, Aghahosseini A. Carbon dioxide direct air capture for effective climate change mitigation based on renewable electricity:

a new type of energy system sector coupling. Mitigation and Adaptation Strategies for Global Change. 2020;25(1):43-65.
8. Schediwy K, Trautmann A, Steinweg C, Posten C. Microalgal kinetics—a guideline for photobioreactor design and process development. Engineering in Life Sciences. 2019;19(12):830-43.
9. Soni RA, Sudhakar K, Rana R. Spirulina–From growth to nutritional product: A review. Trends in food science & technology. 2017;69:157-71.
10. Yim SY, Ng ST, Hossain M, Wong JM. Comprehensive evaluation of carbon emissions for the development of high-rise residential building. Buildings. 2018;8(11):147.
11. Huovila P. Buildings and climate change: status, challenges, and opportunities. 2007.
12. Office Incc. Iran's Third National Communication to UNFCCC. In: environment do, editor. Tehran2017. p. 63.
13. Company NIOPD. Annual statisitics on petroleum products consumption. In: NIODC, editor. Tehran: Public Relations Publications; 2020. p. 336.
14. Zhou W, Wang J, Chen P, Ji C, Kang Q, Lu B, et al. Bio-mitigation of carbon dioxide using microalgal systems: Advances and perspectives. Renewable and Sustainable Energy Reviews. 2017;76:1163-75.
15. Huang G, Chen F, Kuang Y, He H, Qin A. Current techniques of growing algae using flue gas from exhaust gas industry: a review. Applied biochemistry and biotechnology. 2016;178(6):1220-38.
16. Kroumov AD, Módenes AN, Trigueros DEG, Espinoza-Quiñones FR, Borba CE, Scheufele FB, et al. A systems approach for CO_2 fixation from flue gas by microalgae—Theory review. Process Biochemistry. 2016;51(11):1817-32.
17. Thomas DM, Mechery J, Paulose SV. Carbon dioxide capture strategies from flue gas using microalgae: a review. Environmental Science and Pollution Research. 2016;23(17):16926-40.
18. Chen HW, Yang TS, Chen MJ, Chang YC, Lin CY, Eugene I, et al. Application of power plant flue gas in a photobioreactor to grow Spirulina algae, and a bioactivity analysis of the algal water-soluble polysaccharides. Bioresource Technology. 2012;120:256-63.
19. Chiu SY, Kao CY, Huang TT, Lin CJ, Ong SC, Chen CD, et al. Microalgal biomass production and on-site bioremediation of carbon dioxide, nitrogen oxide and sulfur dioxide from flue gas using Chlorella sp. cultures. Bioresource technology. 2011;102(19):9135-42.
20. He L, Subramanian VR, Tang YJ. Experimental analysis and model-based optimization of microalgae growth in photo-bioreactors using flue gas. biomass and bioenergy. 2012;41:131-8.
21. Guruvaiah M, Lee K. Utilization of flue gas from coal burning power plant for microalgae cultivation for biofuel production. Int J Innov Technol Explor Eng. 2014;3(8):1-10.
22. Sumardiono S, Syaichurrozi I, Budi Sasongko S. Utilization of biogas as carbon dioxide provider for Spirulina platensis culture. Current Research Journal of Biological Sciences. 2014;6(1):53-9.
23. Chae SR, Hwang EJ, Shin HS. Single cell protein production of Euglena gracilis and carbon dioxide fixation in an innovative photo-bioreactor. Bioresource technology. 2006;97(2):322-9.
24. Dianati Tilaki R, Jafarsalehi M, Movahedi A. Biofixation of Carbon Dioxide from Kerosene Combustion and Biomass Production by Spirulina. Journal of Mazandaran University of Medical Sciences. 2019;29(172):67-79.
25. Costa JA, de Morais MG, Santana FB, Camerini F, Henrard AA, da Rosa APC, et al. Biofixation of carbon dioxide from coal station flue gas using Spirulina sp. LEB 18 and Scenedesmus obliquus LEB 22. African Journal of Microbiology Research. 2015;9(44):2202-8.
26. Soletto D, Binaghi L, Ferrari L, Lodi A, Carvalho JCMd, Zilli M, et al. Effects of carbon dioxide feeding rate and light intensity on the fed-batch pulse-feeding cultivation of Spirulina

platensis in helical photobioreactor. Biochemical Engineering Journal. 2008;39(2):369-75.
27. Anjos M, Fernandes BD, Vicente AA, Teixeira JA, Dragone G. Optimization of CO_2 bio-mitigation by Chlorella vulgaris. Bioresource technology. 2013;139:149-54.
28. Nakamura T, Senior C, Olaizola M, Masutani S, editors. Capture and sequestration of stationary combustion systems by photosynthetic microalgae. Proceedings of the First National Conference on Carbon Sequestration Department of Energy-National Energy Technology Laboratory, USA; 2001.
29. Jacob-Lopes E, Scoparo CHG, Queiroz MI, Franco TT. Biotransformations of carbon dioxide in photobioreactors. Energy Conversion and Management. 2010;51(5):894-900.
30. Sankar V, Daniel DK, Krastanov A. Carbon dioxide fixation by Chlorella minutissima batch cultures in a stirred tank bioreactor. Biotechnology & Biotechnological Equipment. 2011;25(3):2468-76.
31. Elrayies GM. Microalgae: prospects for greener future buildings. Renewable and Sustainable Energy Reviews. 2018;81:1175-91.
32. Chan AK. Tackling global grand challenges in our cities. Engineering. 2017 Apr 6.
33. Takache H, Pruvost J, Marec H. Investigation of light/dark cycles effects on the photosynthetic growth of Chlamydomonas reinhardtii in conditions representative of photobioreactor cultivation. Algal Research. 2015 Mar 1;8:192-204.

Journal of Air Pollution and Health (Winter 2023); 8(1): 23-42

Original Article

Available online at http://japh.tums.ac.ir

Power aware air quality sensing system with efficient data storage capability

Koel Datta Purkayastha*, Chayan Nath, Sambhu Nath Pradhan

Department of Electronics and Communication Engineering, National Institute of Technology Agartala, India

ARTICLE INFORMATION

Article Chronology:
Received 08 June 2022
Revised 12 January 2023
Accepted 20 February 2023
Published 29 March 2023

Keywords:
Air pollution; Sensor; Wireless network; Low power; Data encoding

CORRESPONDING AUTHOR:

send2koel@gmail.com
Tel: (+91 381) 254 8532
Fax: (+91 381) 2546360

ABSTRACT

Introduction: This paper presents a portable device of Air Quality Monitoring System (AQMS) based on a sensor platform. The purpose of the study is to power awareness, warning indication, and minimal data storage capability.

Materials and methods: AQMS is developed by embedded design methodology. The software part is based on the C programming language. AQMS device is made up of “transmitter” and “receiver” sections through the Zigbee wireless network. The objective is to collect concentrations of CO, NO_2, CO_2, humidity, and temperature to check air pollution for health awareness. A power-saving strategy is adopted in the "transmitter" of AQMS through a Demultiplexer circuit. To minimize the space complexity of storage and availability of long-term data, data encoding techniques are implemented.

Results: By implementing switching activity on the sensors in AQMS, the active mode of sensing operations are controlled and a power saving of 18.41% is achieved. Extending the duration of transmission operation increases data storage in the “receiver” unit. Hence, two encoding techniques are developed where real-time data are encoded in binary form: 2-bit encoding and 3-bit encoding. According to the results, 2-bit encoding saves 50% of storage space and 3-bit encoding saves 25%, compared to not utilizing any encoding strategy, sacrificing data accuracy by less than 5%.

Conclusion: AQMS design is created with the implementations of low power consumption and low storage. Additionally, an alarming condition is set in AQMS for indicating the level of pollutants in the air to determine the risk level of exposure which is dangerous for human health.

Introduction

Environmental contamination has become a widespread problem in the global network as the world's industrialization and urbanization processes accelerate. Air pollution affects the quality of human life and the world’s climate [1]. Contaminated air can be categorized as indoor or outdoor pollution, covering the area where the

Please cite this article as: Datta Purkayastha K, Nath Ch, Pradhan SN. Power aware air quality sensing system with efficient data storage capability. Journal of Air Pollution and Health. 2023;8(1): 23-42.

Copyright © 2023 Tehran University of Medical Sciences. Published by Tehran University of Medical Sciences.
This work is licensed under a Creative Commons Attribution-NonCommercial 4.0 International license (https://creativecommons.org/licenses/by-nc/4.0/). Noncommercial uses of the work are permitted, provided the original work is properly cited.

operation takes place [2]. Ground-level ozone highlights five different polluted parameters comprising carbonic oxide, NO_2, SO_2 and PM [3]. Indoor air pollution, which is defined by the presence of pollutant compounds, has an impact on human health, causing symptoms such as trouble breathing, dizziness, migraines, and heart problems. Maintaining good indoor air quality is necessary for people like the disabled, patients, the elderly, and infants who spent the majority of their life time in confined spaces [4]. The measured level of CO_2, humidity, and temperature present in the environment provides useful information to solve the aforementioned problems [5]. The development of wireless sensor technology has been aided by on-chip controlling systems. People can build industrial and environmental monitoring systems using an architectural design method for sensor nodes. Therefore, the administration must concentrate on this part and take the necessary steps to create several systems and detect the concentration of polluted gases [6-9]. Methods of monitoring air pollutants and measuring the concentrations of CO_2, NO_2, CO and lead are reported in [10, 11]. Most monitoring and sensing stations are using basic techniques to monitor air quality in the environment. A wireless sensor module is developed, which is designed for assessing indoor air quality [12]. A MOS (Metal-Oxide-Semiconductor) based platform is developed for measuring and processing air quality and pollution concentration using a Wi-Fi network and web server [7]. Sensor nodes installed in different rooms consist of tin dioxide sensors which are wirelessly linked to the central unit. Also, in the design of energy-efficient sensor nodes, the application of low power technique is focused on [13, 14]. But the design cannot achieve low data storage for efficient transmission. The issue of storing large-scale data at the sensor network level is discussed [15-18]. Memory is used in the case of data storage whereas the transceiver works as the combined form of transmitter and receiver sections [19]. Another solution represents a measurement of temperature and CO_2 sensors in the company [20]. They do not involve in CO, NO_2, and humidity measurement abilities. The system allows only a Wi-Fi connection process for measuring samples. The monitoring system that is powered by a battery and has power consumption is reported in [21]. The system is presented with a Wireless Sensor Network (WSN) for ambient monitoring, but the solution of minimal data storage is not provided. The review of the literature study informs that the methods used in these works discussed so far are reliable but expensive.

In the proposed article, a cost-effective, portable wireless network 802.15.4 standard-based AQMS is developed with the capability to monitor CO, NO_2, CO_2, and meteorological parameters. The sensing modules used in this work are chosen with improved energy efficiency, area optimization, and low cost. The CO_2 sensor MH-Z14 is having self-calibration capability [22]. The collection and storage of CO_2 during transmission can be done in any place without any internet connection through the Zigbee wireless network compared to [23]. MiCS 4514 is defined as a compact MOS-based sensor where two sensing elements can be detected independently on a single package [24]. This dual sensing module can sense CO gas and NO_2 gas simultaneously and it is suitable for compact design as compared to individual CO and NO_2 sensors used in [11]. The advantage of using zigbee wireless technology in AQMS is that it can cover a large area compared to Bluetooth networks [25]. Also, zigbee wireless communication is best suited for getting data samples without requiring any internet activity as reported in [7, 26]. The proposed AQMS has various characteristics like easy handling, data compression capability, portability, low cost, and power reduction with technically tested accuracy. Collected real-time data from different sensors of the proposed AQMS over the last few years is large in quantity. Hence, there is a

requirement for huge space to store this data. So, it is reviewed that data processing is required before being transferred to storage. In this work, we have proposed data encoding techniques to encode large sets of data into smaller sets so that the storage space requirement is less. The characteristics of the developed AQMS in this work, such as a portable battery-operated system, warning indication, low power consumption and efficient data storage within a limited space make it a suitable node in WSN. For battery-operated AQMS, power consumption is a big issue. So, AQMS should be having low power consumption strategy so that the long use time of the battery can be increased. During energy consumption, a new technique is adapted for increasing the life of the sensor nodes [27]. But, the percentage of power reduction is not mentioned. In this work, a good percentage of saving of power is obtained in real-time and confirms the prolonged existence of sensor nodes.

The remaining sections of this paper are constructed as follows. Section 2 highlights the architectural design of AQMS which comprises transmitter and receiver circuit operation. Section 3 presents the implementation of different encoding techniques for data storage. Section 4 presents the receiver circuit where the alarming condition is activated for warning the level of various polluted gas concentrations. The results of minimal data storage using storage techniques and power consumption of AQMS have been provided in Section 5. This section discusses different storage techniques developed by the encoding method. Next, by using some power reduction techniques in the transmitter design, 18.41% of energy has been saved. Finally, the paper is concluded in Section 6.

Materials and methods

Hardware design of AQMS

The hardware operation of the transmitter and receiver sections of the proposed AQMS along with Secure Digital (SD) card, sensors, microcontroller and wireless communication with their features are discussed in this section.

Transmitter

AQMS has been designed for a 5 V supply. The transmitter circuit shown in Fig. 1 consists of a microcontroller unit as a decision circuit, sensors, a Demultiplexer, memory, and a power supply.

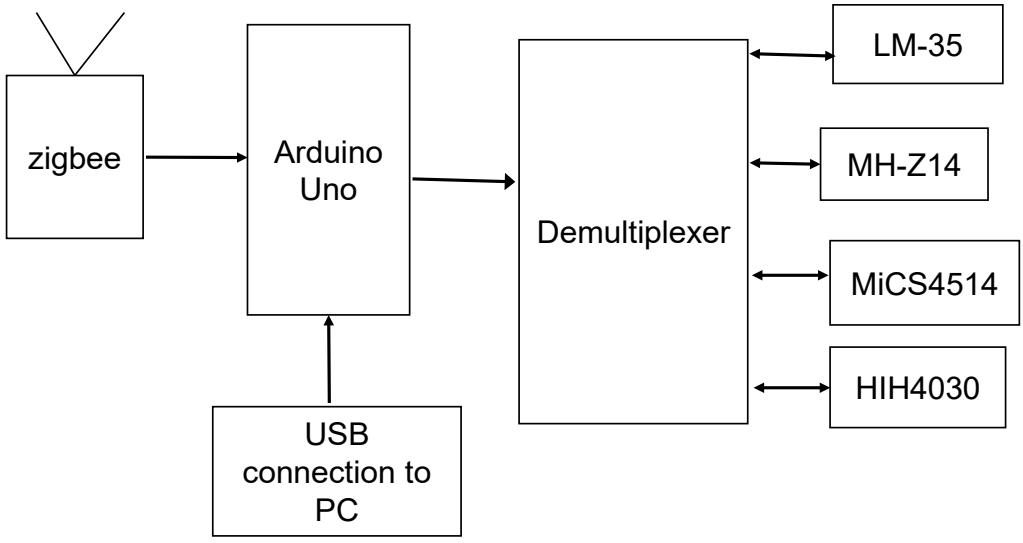

Fig. 1. Block diagram of a transmitter station

To get the correct data from the design, individual sensors are tested in proper working conditions. In the sensor station, Arduino Uno reads gaseous values using sensors along with temperature and humidity through the internal ADC of the processing circuit. The demultiplexer device is implemented for switching operation so that power consumption is controlled. Select lines of demultiplexer help to generate a signal for ON and OFF modes of the power supply for the sensors. Utmost care is given such that no necessary data is lost. The entire sensor data is transmitted serially using zigbee network during the ON time of the sensors.

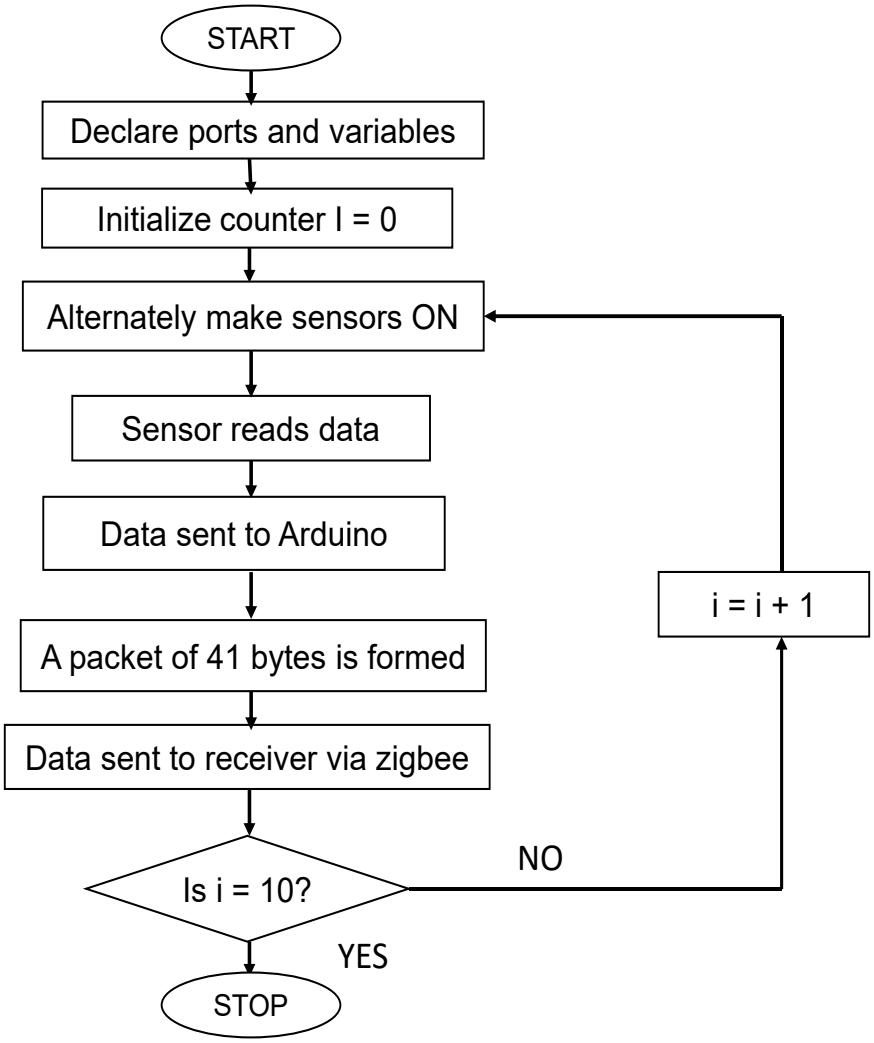

Fig. 2. Flowchart of a transmitter station

The function of the transmitter module is presented through the flowchart shown in Fig. 2. First, all the ports and variables are declared. Next, a sample variable i=0 is assigned to collect the number of readings that may be taken in ON time. Here, i=1 to i=10 is assigned to collect 10 readings. The sensors are powered up periodically with the help of a demultiplexer whose data lines go high as per the inputs given to its select lines. Select line inputs are controlled by the code itself. A small delay is provided between switching on the consecutive sensors. The sensors collect data and those data are converted into a 41 bytes long coded data string which contains the information related to the frame delimiter, length of the packet, sensor values, checksum byte etc. This data string is transmitted via a Zigbee module. The process continues in a loop.

Receiver

In the receiver station, an Arduino Uno microcontroller board, Liquid Crystal Display (LCD), Real-Time Clock (RTC), Secure Digital Card (SD card), Zigbee module, and Light Emitting Diodes (LED) are integrated into the design. During receiving operation, Zigbee receives data serially. Fig. 3 shows the flowchart of the receiver section. The function of the receiver station is discussed here.

On the receiver end, Arduino checks for the validity of the received data by calculating the checksum error byte. The checksum is calculated by following steps:

- First step: All bytes of the Zigbee packet are added except frame delimiter and length bytes. The results of the added bytes are found in hex form.
- Second step: MSB (Most Significant Bit) is extracted from the result obtained in the first step.
- Third step: The remaining value obtained in the second step is subtracted from FF (hexadecimal value).
- Fourth step: The result of subtraction is generated as Zigbee checksum for the data packet.

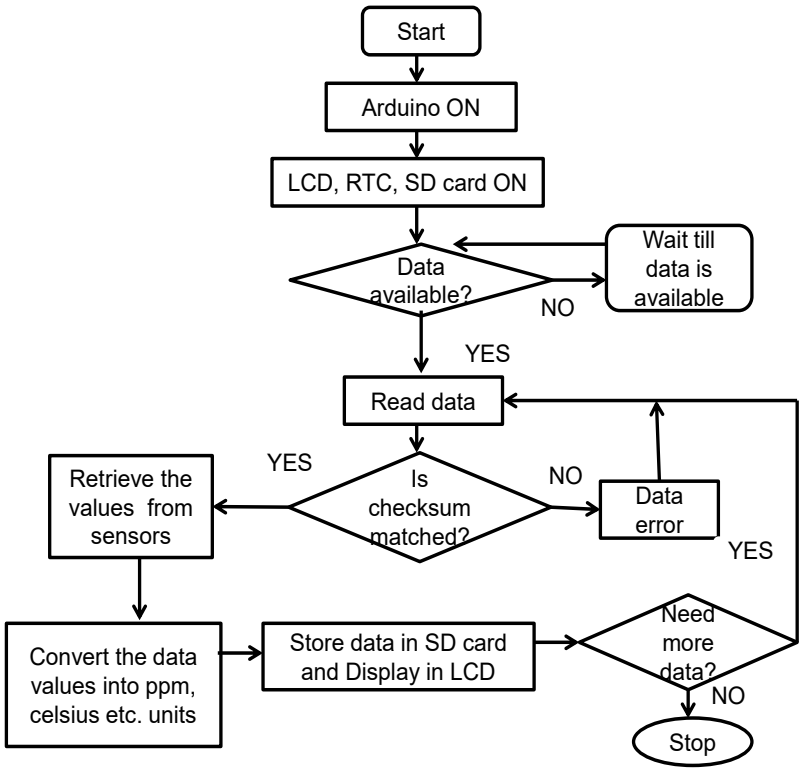

Fig. 3. Experimental flowchart of receiver station

The correct value of the checksum byte indicates successful communication between the transmitter and receiver. The calculated checksum should be matched with the checksum generated by Zigbee for error-free communication. If the API (Application Programming Interface) data packet has an incorrect checksum value, the receiver considers the packet invalid, and the data are ignored. If data is available then it disintegrates the data packets into individual data bytes. The last data byte is the checksum generated in the transmitter Zigbee module. From the received packet, the checksum is again calculated. If the received checksum byte is matched with the calculated checksum byte, it means the data packet is valid. Then each sensor readings is further processed and displayed in the LCD connected to Arduino. If not, the data packet is discarded and waits until the next data packet has been received. As all the data bytes are in hex form, so initially they are converted into their original string format. By identifying the prefixes, each sensor's ADC values are identified. These values are then converted into readings of ppm (parts per million), degree Celsius, etc. After conversion, data are stored in an SD card that is connected to the Arduino board along with the date and time of recording through RTC on the receiver section. Four different colors of LEDs are connected to four sensors to observe air pollution which is discussed in Section 4.

SD card

The SD card is a rewritable, high-capacity storage device. The advantage of using an SD card is that it supports SPI (serial peripheral interface) communication. In the developed AQMS, a 2 GB SD card has been used. Fig. 4 shows a flowchart of received data stored in an SD card.

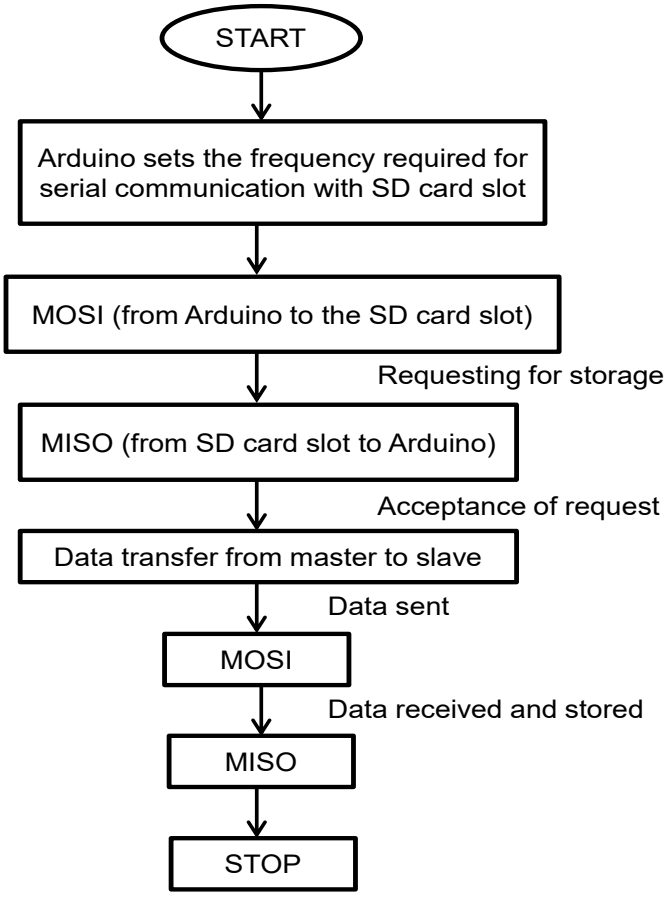

Fig. 4. Flowchart of the storing process for data in SD card

During the storing operation of received data in the SD card, a MOSI (Master Output Slave Input) signal flows from Arduino (master) to the SD card (slave). The MOSI signal sends a request for storing data. If space is available then a signal MISO (master input slave output) flows from the SD card to Arduino and sends a response, confirming the transfer and storage of data as requested by the MOSI signal. Then the data get transferred from Arduino. After that Arduino sends another MOSI signal, indicating the completion of transferring data. In reply, the SD card sends a MISO signal, informing that data is received and stored.

Sensors of AQMS

In the proposed AQMS, CO_2, CO, NO_2, relative humidity, and temperature sensors are used for measuring pollutant levels in the air. The details of all these sensors are discussed below.

CO_2 sensor

An MH-Z14 NDIR sensor has been selected for measuring the concentration level of carbon dioxide in the air. The sensor can be non-oxygen dependent and has good selectivity. This sensor can measure the concentration of CO_2 between 0 to 10000 ppm, where the operating voltage level ranges between 0 and 5 V signal. The average current is less than 60 mA at 5 V input. It is important to know that the level of CO_2 is affected by the change of absolute temperature and relative humidity parameters in the outdoor environment as well as in the indoor environment. The microcontroller through its internal ADC records data with a 16 MHz clock frequency on the UNO board. The response time of the CO_2 sensor is observed to be 120 s.

Temperature and humidity sensors

LM35 is a low cost precise integrated temperature measurement device where the output voltage is linearly proportional to the centigrade scale. It is an analog sensor and auto-calibrated in degree Celsius. The accuracy of the LM35 temperature sensor is within acceptable limits and the variation is between ±2 to ±5 ºC. The power consumption of the sensor module is observed to be 1.8 mW. This sensor is suitable to measure the temperature in the range of 0ºC to 60ºC.

The humidity sensor HIH-4030 is chosen for its low power consumption and fast response time. The relative humidity range of the HIH-4030 sensor lies between 0% to 90%, which matches with an ambient humidity range of India (50-80%).

CO and NO_2 sensor

MiCS-4514 dual sensor is chosen for measuring CO and NO_2 gases in the atmosphere. It can sense both gases simultaneously. The power consumption of this dual sensor module is observed to be 150 mW and the response time is less. The CO and NO_2 gases are observed in the millivolt using the MiCS-4514 sensor module. Another resistive sensor MQ-7 is selected for measuring CO gas in ppm level. The power consumption of this sensor is observed to be 400 mW.

Microcontroller

The data transmission and receiving functions are developed on Arduino Uno (https://www.arduino.cc) microcontroller board. ATmega328P microcontroller chip is inserted into the board. It is a 32-bit open-source platform supporting the addition of sensors in the physical environment. The microcontroller units are used for designing signal processing unit modules, control units, and external memory & memory interfacing units attached to the processor in the AQM system. In this

work, the microcontroller unit is designed for decision- making, processing, and data storage activities. The microcontroller unit is programmed in C language. Moreover, this microcontroller platform is easily accessible in both hardware and software. The current consumption at 1 MHz is observed to be 0.2 mA in active mode [28].

Wireless communication

A wireless sensor network is a sensor platform used for developing AQM systems with communication capabilities. Zigbee communication has been used in this research work. The IEEE 802.15.4 Zigbee network is the defined standard. This network is well suited for long battery life, high reliability, and low power consumption [29, 30]. The applications of Zigbee networks include home automation systems, appliance control, surveillance, etc. Zigbee wireless network has various well-known applications namely telemedicine services, smart farming, indoor device control, military, and some commercial applications [31]. Air quality monitoring in the real world is one area of application where researchers are concerned about global warming, all over the world. For Zigbee wireless communication, the XBee-Pro S2 communication module is chosen in this work. The XBee Pro RF communication modules are useful for data transmission in the case of both outdoor and indoor sides [32]. To start with, a network has been created between the sensor node (transmitter) and coordinator (receiver station) using the X-CTU terminal. The PAN (private area network) ID of all the developed modules (transmitter and receiver) must be the same. This kind of RF module is capable to operate in four ways such as receive, transmit, sleep mode, and idle [29].
The transmitter is set to AT mode. In AT mode, zigbee sends information from sensors to the common receiver. The receiver is set to API mode. Since the AQMS is a multimode system, it is easier to handle information from multiple nodes in API mode. Once zigbee is configured, the system is ready to transmit and collect information from sensors. The details of the settings of sensors and measurement analysis are presented in Table 1. The messages received from zigbee wireless communication are of numerical codes. These describe the measurement results of four sensors.
Zigbee network is associated with a host device via a logic-level asynchronous serial port. By this serial port, Zigbee communicates with a universal asynchronous receiver/ transmitter (UART) to transfer and collect serial data. The recorded sensor data are not sent directly to Zigbee as it causes more time-consuming and becomes an inefficient data transmission operation. Therefore, data must be encoded before sending it. Each sensor data is identified by a particular letter. Five different parameters are measured namely CO_2, temperature, CO, NO_2 and relative humidity. Measured values are denoted by a coded format. In API mode data are received in the form of packets known as data packets of 1-byte each. These bytes carry information about sensor readings, sensor node address bytes, checksum bytes, length of the packet, etc. And these are sent via Zigbee. The data packet receives in hex form and is equivalent to ASCII values. The checksum byte is used to validate each packet. Packets generated from the transmitter node are sent to the receiver station through WSN. All sorts of information have been included in the string form. While configuring the receiver station, the address of the Zigbee to be used in the receiver is provided. This configuration is saved and uploaded to Zigbee which acts as a router. The data packets are sent at regular intervals until the manual transmission is stopped.

Table 1. Zigbee data packet

Function	Description	Example
61 30 31 37 34	The value measured by the MH-Z14 sensor for CO_2 in ASCII	61 30 31 37 34 'a' '0' '1' '7' '4' 'a' indicates CO_2 data. CO_2=174ppm
62 30 30 37 32	The value measured by the LM35 sensor for temperature	62 30 30 37 32 62-'b'indicates temperature. ADC value of 72 which is equivalent of 35.19ºC
63 30 32 31 38	The value measured by the MiCS-4514 sensor for CO	63 30 32 31 38 63- 'c' indicates CO data. Analog Voltage of 218 mV corresponding to CO concentration
64 30 35 31 39	The value measured by the MiCS-4514 sensor for NO_2	64 30 35 31 39 64-'d' indicates NO_2 data Analog Voltage of 519 mV corresponding to NO_2 concentration
65 30 33 31 34	The value measured by the HIH-4030 sensor for relative humidity	65 30 33 31 34 65-'e' indicates humidity data ADC value of 314 which corresponds to Relative Humidity of 23.60%

* ºC = degree Celsius, % = percentage, mV = millivolt, CO_2 = concentration of CO_2, ppm = parts per million.

Proposed encoding techniques adopted in AQMS

This section highlights the storing procedure of CO data in the receiver station. However, data from other sensors can also be taken and the effectiveness of the proposed encoding scheme may be established. MQ-7 sensor is used in this work for CO gas. The air quality standard of CO and CO_2 gas given by the central pollution control board (CPCB) is presented in Table 2. The air quality index (AQI) range of the concentration of CO-polluted gas is used in this work for encoding datasets.

Table 2. Ambient air quality index (AQI)

AQI range	CO range (ppm)	CO_2 range (ppm)
Good	0-0.87	0-350
Satisfactory	0.88-1.75	350-450
Moderate	1.76-8.73	450-600
poor	8.74-14.85	600-1000
Very Poor	14.86-29.7	1000-2500
Severe	29.8+	2500-5000

Table 3. Text value to 2-bit binary representation

AQI range	ppm range of CO	Binary values
Good	0-1.75	00
Moderate	1.76-8.73	01
Poor	8.74-29.7	10
Severe	Above 29.7	11

In this case, measured CO concentrations in the ppm range are compared with the CPCB range. To store plenty of CO values within minimum storage space two encoding techniques have been proposed. As the sensor data are stored in a local PC, the use of an encoding technique in efficient form is developed to save previous text data. The intention of using the encoding technique in this work is to save past text data in binary form. In these techniques, values of the CO sensor within the corresponding AQI range are encoded and stored in binary form. That is, the sensor data will thus be encoded in a small number of bits. Then the number of bits is calculated and compared with the data stored without having any encoding technique.

2-Bit encoding

In this process, text data of CO values received are encoded in 2-bit binary representation as follows: 00, 01, 10, and 11. Table 3 shows the encoded binary form of text data for the corresponding AQI range. To begin with 2-bit binary conversion, CO values received in the AQI range of 0-1.75 ppm are encoded with 00 binary numbers. In the next step, CO values received within 1.76-8.73 ppm are encoded with 01 binary conversions. This process continues up to 11 binary forms. For example, if any CO data is found between 1.76-8.73 ppm, it is clear that the value is detected in the "Moderate" range and is stored by encoding in 01 binary forms.

Table 4. Text value to 3-bit binary representation

AQI range	ppm range of CO	Binary values
Good	0-0.87	000
Satisfactory	0.88-1.75	001
Moderate	1.76-8.73	010
poor	8.74-14.85	011
Very Poor	14.86-29.7	100

3-Bit encoding

A similar technique is followed in 3-bit encoding. Here, real-time CO values are encoded in 3-bit binary values, i.e. 000, 001, 010, 011, 100, 101. Thus, six AQI ranges are taken from the CPCB report for 000 to 101 binary forms. Table 4 shows the encoding of text data of CO values in 3-bit binary representation.

Implementing alarming conditions in the receiver section of AQMS

The experimentation in this work is carried out to get an idea about the level of pollution in the environment. In the "receiver" of AQMS, LEDs are set as a warning indicator for gases and environmental conditions. For maintaining awareness conditions, threshold values of CO and CO_2 are considered after observing CPCB data given in Table 2. Regarding nature, temperature ranges in India from 2 to 40 ºC, and relative humidity are between 50-80%. The threshold values of CO and CO_2 are comparable to CPCB standard value in Table 2. If the level of CO exceeds the threshold level of 8.73 ppm which is in the CPCB report in the 'Moderate' range, a warning indicator is issued through the Light Emitting Diode (LED) which is indicated as a visual indicator. Similarly, if CO_2 gas exceeds an acceptable level that is set at 600 ppm then the alarming index becomes high. Whenever the pollution level is above the normal level then the glowing LED is indicated as an alarm. In the case of temperature and humidity, if current values are significantly different from previous values then results are indicated by LED and displayed on the PC. The overall test is carried out for 1-2 weeks continuously for 1 h. Fig. 5 shows the receiver circuit of AQMS. Four LEDs are used in this work. Green LED indicates CO concentration, red LED for CO_2, blue LED for temperature, and yellow LED is an indicator for humidity value.

Fig. 5. Receiver section consisting of LEDs indicator for sensors

Results and discussion

In the design of AQMS, building individual circuit blocks and integrating these blocks are the major activities, which are already explained in prior sections. The objective of AQMS is to present a device that informs about the levels of air pollutants, stores the pollutants data in relatively low space and consumes low power. The section starts with a discussion on the storage of CO data using the proposed encoding schemes. The proposed method of data retrieval from the encoded data is presented. The error analysis at the time of data retrieval is mentioned in this section. The way of applying the power reduction strategy in the AQMS and the power saving result after experimenting is presented in this section.

Data storage

The polluted gases are measured with the developed AQMS on the campus of the National Institute of Technology, Agartala, Tripura, India. To have access to all previous data at any time, past data is to be stored. As we have to make predictive analyses with the proper dataset, storing data in a convenient form is a challenging task. As the amount of data acquisition becomes huge, encoding dataset in an efficient form is important. This paper attempts to encode the data in such a way that a large number of data can be stored in the limited possible space. The proposed encoding techniques have been discussed in Section 3. Two data encoding techniques are applied to the dataset of sensor values where data are encoded and stored in the binary value. The encoding datasets are given as supplementary documents in another file. The number of bits calculated displays the CO gas information which is given in Table 5 when the AQMS device is ON. The percentage of storage space saved in encoding strategies compared to all text data stored without using any strategy is given as follows:

Table 5. Storage analysis using two encoding techniques

Sl. No.	2-Bit storage	3-Bit storage	All data storage
No. of bits in 1 h	836	1260	1680
Percentage (%)	50	25	

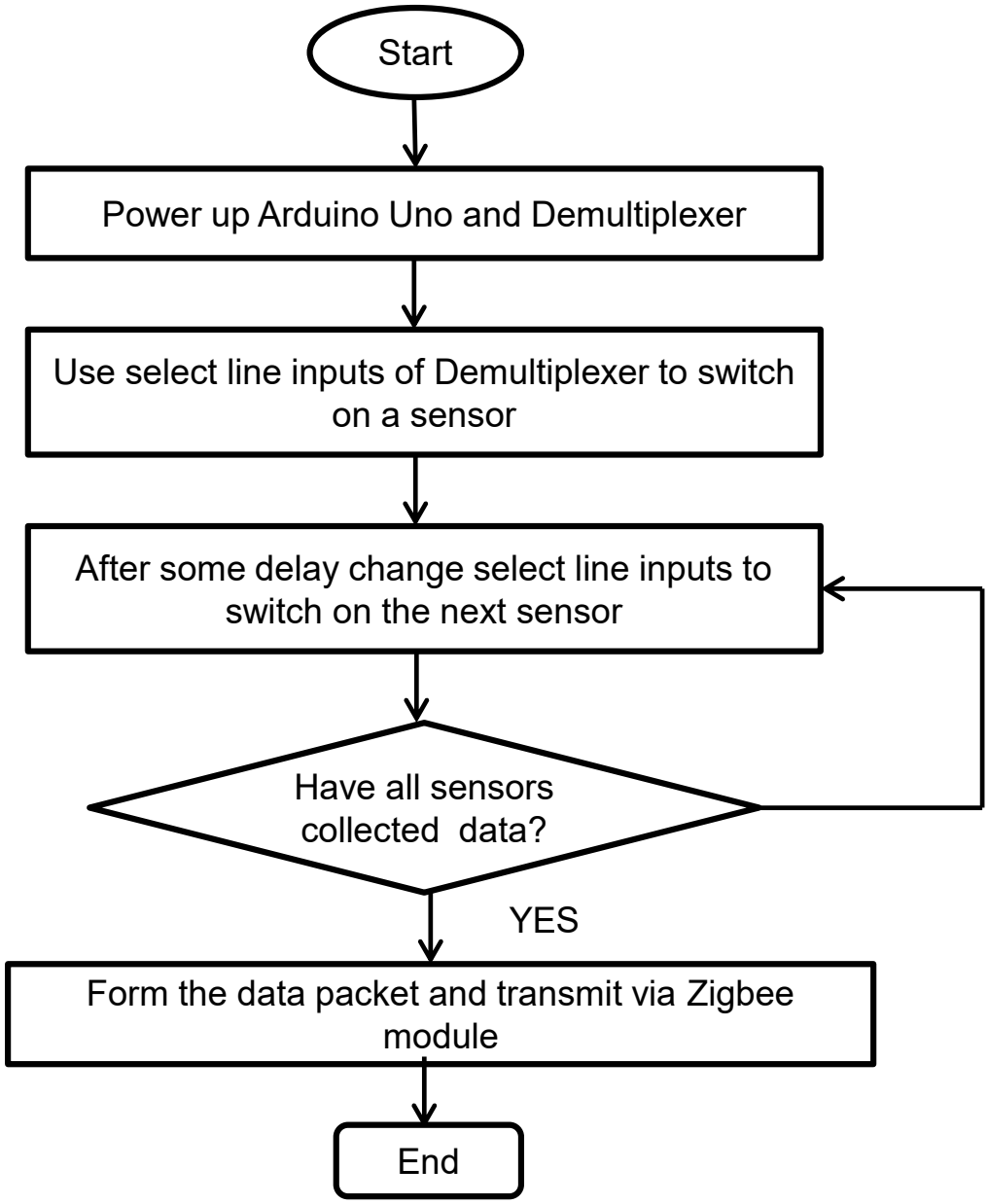

Fig. 6. Low power application flow diagram

The result of data encoding indicated the requirement for storage space in this work. AQMS can be installed in any place, any environmental situation to collect data. From Table 5, 2-bit encoding is seen as an effective technique for data storage capacity as it produces a result that requires the least storage space. Results clearly show that amount of storage space saved in the 2-bit encoding technique is 50% of the space required by 3-bit encoding. After storing data in binary value and text form it is observed that the error obtained during data retrieving is less than 5%. So, it can be said that almost exact data is going to be retrieved without sacrificing error.

Low power design of AQMS

Power saving is an important object in designing a prevalent monitoring system. Because reducing the total power consumed, implies more battery life for any portable device. For a particular sensor node, monitoring every instant of time is not required. However, focusing on minimizing power at the sensor node makes the system run for a longer time. The purpose of this work is to create a new strategy for how much energy can be saved by AQMS. For low-power operation, a new technology by choosing demultiplexer 74HC238 IC (integrated circuit) is implemented in the transmitter station. This IC is a combinational logic with an active high output, which has one data input line and eight data output lines. Select line inputs of the demultiplexer are used to control the outputs that are connected to four sensors. Through a demultiplexer device sensors are switched periodically. Select line inputs are altered to make sure that only one sensor will be turned ON at a time. It can be noticed that rather than keeping the sensors ON all the time we can periodically turn a sensor ON and OFF in the sensor station. The steps of low-power application are presented in the flowchart in Fig. 6.

The transmitter section of AQMS is made ON for 1 h. Different sets of readings are taken for power calculation. A multimeter is used to determine the current value of each sensor in the traditional method. For analysis of power consumption, the runtime of all sensors is calculated. The runtime operation for 1 h is given below:

- First, the runtime is measured in 60 s
- The individual runtime of sensors is multiplied by 60
- Finally, the total runtime of sensors is prepared for 1 h.

After testing each sensor individually, it is found that the power saving in the humidity sensor is the highest. The switching operation by using a demultiplexer starts from the CO_2 sensor and ends on the humidity sensor. First, the CO_2 sensor is made ON for 4 s. The temperature sensor and combined CO and NO_2 sensors were for 4 s each. At last, the humidity sensor remains ON for 8 s. The whole runtime process consists of a total 20 s period. Therefore, in 1 min, three cycles are completed. As the humidity sensor consumes the least power, it is chosen to be operated at the end of the cycle respectively. So, if at any time, the humidity sensor is operated for a long time, it will not affect total energy consumption. Therefore, it is clear that three sensors (CO_2 sensor, temperature sensor, and CO and NO_2) are individually ON for a total of 12 s/min,

i.e. 3 cycles×4 s/cycle = 12 s.

Hence, in 1 h each sensor remains ON=12×60 =720 s. On the other hand, the humidity sensor is turned ON for 8 s/cycle.

i.e. 3 cycles×8 s/cycle = 24 s

Thus, in 1 h remains ON=24×60 = 1440 s.

Fig. 7 represents the duty cycle D (CO_2, CO, NO_2, temp) of three sensors. The graph shows that each sensor is ON for 4 s and OFF for 16 s in one cycle. Therefore, the duty cycle of these sensors is:

$$D(CO_2,CO,NO_2,\text{temperature}) = \left(\frac{12}{60} \times 100\right)\% = 20\% \quad (1)$$

Eq.1 shows the result of the duty cycle.

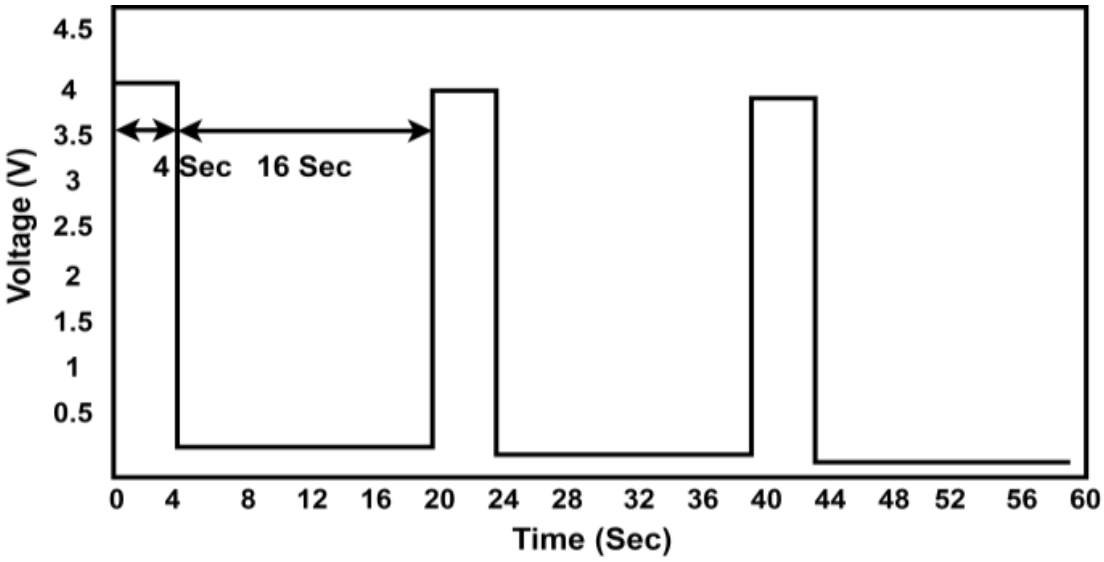

Fig. 7. Duty cycle of CO_2, temp erature, CO and NO_2 sensor

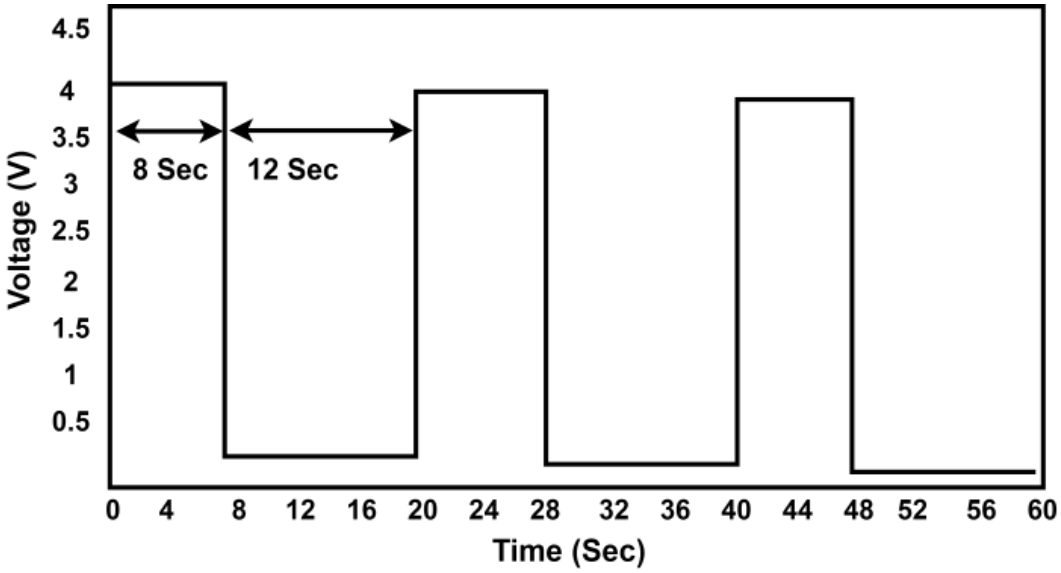

Fig. 8. Duty cycle of the humidity sensor

Similarly, Fig. 8 presents the plot of the duty cycle of humidity sensor D (humidity). This sensor lasts for 8 s and stays off for 12 s. Therefore, after completing three cycles 24 s stays ON in 60 s. Thus, the duty cycle for the humidity sensor is:

$$\text{D(humidity)} = \left(\frac{24}{60} \times 100\right)\% = 40\ \% \quad (2)$$

Eq. 2 presents the duty cycle of the humidity sensor. The average current and voltage drawn by the sensors have been calculated considering 1 h during the operation. Hence, the measured power in AQMS using the creative approach of making switching operations on each sensor is shown in Table 6. In this case, the voltage (V) and current value (I) of all sensors are measured when they are always ON. Power consumption has been calculated by, the P=V×I relationship.

According to the above results, energy is derived from the E=P×t relationship. Here, t represents time. It is measured in seconds. Table 7 shows the outcome of total power without using any power-saving approach.

Table 6. The calculated energy using a demultiplexer

Sl. No.	Name of components	Voltage (V)	Current drawn (mA)	Total runtime (s)	Energy consumed (J)
1	LM-35	4.01	8.40	720	24.25
2	MH-Z14	4.01	8.40	720	24.25
3	MiCS-4514	4.01	0.002	720	5.76
4	HIH-4030	4.01	0.2	1440	1.15
5	Arduino Uno	5	46.5	3600	837
6	Zigbee	3.27	22	3600	259.20

Total=1151.61

Table 7. The energy calculated without using demultiplexer

Sl. No.	Name of components	Voltage (V)	Current drawn (mA)	Total Runtime (s)	Energy consumed (J)
1	LM-35	4.4	8.67	3600	137.33
2	MH-Z14	4.4	8.67	3600	137.33
3	MiCS-4514	4.4	0.002	3600	31.68
4	HIH-4030	4.4	0.2	3600	3.17
5	Arduino Uno	5	46.5	3600	837
6	Zigbee	3.20	23	3600	264.96
		Total			1411.47

Table 8. Monitoring systems related to power awareness designed by well-known organizations

Reference or systems	Measured pollutants	Voltage (v)	Power consumption (mW)
AQMS (proposed)	CO, CO_2, NO_2, temperature, humidity	5	372.6
[30]	CO_2, VOC, PM	12	1440
RAE Systems, WGM, San-Jose, Inc., USA	CO, SO_2, O_2, VOC, NO_2	7.4	629

Hence, during the runtime operation of AQMS, energy is measured. It is clear that by applying the switching method in the sensors, energy of (1411.47-1151.61) Joules i.e. about 260 Joules have been saved. Therefore, by switching all sensors through a demultiplexer circuit total power consumed in the developed AQMS is 0.372 watts. Thus, the result of power saving is achieved at about 18.41% compared to the system where the power saving strategy is not adopted. Table 8 represents different monitoring systems compared to the proposed AQMS related to power consumption.

Additionally, in terms of easy operation, portability and accuracy, the quality of measured values is appreciable. The sensors used in this work add benefits such as low cost, fast response time, low power, etc. In this work, the new concept of switching the sensors using a demultiplexer has been implemented for the first time. After receiving the tested results, it is evident that this technique serves as a favorable idea for low-power AQMS design, which can have energy harvesting viable.

Conclusion

The proposed AQMS has been successfully designed and the sensor network is based on IEEE 802.15.4 network standard. The system is compact, easy to use, continuous transmission, automatic storage, and real-time display which provides information about air quality for future analysis. The monitoring system raises an alarm in case of a drastic changes in air quality. Efficient encoding techniques are implemented for data storage where a large volume of data is stored in binary numbers. The power consumption of the AQMS device is tested. All sensors are properly controlled by using a demultiplexer, indicating a switching technique and making the design energy efficient. The data integrity and security are checked with even better accuracy. Furthermore, predictions about the trend of data in the future will be explored.

Financial supports

No funds or any other financial assistance has been received to continue the research work and prepare the manuscript.

Competing interests

The authors declare that they have no competing interests.

Acknowledgements

The research is completed with the resources of a special manpower development program (SMDP) project.

Ethical considerations

Ethical issues (Including plagiarism, Informed Consent, misconduct, data fabrication and/or falsification, double publication and/or submission, redundancy, etc) have been completely observed by the authors.

References

1. Sharma A, Mitra A, Sharma S, Roy S. Estimation of air quality index from seasonal trends using deep neural network. In proceedings of the International Conference on Artificial Neural Networks. 2018; pp. 511-521.

2. Leung DY. Outdoor-indoor air pollution in urban environment: Challenges and opportunity. Frontiers in Environmental Science. 2015 Jan 15;2:69. [CrossRef] https://doi.org/10.3389/fenvs.2014.00069

3. Chen M, Yang J, Hu L, Hossain MS, Muhammad G. Urban healthcare big data system based on crowd sourced and cloud-based air quality indicators. IEEE Commun. Mag. 2018; 56:14-20. {CrossRef]

4. Marques G. Ambient assisted living and internet of things. In harnessing the internet of everything (IoE) for accelerated innovation opportunities, IGI Global: Hershey, PA, USA. 2019; pp. 100-115.

5. United States Environmental Protection Agency (USEPA). Indoor air facts no. 4 (revised) sick building syndrome. Air and Radiation (6609J), Research and Development (MD-56), Tech. Rep. 1991. [Online]. Available: http://www.epa.gov/iaq/pdfs/sick_building_factsheet.pdf

6. Gungor VC, Hancke, GP. Industrial wireless sensor networks: Challenges, design principles, and technical approach. IEEE Trans. Ind. Electron. 2009; 56(10):4258–4265.

7. Postolache OA, Pereira JMD, Girao PMBS. Smart sensors network for air quality monitoring applications. IEEE Trans.

Instrum. Meas. 2009; 58(9):3253–3262.

8. Kumar A, Singh IP, Sud SK. Energy efficient and low cost indoor environment monitoring system based on the IEEE 1451 standard. IEEE Sensors Journal. 2011; 11(10):2598–2610.

9. Rodriguez-Sanchez MC, Borromeo S, Hernandez-Tamames JA. Wireless sensor networks for conservation and monitoring cultural assets. IEEE Sensors Journal. 2011; 11(6):1382–1389.

10. Kularatna N, Sudantha BH. An environmental air pollution monitoring system based on the IEEE 1451 Standard for low cost requirements. IEEE Sensors Journal. 2008; 8(4):415-422.

11. Kumar A, Hancke GP. Energy efficient environment monitoring system based on the IEEE 802.15.4 Standard for low cost requirements. IEEE Sensors Journal. 2014; 14(8):2557-2566.

12. Oh SJ, Chung WY. Room environment monitoring system from PDA terminal. In Proc. International Symposium Intelligent Signal Processing and Communication Systems (IEEE-ISPACS 2004). 2004; pp.497-501.

13. Yan R, Sun H, Qian Y. 'Energy-aware sensor node design with its application in wireless sensor networks', IEEE Trans. Instrum. Meas., Vol. 62, No. 5, pp.1183–1191.

14. Yan R, Ball D, Deshmukh A, Gao RX. A Bayesian network approach to energy-aware distributed sensing. In Proc. IEEE Sensors, Vienna, Austria. 2004; pp.44-47.

15. Nature. Big data: Science in the petabyte era: community cleverness required. International Journal of science. 2008; 455(7209).

16. Tsuchiya S, Sakamoto Y, Tsuchimoto Y, Lee V. Big data processing in cloud environments. Journal of FUJITSU Science and Technology. 2012; 48(2):159-168.

17. Aich A, Krishna A, Akhilesh V, Hegde C. Encoding web-based data for efficient storage in machine learning applications. In 2019 IEEE International conference on Information processing, IEEE. 2019.

18. Ljungquist B, Petersson P, Johansson AJ, Schouenborg J, Garwicz M. A bit-encoding based new data structure for time and memory efficient handling of spike times in an electrophysiological setup. Neuroinformatics. 2018; 16(2):217-229.

19. Jalil ME. Positioning and location tracking using wireless sensor network. Universiti Teknologi Malaysia. 2011.

20. PointSix. WiFi 2000 ppm CO_2 and Temperature Transmitter 3008-40-V6. Point Six Wireless. Data Sheet. http://www.pointsix.com/PDFs/3008-40-V6.pdf

21. Folea SC, Mois G. A low-power wireless sensor for online ambient monitoring. IEEE Sensors Journal. 2015;15:742-749.

22. Winsen. Zhengzhou Winsen Electronics Technology Co., LTD. 2014. [Online]. Available: https://www.winsen-sensor.com/d/files/MH-Z14.pdf

23. Yang H, Qin Y, Feng G, Ci H. Online monitoring of geological CO_2 storage and leakage based on wireless sensor network. IEEE Sensors Journal. 2013; 13(2):556–562.

24. Sgxsensortech. (2014). [Online]. Available: https://www.sgxsensortech.com/content/uploads/2014/08/0278_Datasheet-MiCS-4514.pdf

25. Kim Y, Evans RG, Iversen WM. Remote sensing and control of an irrigation system using a distributed wireless sensor network. IEEE Transactions on Instrumentation and Measurement. 2008; 57(7):1379-1387. https://doi.org/10.1007/s12021-018-9367-z

26. Dhanalakshmi S, Poongothai M, Sharma K. IoT based indoor air quality and smart energy management for HVAC system. In Proc. International Conference on Computing and Network Communications (CoCoNet'19). Procedia Computer Science, Elsevier. 2020; 171:1800-1809.

27. Hilmani A, Maizate Abderrahin,

Hassouni L. Designing and managing a smart parking system using wireless sensor networks. Journal of Sensor and Actuator Networks. 2018; 7. https://doi.org/10.3390/jsan7020024

28. AC (Atmel Corporation). 8-Bit AVR Microcontroller with 4/8/16/32K bytes in-system programmable flash. 2017. https://www.atmel.com/pt/br/devices/ATMEGA328P.aspx. Accessed 09 Feb 2017. https://doi.org/10.1109/ICInPro47689.2019.9092264

29. Jelicic V, Magno M, Brunelli D, Paci G, Benini L. Context adaptive multimodal wireless sensor network for energy-efficient gas monitoring. IEEE Sensors Journal. 2013; 13(10):328–338.

30. IEEE Standard for Information Technology- telecommunications and Information Exchange Between Systems-Local and Metropolitan Area Networks. IEEE Standard 802.15.4-2003. 2003.

31. Akyildiz IF, Vuran MC. Factors influencing WSN design. Wireless Sensor Networks, 1st ed. New York, NY, USA: Wiley. 2010; pp. 37-51.

32. Digital International Inc., Minnetonka, MN, USA. 2015. XBee-PRO RF Module [Online]. Available: http://store.express-inc.com/pdf/xa-a.pdf

Journal of Air Pollution and Health (Winter 2023); 8(1): 43-58

Original Article

Available online at http://japh.tums.ac.ir

Source characterization of PM_{10} using CMB receptor modeling for the western industrial area of India

Seema Nihalani, Anjali Khambete, Namrata Jariwala*

Civil Engineering Department, Sardar Vallabhbhai National Institute of Technology, Surat, India

ARTICLE INFORMATION

Article Chronology:
Received 26 November 2022
Revised 28 January 2023
Accepted 01 March 2023
Published 29 March 2023

Keywords:
Particulate matter; Vehicle emissions; aerosols; Ankleshwar; Vapi

CORRESPONDING AUTHOR:

seemanihalani@yahoo.com
Tel: (+91 261) 220 1505
Fax: (+91 261) 220 1505

ABSTRACT

Introduction: Receptor models use the chemical characterisation of particulate matter to distinguish the source and analyse the source contributions. The main aim of this study is to carry out source apportionment of PM_{10} for industrial locations of Vapi and Ankleshwar in Gujarat, using the Chemical Mass Balance (CMB) receptor model.

Materials and methods: At six distinct locations of Ankleshwar and Vapi, respirable dust samplers were used to collect particulate matter on quartz filter sheets for the current study. Filter papers containing PM_{10} mass were subsequently examined for Water Soluble Ions (WSIs), major and trace elements, elemental and organic carbon followed by source apportionment study.

Results: Using CMB, the contributions obtained for Ankleshwar are 27.85% for crustal or soil dust, 26.31% for fossil fuel combustion, 21.06% for vehicle emissions, 14.20% for secondary aerosols, 9.30% for biomass, and 1.20% for industrial emissions. CMB for Vapi revealed the chief source signatures as fossil fuel combustion including industries contributing 35%, crustal or soil dust contributing 22.90%, biomass burning contributing 19.12%, vehicular emissions contributing 16.18%, and secondary aerosols contributing 6.79%.

Conclusion: By applying the CMB model, the primary source is found to be crustal or soil dust followed by burning fossil fuels, vehicular emissions, and secondary aerosols for Ankleshwar and Vapi, respectively. A quantitative assessment of source contributions to particulate matter is required to create emission control measures. The findings of this study will be beneficial for the environmental management of particle concentrations in the study region.

Introduction

Airborne particulate matter and other gaseous pollutants are becoming more prevalent, especially in developing nations like India, as a result of rapid industrialisation, urbanisation, fossil fuel consumption, and economic expansion. According to research studies, increased morbidity and high particle concentration are strongly

Please cite this article as: Nihalani S, Khambete A, Jariwala N. Source characterization of PM_{10} using CMB receptor modeling for the western industrial area of India. Journal of Air Pollution and Health. 2023;8(1): 43-58.

Copyright © 2023 Tehran University of Medical Sciences. Published by Tehran University of Medical Sciences.
This work is licensed under a Creative Commons Attribution-NonCommercial 4.0 International license (https://creativecommons.org/licenses/by-nc/4.0/). Noncommercial uses of the work are permitted, provided the original work is properly cited.

correlated. When inhaled, the respirable portion of particulate matter known as Particulate matter (PM_{10} or $PM_{2.5}$) can cause several respiratory and heart health problems in people [1]. Numerous studies have demonstrated a correlation between particulate matter parameters, such as size, distribution, mass concentration, and the impacts on human health. Even better than any other indicator, this knowledge serves as a guide for predicting the effects of the particles on human health. [2, 3]. Due to its immediate as well as long-term detrimental impacts on health, chemical characterization of airborne particulate matter, particularly heavy metal tracer indicators, is of great interest. Along with having a negative impact on health, particulate matter also affects several atmospheric functions, such as solar radiation, visibility, precipitation, cloud formation, etc. Many stern measures have already been taken to reduce the threat of air pollution, but many big towns and cities are still dealing with this issue. The main anthropogenic sources of particulate matter include emissions from moving vehicles or traffic, industrial activity emissions, burning fossil fuels, burning biomass, construction and demolition activities, suspended or re-suspended road dust, and so on [4]. The concentration of particulate matter and its chemical characterization in ambient air can indicate characteristics of the activities involved in addition to providing details on human exposure to such heavy metal pollution [5]. Hence, thorough monitoring of ambient air quality is necessary to determine the current state of air quality in any given place.

Receptor models are often used to identify the sources of air pollution and assess the impact of each source on the receptor. Receptor models typically use the elemental features of particles identified from the source to recognize the presence of distinct sources and compute their contributions to the receptor. Different receptor models, including CMB, Principal Component Analysis (PCA), PCA-MLR, UNMIX, Positive Matrix Factorisation (PMF), and others, have been used in research studies throughout the world to carry out source apportionment [6-8]. The CMB model, among these several receptor models, is quite reliable for source apportionment of both coarse and fine particulates. To analyze the contribution from various sources, the CMB model chooses the most optimal combination of the chemical composition of PM_{10} and emission source characteristics [9]. Since Factor Analysis (FA) or PMF have been frequently employed, source apportionment studies with CMB in India are limited. It is crucial to understand the impact of each emission source separately to create efficient strategies for risk reduction and air pollution control. The CMB receptor model has been used in this work to evaluate the various sources of coarse particles in Ankleshwar and Vapi. For the industrial areas of Ankleshwar and Vapi in Gujarat, the current work presents the chemical characterization of atmospheric PM consisting of EC, OC, WSIs comprising cations and anions, major and trace elements in PM_{10} mass. A source apportionment investigation using the CMB model, enrichment factor analysis, and mass closure is used to understand this. The findings of this study will help manage the environment of particle concentrations that exceed regulatory standards in the study area.

Materials and methods

Site description

The first study area, Ankleshwar, is the largest industrial complex in Asia and home to several chemical firms, is situated at 21.62° N and 73.01° E, about 10 km from Bharuch. Production of dyes, paints, insecticides, chemicals, and medicines are among the main industries of Ankleshwar. In Ankleshwar, the average air temperature ranges from 13.3 °C to 41.9 °C, while the average relative humidity

is between 12% and 99.4%. The average wind speed is observed to be between 3.1 m/s to 9 m/s, with prominent wind direction being south-west. Second study area, Vapi is located at 20°23'21.48" N and 72°54'38.16" E, with a mean sea height of approximately 30 m. The average annual temperature of Vapi is 27 °C, with 70% annual relative humidity and 2000 mm of average precipitation. The prevailing wind direction most of the year is West-South-West, with an average yearly wind speed of 3.6 m/s. The main contributors to atmospheric particulates in both the study areas include secondary aerosols, resuspended dust, fossil fuel burning, industrial pollutants, vehicle emissions and biomass burning. Fig. 1 displays the sampling locations for both Ankleshwar and Vapi. For both the sites, at each of the six sampling locations, respirable dust samplers were employed to measure the particle content. Filter papers were then further digested to measure the elements NO_3, SO_4, NH_3, K-S, Cl, Na, Ca, EC, OC, Al, Si, Br, Cr, Cu, Ni, Zn, Pb, Fe, K, Mn, S, Ti, and V.

Experimental techniques and methods

The PM_{10} samples for Ankleshwar and Vapi were collected between December 2019 and February 2020 at the locations depicted in Fig. 1. Using a respirable volume sampler (RDS with Model 460 NL, make - Envirotech Pvt. Ltd) placed at a height of 1.5 m from the ground, PM_{10} samples were collected for 24 hours on quartz filter sheets that are 20.3 cm long by 25.4 cm wide, with a flow rate of 1.13 m3/min. 120 samples were collected using filter sheets for both the study areas. The filter papers used in particulate matter monitoring were conditioned for two days in a desiccator at 25 ° C temperature and 50% relative humidity, before and after sampling. A five-digit weighing balance was used to determine the gravimetric weight of fiber filters. The difference between the original and final weights of the filter was used to calculate the particulate concentration. The scientific techniques utilised in this study include gravimetric analysis for particulate matter concentration, ion chromatography for WSIC analysis, ICP-AES for heavy metal analysis, and EC-OC carbon analyzer for elemental and organic carbon analysis.

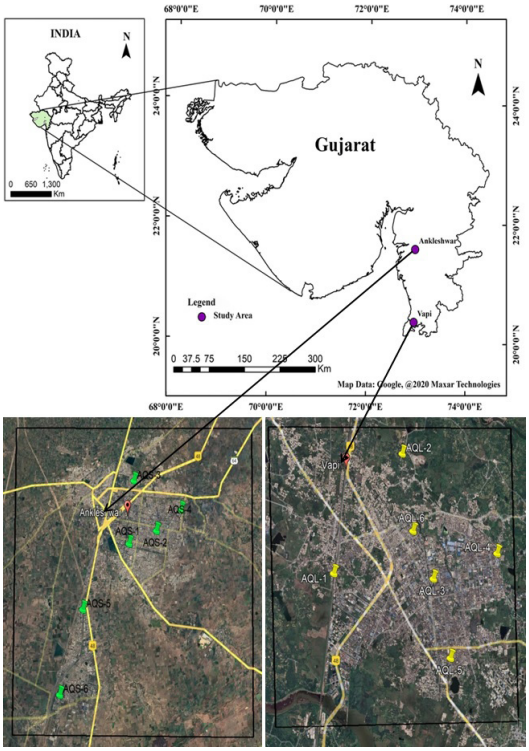

Fig. 1. Sampling locations in the study area

The filter sheets were subsequently separated into three portions for the examination of heavy metals, ions, and EC-OC after identifying the particulate matter concentration. Digestion and further heavy metal extraction from one part of the filter sheet was done on a hot plate. In a closed vessel, the filter papers were digested and dissolved in 15 mL HNO_3-HCl solution over the course of two hours at 150° C. Following digestion, the sample was filtered using Whatman filter paper, and it was then kept in a refrigerator until examination. The separated and chilled sample was utilised for the analysis of Al, Si, Br, Ca, Cl, Cr, Cu, Fe, K, Mn, Ti, Ni, Zn, Pb, S, and V using ICP-AES (Model ULTIMA 2000). According to the CPCB's standard process, the second portion of the filter paper was utilised for ion analysis, and it was extracted using ultra-pure or deionized water with a resistivity of 18 MU. A syringe filter was used to filter the extracted water sample, which was then saved for subsequent examination using an ion chromatograph (IC Basic 792: Metrohm). Four cations- ammonium (NH_3), potassium (K^+), potassium (K-S) salt, and calcium ($Ca2^+$) and two anions- nitrate (NO_3) and sulfate (SO_4) are included in the ion analysis. An EC-OC carbon analyzer (model DRI2001, Protocol Improve A) was used to analyse the third and final portion of the filter paper in accordance with U.S. Environmental Protection Agency)USEPA(protocol. The controlled oxidation of EC and OC, which liberates carbon compounds at various temperatures, is the basis for the operation of the EC-OC carbon analyzer.

Quality control and quality assurance

To keep the accuracy and precision throughout the investigation, a rigorous quality control program was put in place. The current sampling and analysis ensured the further quality control measures:

With clean forceps, filters were handled with caution.

It was made sure to collect representative samples with the appropriate labeling (such as sample type, location, time and date of collection, environmental factors, etc.).

The disposable materials, such as glassware, solvents, etc., were used appropriately.

Every precaution was taken to prevent contamination while sampling, sample handling, processing, and analysis.

Quality assurance was done during chemical reagent handling and field operations.

Collaborative sampling, flow audits, spot checks, and duplicate analysis to ensure data quality control.

Competency assessments were conducted for field operators and laboratory analysts.

Acceptance tests were performed on the tools and equipment being utilised.

Enrichment factor

The Enrichment Factor (EF) provides information about the element's fundamental characteristics, including whether it is of crustal origin or originates from human activity. The ratio of the two components is used to compute the enrichment factor. The numerator is obtained by dividing the element concentration by the reference element concentration in the sample whereas the denominator is derived by dividing the element concentration by a chosen reference element concentration in the earth's crust [10]. Fe, Al, and Si are the primary reference elements used to calculate EF, while Aluminum (Al), which has been widely used in numerous past research, has been chosen as the reference element for the current investigation [11].

EF is calculated through Eq. 1:

$$EF=(E\_Sample⁄X\_(Sample))/(E\_Crust⁄X\_Crust) \quad (1)$$

Where Esample=element concentration in the sample

Xsample=reference element concentration in the sample

Ecrust=element concentration in the earth's crust.

Xcrust=reference element concentration in the earth's crust.

Mass closure

To evaluate the relative contribution of measured elemental species and their correlation with an estimated mass of PM_{10}, the chemical species constituting PM_{10} mass are rebuilt ($RCPM_{10}$). The mass closure is accomplished using the IMPROVE equation, as illustrated in Eq. 2 below, and the reconstructed PM_{10} mass is referred to as $RCPM_{10}$ [12].

$RCPM_{10}$=[AS]+[AN]+[POM]+[LAC] +[SS]+[SOIL] (2)

Where $RCPM_{10}$ is the reconstructed mass of PM_{10}, AS is ammonium sulfate, AN is ammonium nitrate, POM is particulate organic matter, LAC is light-absorbing carbon and SS is sea salt.

The product of each element's concentration and its conversion index is used to calculate the concentration of each factor specified in Eq. 2. By deducting the reconstructed mass $RCPM_{10}$ from the observed mass PM_{10}, the mass difference (MD) for PM_{10} is calculated (i.e., MD = PM_{10} - $RCPM_{10}$).

Chemical mass balance (CMB)

The fundamental idea underlying various receptor models is to utilise the classical theory of mass equilibrium to determine the likely sources of PM_{10} or $PM_{2.5}$ emissions while assuming that mass is conserved [13]. The concentration of chemical species bound to PM_{10} as well as specific source profiles constitutes the input dataset for the receptor model. By calculating the relative source contributions of selected sources at the specific monitoring location, these input datasets are utilised to identify and carry out source apportionment of ambient particulates [14]. Due to the retroactive character of receptor models, it can only assess the effects of source profiles that have previously been examined. CMB is a novel receptor model that computes the source contributions by using the information on source profiles as well as the chemical composition of the elements in PM_{10}. To calculate the individual source contributions in comparison to similar emission sources, it is advised that the likely sources that are chemically different be employed [15]. The receptor element concentration is expressed as a direct aggregation of the sum of the products of the source contributions and source profiles in the CMB model's linear regression equation.

Thus, using multiple linear regression techniques, the CMB model uses source profiles and receptor concentrations with uncertainties as input to produce distinct source involvement [16]. However, it is advised to avoid linearity and the likelihood of identifying geographic locations in the source profile selection to maintain a high level of model relevance [17]. By combining a comparable set of sources, the linearity in source profiles can be decreased [18]. The application of the CMB model is appropriate when limited monitoring data is available. Utilizing in-depth information on source profiles may allow for a reduction in the number of samples or data that can be used as input, but a smaller dataset may raise the amount of uncertainty.

Watson provided the CMB model's fundamental equation (Eq. 3) in 1984 as a statement of mass conservation:

$$C_i = \sum_{j=1}^{m} F_{ij}\, S_j + E_i \quad (3)$$

Where i=number of species
j=number of sources

Ci=ambient concentration of species i
Fij=fraction of species i in source j
Sj=source contribution of source j
Ei=residual error in species i

The fundamental premises on which the CMB model is applied are [2]:

- A linear independence between the source profiles
- The number of sources must be smaller than the number of species
- Source emission compositions remain stable during the monitoring period
- Chemical species do not interact with one another and accumulate linearly.
- Identification and characterization of receptor emissions from all likely sources that will affect the receptor
- The measured uncertainties are distributed normally, random, and not correlated.

For CMB model investigation, the following basic steps are applied:

- Measuring PM_{10} concentration and chemical species bound to PM_{10}
- Determining the details of selected source profiles used for the CMB analysis such as:
- Vehicular source profiles
- Refuse or biomass burning
- Crustal or soil dust
- Fossil fuel combustion
- Industrial emissions
- Secondary aerosols
- Using the CMB receptor model, the chemical mass balance equation is solved.
- Determining the contributing sources by averaging daily samples over the course of the monitoring period.

CMB model performance parameters

The CMB model must be used to assess contributions from chemically distinct sources since sources with identical physical or chemical features cannot be distinguished by them. The CMB model includes a variety of performance metrics for each model run, including the regression coefficient, degree of freedom, chi-square, and percent mass. For each of these diagnostic tests, the CMB guide from the USEPA lists a range of values. A Source Contribution Estimate (SCE) is the primary output provided by the CMB model. The overall mass concentration is often approximated by the sum of all source contribution estimations. When the SCE exceeds the standard error, it is taken into account for output; however, if the SCE is less than the standard error, the source contribution cannot be identified. The coefficient of determination (R^2), chi-square (χ^2), degree of freedom, and percent mass are typically the goodness of fit metrics used for computation using the least square approach [19].

- R^2 is derived using the linear regression of values obtained from the CMB model against observed concentrations. R^2 has values between 0 and 1. When R^2 is close to 1, the SCEs provide a better explanation for the observed concentrations, however, when R^2 is less than 0, the SCEs don't demarcate the source profiles.
- To calculate the weighted sum of squares, the difference between the estimated and measured concentrations for the fitted species is first determined and then divided by variance and degree of freedom. The chi-square value indicates the goodness of the data. Values of χ^2 smaller than one suggest a good fit data while values of χ^2 greater than 4 reveal that the linked species concentrations are not properly related to the SCEs.
- The percentage of mass is determined by dividing the total SCEs from the CMB model by the actual mass concentration. Percent mass

levels between 80% and 120% are regarded as sufficient.

- By deducting the number of fitting sources from species, the degree of freedom is calculated. According to the CMB handbook, a solution should be regarded as reasonable if its degree of freedom value is more than 5.

Results and discussion

Ambient air quality in the study area

For Ankleshwar, the mass concentration of PM_{10} varied between 100.98 to 225.47 µg/m^3, while for Vapi, it varied between 115.88 to 226.50 µg/m^3. Fig. 2 shows the levels of PM_{10} and $PM_{2.5}$ in the study area.

The average value of PM_{10} for six locations in Ankleshwar is 1.6 times higher than National Ambient Air Quality Standard (NAAQS, 2009) value of 100 µg/m^3, while for Vapi it is two times higher. Additionally, the average PM_{10} concentrations in Ankleshwar and Vapi are found to be almost 10 times higher than the PM_{10} air quality threshold set by the World Health Organization, which is 20 µg/m^3 (WHO, 2006). For Ankleshwar, the concentration of $PM_{2.5}$ is found between 69.64 to 122.15 µg/m^3, while for Vapi, it is between 69.38 to 120.52 µg/m^3. Therefore, it can be seen that the ratio of $PM_{2.5}$ to PM_{10} in the study area ranges from 0.49 to 0.69, with an average value of 0.60, indicating the effect of combustion-related activities [19].

Chemical characterization of PM_{10}

Following the chemical characterization of PM_{10}, the elements are divided into four categories total carbon, WSIs, major and trace elements, as shown in Fig. 2. The carbon fraction has the largest concentration of the four identified components, followed by major elements, water-soluble ions, and trace elements. In Ankleshwar and Vapi, the mean concentration of water-soluble ions is found to be 26.90 and 25.87 µg/m^3, respectively whereas the mean concentration of total carbon is recorded as 49.72 and 51.18 µg/m^3, respectively. For Ankleshwar and Vapi, the mean concentration of the main elements is found to be 31.49 and 31.08 µg/m^3, respectively and the measured trace element concentrations are 1.60 and 1.58 µg/m^3, respectively

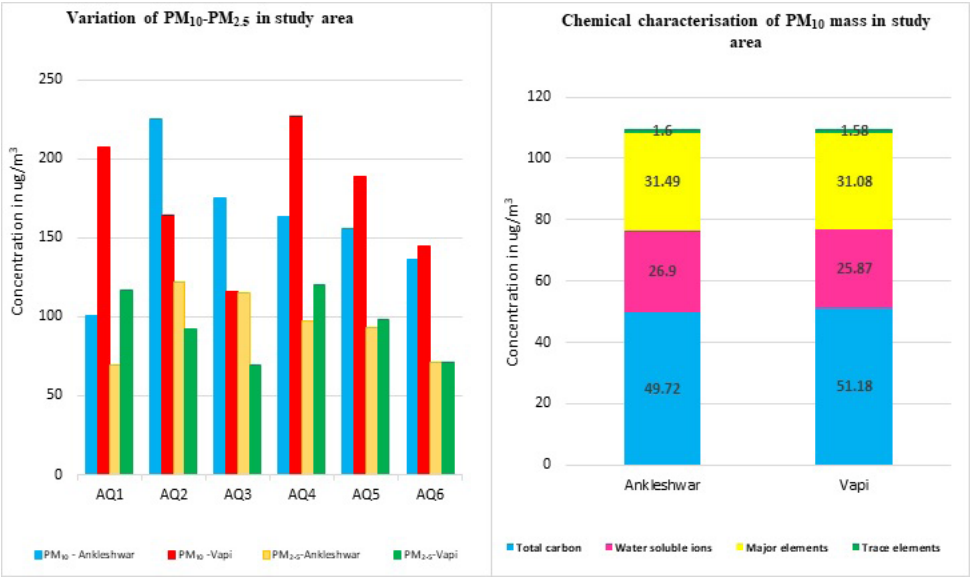

Fig. 2. Variation of PM_{10} - $PM_{2.5}$ and Chemical characterization of PM_{10} in the study area

As indicated in Fig. 3, the mean concentration of OC is recorded as 29.39 µg/m^3 for Ankleshwar and 29.40 µg/m^3 for Vapi, whereas the mean concentration of EC is obtained to be 20.33 µg/m^3 for Ankleshwar and 21.78 µg/m^3 for Vapi. The concentration of OC and EC is significantly influenced by vehicle emissions and the burning of agricultural waste [11]. The value of the OC/EC ratio between 0.3 and 1 denotes diesel vehicle emissions, whereas, the number between 1.4 and 4 denotes gasoline car emissions [11, 14]. According to the current study, the OC/EC ratio for Ankleshwar and Vapi is around 1.45 and 1.41 respectively, indicating emissions a mix of diesel as well as gasoline-powered automobiles. A similar trend is observed for OC and EC at both the locations.

As shown in Fig. 3, the average concentrations of the water-soluble cations K, Ca, NH_3, and Na are 4.15, 3.32, 3.27, and 1.32 µg/m^3 for Ankleshwar and 3.99, 2.93, 2.79, and 1.32 µg/m^3 for Vapi, respectively. For Ankleshwar, the average concentration of water-soluble anions SO_4, NO_3, and Cl in PM_{10} is 8.37, 3.66, and 2.81 µg/m^3, whereas, for Vapi, it is 8.04, 4.12, and 2.68 µg/m^3. The long-distance transmission of secondary aerosols, in addition to secondary emissions from nearby sources like factories and cars, can be blamed for the effect of water-soluble ions [14]. A similar trend is observed for WSIs that is cations as well as anions at both the locations.

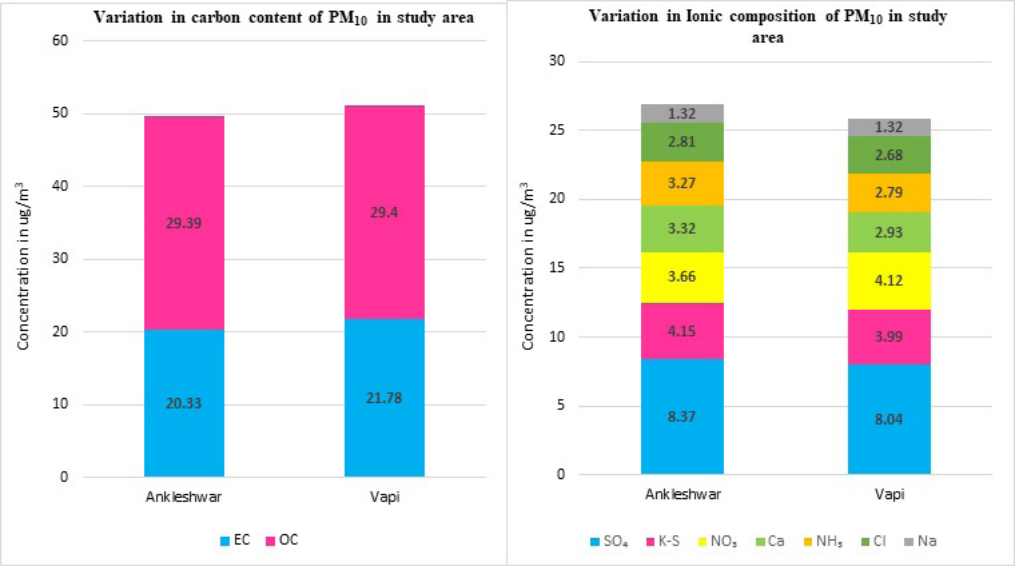

Fig. 3. Variation in Carbon content and Ionic composition of PM_{10} in the study area

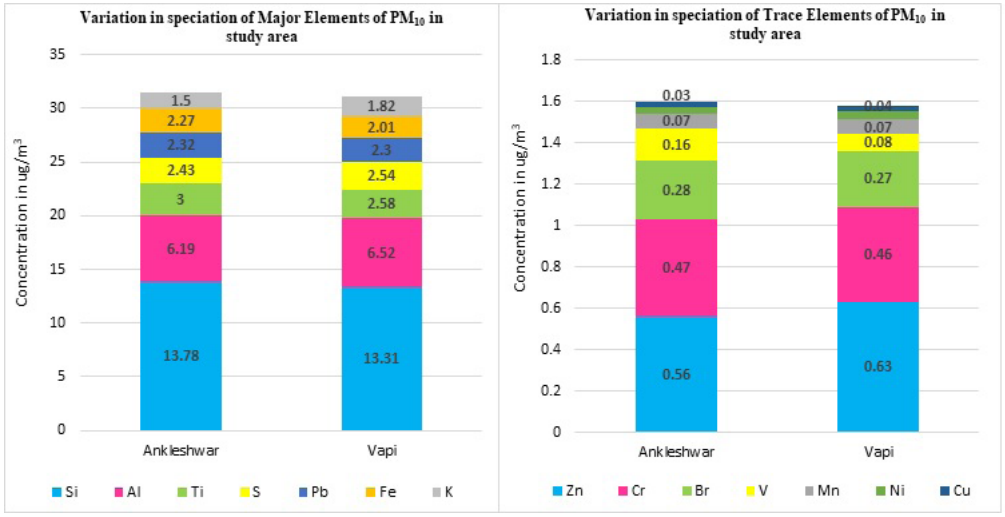

Fig. 4. Variation in speciation of major and trace elements of PM_{10} in the study area

In this study, the elements are divided in two categories, major and trace elements. In general, the major elements are Si, Al, Ti, S, Pb, Fe, and K, with average concentrations of 13.78, 6.19, 3, 2.43, 2.32, 2.27, and 1.5 µg/m^3 for Ankleshwar and 13.31, 6.52, 2.58, 2.54, 2.30, 2.01, and 1.82 µg/m^3 for Vapi, as shown in figure 4.0. The trace elements include anthropogenic trace indicators such as Zn, Cr, Br, V, Mn, Ni, and Cu, with mean concentrations of 0.56, 0.47, 0.28, 0.16, 0.07, and 0.03 µg/m^3 for Ankleshwar and 0.63, 0.46, 0.27, 0.08, 0.07, 0.04, and 0.03 µg/m^3 for Vapi, respectively. Based on the location of the air mass and its path of travel, the main and trace elements can be identified as originating from either a natural or manmade source, which can be further substantiated using Enrichment Factor (EF) analysis [14]. The CPCB has established annual regulatory limits for several metals, including As, Pb, Cd, and Ni (MoEF, 2009). The mean Pb concentration is analysed as 2318 ng/m^3 and 2305 ng/m^3 for Ankleshwar and Vapi, respectively, comparing the CPCB limit of 500 ng/m^3, while the concentration of Ni is found to be 34 ng/m^3 and 37 ng/m^3 for Ankleshwar and Vapi, respectively, exceeding the CPCB limit of 20 ng/m^3.

Enrichment factor

Elements with EF values less than 10 are significantly associated with crustal sources and are marginally enriched. Elements with EF values between 10 and 100 indicate that the elements come from both crustal and anthropogenic sources, while elements with EF values greater than 100 imply that the majority of the elements come from anthropogenic sources [14]. For both Ankleshwar and Vapi, the order of the EF values for the elements taken into consideration in this study is Pb> Br>S>Zn>Cr>>V>Ti>Cu>Ni>Al (Fig. 5). For the metals Fe, Mn, Si, and K, the values of EF are less than 10, indicating that the sources of these elements are crustal processes including natural rock weathering, forest fires, sea salt, and wind-blown soil components [20]. The measured EF values for Ni, Ti, Cr, Cu, and V range from 10 to 100, indicating moderate enrichment from both crustal and anthropogenic sources. Examples of anthropogenic sources include the burning of fossil fuels like coal, vehicle emissions, and industrial emissions. The elements Zn, S, Br, and PB had EF values greater than 100, indicating that they probably originate from anthropogenic sources such as burning coke or biomass, traffic emissions, industrial emissions from the steel or foundry industries, and resuspended dust.

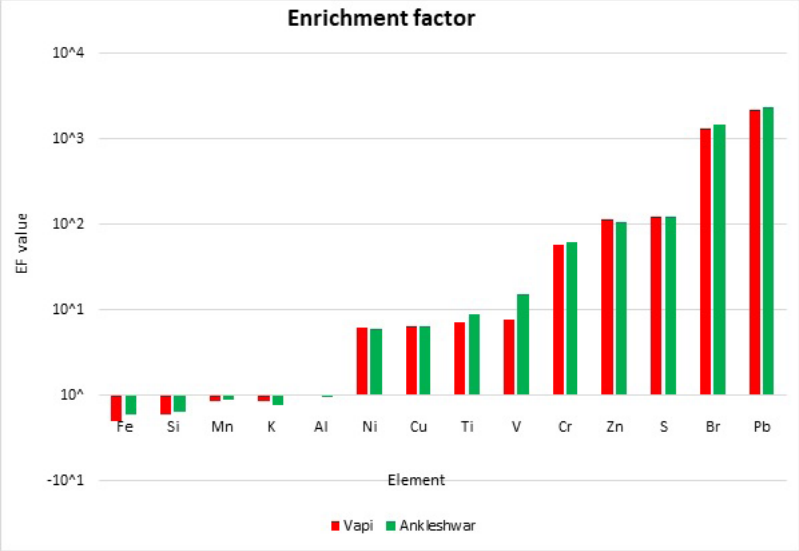

Fig. 5. Enrichment factors for elements in the study area

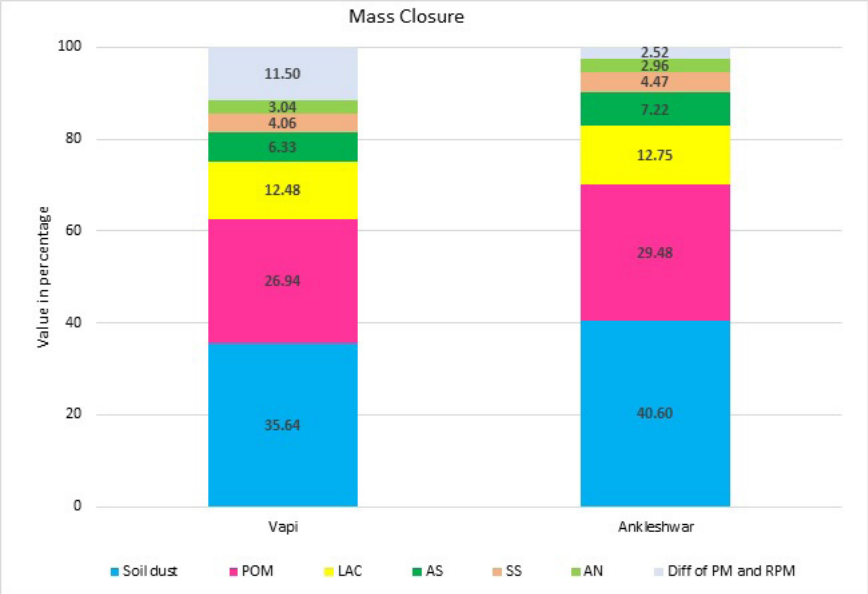

Fig. 6. Factors for Mass closure in the study area

Mass closure

Using IMPROVE equation, stated above, for Ankleshwar and Vapi, the MD for PM_{10} is determined as 2.52% and 11.5% of PM_{10} mass, respectively. The unidentified mass of PM_{10} is responsible for the mass difference. Using IMPROVE equation, the computed contribution of soil dust is obtained as 40.60% and 35.64% of the $RCPM_{10}$ mass, for Ankleshwar and Vapi respectively, which is greater than anticipated. The effect of regional as well as transboundary migration of soil dust from neighbouring regions may be responsible for the high value of soil dust. For Ankleshwar and Vapi, the effect of POM is seen to be 29.48% and 26.94% of the $RCPM_{10}$ mass, respectively. The primary POM sources in the atmosphere include burning fossil fuels or burning biomass, whereas secondary sources are secondary aerosols released after the oxidation of gaseous precursors.

For Ankleshwar and Vapi, the estimated contribution of LAC to the $RCPM_{10}$ mass is 12.75% and 12.47%, respectively. LAC typically consists of black, elemental, or graphite carbon that is released as a result of incomplete fossil fuel combustion or biomass burning. For Ankleshwar and Vapi, the contribution from AS is observed to be 7.22% and 6.33%, respectively. Typically, AS is created in the atmosphere as a result of several chemical reactions that occur with SO_2, which is released through the combustion of fossil fuels. For Ankleshwar and Vapi, the effect of sea salt is determined to be 4.47% and 4.09% of PM_{10} mass respectively. The concentration of AN is 2.96% and 3.04% of $RCPM_{10}$ mass for Ankleshwar and Vapi respectively. When NO_x from the burning of fossil fuels or vehicle emissions undergoes reversible interactions with the gaseous phases of NH_3 and HNO_3, AN is created. According to Fig. 6, the percentage contribution of various factors of $RCPM_{10}$ mass is observed to be in the sequence of Soil>POM>LAC>AS>SS>AN.

Source apportionment-using CMB

For source apportionment investigation for the industrial districts of Ankleshwar and Vapi, the CMB receptor model is used. This scientific investigation is conducted to identify potential sources of PM_{10} emissions and to calculate the source contributions to PM_{10} mass. The estimations of the CMB model are not unique since they are based on least squares linear regression; as a result, it is difficult to demonstrate their correctness. For the current study, the CPCB-developed source profiles for the CMB model for several Indian metropolitan cities are used. The emission sources taken into account are biomass burning, vehicular emissions, crustal or soil dust, and fossil fuel combustion, including industrial sources.

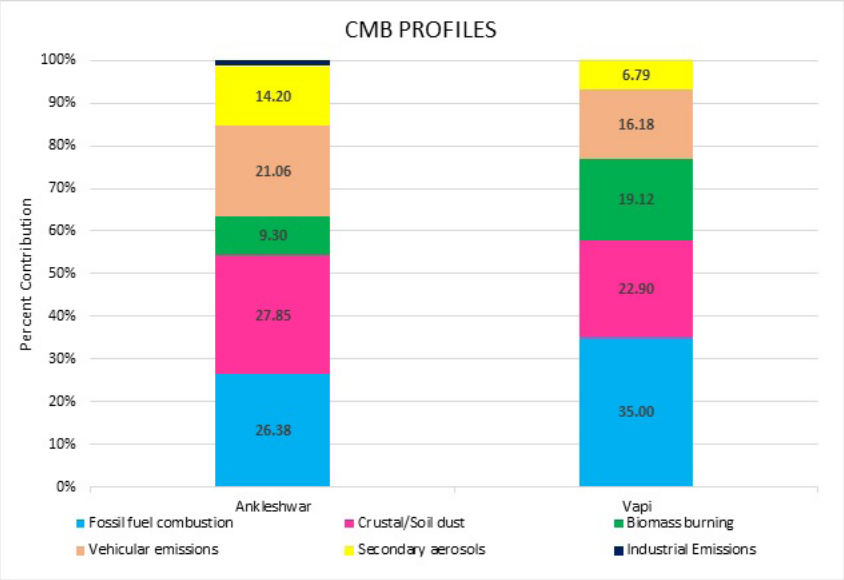

Fig. 7. PM_{10} Source contributions at Ankleshwar and Vapi using the CMB model

The factors for source apportionment using CMB are shown in Fig. 7, which reveals that the source contributions for Ankleshwar and Vapi are marginally different. With a percentage of 26.38% from Ankleshwar and 35% from Vapi, fossil fuel combustion is the leading source of emissions. The burning of any type of fossil fuel, such as coal, gasoline, diesel, natural gas, or oil, Light Diesel Oil (LDO), Heavy Diesel Oil (HDO) is a composite source of PM_{10}, and the several marker species linked to this source include Al, SO_4, Cl, Fe, Cr, and Zn [21]. The second major source of emissions at both locations is crustal or soil dust, which Ankleshwar contributing 27.85% and Vapi contributing 22.90% of the mass of PM_{10}. Crustal or soil dust is a complex and heterogeneous mixture of dust that contains a high concentration of crustal elements like Si, Al, Ca, K, Na, and Mg. It can be produced by a variety of activities, including soil dust, resuspended dust, construction activities, fuel combustion, and vehicular emissions [22]. Vehicular emissions are the third-largest source of emissions, with EC, OC, Cu, Zn, Mn, Pb, and Ni serving as the primary marker species [23]. Vehicular emissions include combined emissions from several sources, such as gasoline and diesel cars, lubricants, beak liners, etc. Ankleshwar and Vapi as shown in Fig. 7, contribute 21.06% and 16.18%, respectively, to vehicular emissions. With an impact of 9.3% from Ankleshwar and 19.12% from Vapi, biomass burning is the fourth-largest component. Sources such as the burning of household fuelwood, agricultural waste, cow dung, solid waste, wildfires, and other biomass waste are included in biomass burning. The presence of element markers like SO_4, NH_4, or OC in combination with K^+ is often used to differentiate K^+ as a source of biomass-related burning [14].

Secondary aerosols, which comprise ammonium sulphate and ammonium nitrate, are identified as the fifth emission source. Secondary aerosols of atmospheric particles that are created in the atmosphere can typically come from anthropogenic or natural sources and are mostly derived from their gaseous predecessors such as SO_2, NO_x, and NH_3 [14]. Secondary aerosols are shown to contribute 14.20% for Ankleshwar and 6.79% for Vapi. For the current study, industrial emissions could not be distinguished as a separate source by the CMB model, however, for Ankleshwar, a very weak contribution of 1.2% is shown as the sixth emission source.

R^2, chi-square (χ^2), degree of freedom, fit measure and percent mass are the several performance measurements and statistics used to assess the CMB model. The R^2 values are observed to be 0.77 and 0.86 for Ankleshwar and Vapi indicating that the SCEs provide a better explanation for the observed concentrations. The χ^2 is observed to be 3.56 and 5.80 for Ankleshwar and Vapi respectively depicting average linkage between SCEs and species concentration. The percentage of mass determined by the CMB model is 105.7% and 95.1% for Ankleshwar and Vapi, which can be termed as sufficient. The obtained solution by CMB can be regarded as reasonable with a degree of freedom values of 13 and 14 for Ankleshwar and Vapi respectively. The largest fit measures achieved for obtained solutions are 0.70 and 0.72 for Ankleshwar and Vapi, indicating a rational solution.

Table 1 provides an overview of the CMB source apportionment studies that are conducted in the Indian context.

Table 1. Summary of the percentage contribution of PM sources for CMB studies conducted in India

Sr. No.	Location	PM	Fossil fuel combustion	Crustal /Road dust	Vehicles	Industrial	Refuse/ Field burning	Secondary/ Marine aerosols	Other	Ref
1	Bangalore	PM_{10}	4.2	50.6	19	4.5	---	8.7	13	[24]
2	Bangalore	$PM_{2.5}$	5.8	3.5	49.9	3.5	---	12.7	24.7	[24]
3	Delhi	PM_{10}	---	64	29	3	---	---	4	[25]
4	Delhi	$PM_{2.5}$	---	35	62	2	---	---	1	[25]
5	Delhi	$PM_{2.5}$	---	35	20	20	16	---	9	[26]
6	Delhi	PM_{10}	---	43	17	20	13	---	7	[26]
7	Hyderabad	PM_{10}	12	40	22	9	7	---	10	[27]
8	Hyderabad	$PM_{2.5}$	9	26	31	7	6	---	21	[27]
9	Hyderabad	PM_{10}	6.1	33.6	43.6	---	6.9	9.7	---	[28]
10	Hyderabad	$PM_{2.5}$	9.7	18.1	35.9	---	16.4	18.8	---	[28]
11	Kanpur	$PM_{2.5}$	13	6	37	---	23	15	---	[29]
12	Kolkata	PM_{10}	42	21	---	---	7	---	29	[30]
13	Kozhikode	PM_{10}	---	46	18	---	18	17	6	[31]
14	Mumbai	PM_{10}	20.6	10	36.3	2.1	---	---	---	[32]
15	Nagpur	$PM_{2.5}$	---	6	57	---	15.1	16	6	[33]

Conclusion

The current research presents an exhaustive insight of PM_{10} levels, elemental species bound to PM_{10}, and the emission sources contributing to PM_{10} mass for Ankleshwar and Vapi industrial areas. The results showed that the PM_{10} mass is higher than the NAAQS standard value of 100 µg/m^3 and ranged between 100.98 and 225.47 µg/m^3 for Ankleshwar and 115.88 to 226.5 µg/m^3 for Vapi. According to the chemical examination, the total mass of carbons ranged from 44 to 48 percent of PM_{10} mass in Ankleshwar and from 45 to 48 percent in the industrial region of Vapi. For Ankleshwar and Vapi, water-soluble ions constitute 21 to 26% and 22 to 26% of the PM_{10} mass, whereas significant elements ranged in proportion between 28 and 30% and 26 to 29% respectively. In all six locations for Ankleshwar and Vapi, the average lead and nickel concentrations are higher above the CPCB

limits of 500 ng/m^3 and 20 ng/m^3, respectively. The elements Ni, Cu, Ti, and V have a natural and anthropogenic source, while Fe, Si, Mn, and K are found to have crustal origins. The enrichment factors for the marker elements Cr, Zn, S, Br, and Pb showed that their source is anthropogenic. When assessing the sources that contribute to PM_{10} mass, a well-known receptor model (CMB) is used and the best-fitting source profiles include fossil fuel combustion including industrial sources, crustal or soil dust, vehicle emissions, biomass burning, and secondary aerosols. According to the CMB model for Ankleshwar, source contributions are 27.85% from crustal or soil dust, 26.31% from burning fossil fuels, 21.06% from vehicle emissions, 14.20% from secondary aerosols, 9.30% from burning biomass, and 1.20% from industrial emissions. According to the CMB model findings for Vapi, the contribution from fossil fuel combustion, including industrial sources, is 35%, followed by contributions from crustal or soil dust (23%), biomass burning (19%), automobile emissions (16%), and secondary aerosols (7%). The current study is limited to the winter season because in the study area, winter is considered as worst climate scenario since dispersion of air pollutants is limited in winter season [34]. In developing countries, the generation of source profiles for specific areas takes long time. Hence, source apportionment study using the CMB model can give us a brief insight about source profiles present in the study area. The current research helps to estimate the pollutant load in the study region and creates a strategy for improving urban air quality. Further CMB, receptor model can be applied for $PM_{2.5}$ in the future to study the health impact on the workers and people residing in nearby areas.

Financial supports

Not applicable. No funding is received for conducting this study.

Competing interests

The authors declare they have no conflicts of interest or competing interests.

Acknowledgements

The authors would like to thank the editor in handling this paper, and also acknowledge the anonymous reviewers for their great comments and edits which helped us to improve the quality of this paper significantly.

Ethical considerations

"Ethical issues (Including plagiarism, Informed Consent, misconduct, data fabrication and/ or falsification, double publication and/ or submission, redundancy, etc) have been completely ob-served by the authors."

References

1. Das R, Khezri B, Srivastava B, Datta S, Sikdar PK, Webster RD, Wang X. Trace element composition of $PM_{2.5}$ and PM_{10} from Kolkata–a heavily polluted Indian metropolis. Atmospheric Pollution Research. 2015 Sep 1;6(5):742-50.

2. Belis CA, Karagulian F, Larsen BR, Hopke PK. Critical review and meta-analysis of ambient particulate matter source apportionment using receptor models in Europe. Atmospheric Environment. 2013 Apr 1;69:94-108.

3. Nabizadeh R, Yousefi M, Azimi F. Study of particle number size distributions at Azadi terminal in Tehran, comparing high-traffic and no traffic area. MethodsX. 2018 Jan 1;5:1549-55.

4. Nihalani SA, Khambete AK, Jariwala ND. Receptor modelling for particulate matter: review of Indian scenario. Asian Journal of Water, Environment and Pollution. 2020 Jan 1;17(1):105-12.

5. Saradhi IV, Prathibha P, Hopke PK, Pandit GG, Puranik VD. Source apportionment

of coarse and fine particulate matter at Navi Mumbai, India. Aerosol and Air Quality Research. 2008;8(4):423-36.

6. Hopke PK, Ito K, Mar T, Christensen WF, Eatough DJ, Henry RC, Kim E, Laden F, Lall R, Larson TV, Liu H. PM source apportionment and health effects: 1. Intercomparison of source apportionment results. Journal of exposure science & environmental epidemiology. 2006 May;16(3):275-86.

7. Pant P, Harrison RM. Critical review of receptor modelling for particulate matter: a case study of India. Atmospheric Environment. 2012 Mar 1;49:1-2.

8. Parthasarathy K, Sahu SK, Pandit GG. Comparison of two receptor model techniques for the size fractionated particulate matter source apportionment. Aerosol and Air Quality Research. 2016 Jun;16(6):1497-508.

9. Viana M, Kuhlbusch TA, Querol X, Alastuey A, Harrison RM, Hopke PK, Winiwarter W, Vallius M, Szidat S, Prévôt AS, Hueglin C. Source apportionment of particulate matter in Europe: a review of methods and results. Journal of aerosol science. 2008 Oct 1;39(10):827-49.

10. Sudheer AK, Rengarajan R. Atmospheric mineral dust and trace metals over urban environment in western India during winter. Aerosol and Air Quality Research. 2012 May;12(5):923-33.

11. Sharma SK, Mandal TK, Jain S, Sharma A, Saxena M. Source apportionment of $PM_{2.5}$ in Delhi, India using PMF model. Bulletin of environmental contamination and toxicology. 2016 Aug;97:286-93.

12. Matawle J, Pervez S, Dewangan S, Tiwari S, Bisht DS, Pervez YF. $PM_{2.5}$ chemical source profiles of emissions resulting from industrial and domestic burning activities in India. Aerosol and Air Quality Research. 2014 Jul;14(7):2051-66.

13. Srimuruganandam B, Nagendra SS. Source characterization of PM_{10} and PM2. 5 mass using a chemical mass balance model at urban roadside. Science of the total environment. 2012 Sep 1;433:8-19.

14. CSIR-NEERI, PM_{10} and $PM_{2.5}$ source apportionment study and development of emission inventory of Twin cities Kolkata and Howrah of west Bengal, 2019.

15. Clements AL, Fraser MP, Herckes P, Solomon PA. Chemical mass balance source apportionment of fine and PM_{10} in the Desert Southwest, USA. AIMS Environmental Science. 2016;3(1):115-32.

16. Gadkari N, Pervez S. Source apportionment of personal exposure of fine particulates among school communities in India. Environmental monitoring and assessment. 2008 Jul;142:227-41.

17. Selvaraju N, Pushpavanam S, Anu N. A holistic approach combining factor analysis, positive matrix factorization, and chemical mass balance applied to receptor modeling. Environmental monitoring and assessment. 2013 Dec;185:10115-29.

18. Chowdhury Z, Zheng M, Schauer JJ, Sheesley RJ, Salmon LG, Cass GR, Russell AG. Speciation of ambient fine organic carbon particles and source apportionment of $PM_{2.5}$ in Indian cities. Journal of Geophysical Research: Atmospheres. 2007 Aug 16;112(D15).

19. Thammadi SP, Pisini SK, Shukla SK. Estimation of $PM_{2.5}$ emissions and source apportionment using receptor and dispersion models. International Journal of Environmental and Ecological Engineering. 2018 Jun 1;12(7):513-9.

20. Behera SN, Sharma M. Reconstructing primary and secondary components of $PM_{2.5}$ composition for an urban atmosphere. Aerosol Science and Technology. 2010 Sep 30;44(11):983-92.

21. Behera SN, Sharma M. Reconstructing primary and secondary components of $PM_{2.5}$ composition for an urban atmosphere. Aerosol Science and Technology. 2010 Sep 30;44(11):983-92.

22. Pipal AS, Jan R, Satsangi PG, Tiwari S, Taneja A. Study of surface morphology, elemental composition and origin of atmospheric aerosols ($PM_{2.5}$ and PM_{10}) over Agra, India. Aerosol and Air Quality Research. 2014 Jun;14(6):1685-700.

23. Chakraborty A, Gupta T. Chemical characterization and source apportionment of submicron (PM1) aerosol in Kanpur region, India. Aerosol and Air Quality Research. 2010 May;10(5):433-45.

24. CPCB, In: C.P.C.B (Ed.), Air Quality Assessment, Emissions Inventory, and Source Apportionment Studies Bangalore, India. The Energy and Resources Institute, India. 2010.

25. Srivastava A, Jain VK. Seasonal trends in coarse and fine particle sources in Delhi by the chemical mass balance receptor model. Journal of Hazardous Materials. 2007 Jun 1;144(1-2):283-91.

26. CPCB, In: C.P.C.B (Ed.), Air Quality Assessment, Emissions Inventory, and Source Apportionment Studies Delhi, India. National Environmental Engineering Research Institute, India; 2010.

27. Gummeneni S, Yusup YB, Chavali M, Samadi SZ. Source apportionment of particulate matter in the ambient air of Hyderabad city, India. Atmospheric Research. 2011 Aug 1;101(3):752-64.

28. Guttikunda SK, Kopakka RV, Dasari P, Gertler AW. Receptor model-based source apportionment of particulate pollution in Hyderabad, India. Environmental monitoring and assessment. 2013 Jul;185:5585-93.

29. CPCB, In: C.P.C.B (Ed.), Air Quality Assessment, Emissions Inventory and Source Apportionment Studies for Kanpur City, India. Indian Institute of Technology Kanpur, India;2010.

30. Gupta AK, Karar K, Srivastava A. Chemical mass balance source apportionment of PM_{10} and TSP in residential and industrial sites of an urban region of Kolkata, India. Journal of hazardous materials. 2007 Apr 2;142(1-2):279-87.

31. Keerthi R, Selvaraju N, Alen Varghese L, Anu N. Source apportionment studies for particulates (PM_{10}) in Kozhikode, South Western India using a combined receptor model. Chemistry and Ecology. 2018 Oct 21;34(9):797-817.

32. Chelani AB, Gajghate DG, Devotta S. Source apportionment of PM_{10} in Mumbai, India using CMB model. Bulletin of environmental contamination and toxicology. 2008 Aug;81:190-5.

33. Pipalatkar P, Khaparde VV, Gajghate DG, Bawase MA. Source apportionment of PM2. 5 using a CMB model for a centrally located Indian city. Aerosol and Air Quality Research. 2014 Mar;14(3):1089-99.

34. Li TC, Yuan CS, Huang HC, Lee CL, Wu SP, Tong C. Inter-comparison of seasonal variation, chemical characteristics, and source identification of atmospheric fine particles on both sides of the Taiwan Strait. Scientific reports. 2016 Mar 14;6(1):1-6.

Journal of Air Pollution and Health (Winter 2023); 8(1): 59-76

Original Article

Available online at http://japh.tums.ac.ir

Road traffic-induced particle matter dispersion in a calm wind environment at the main roundabout in Douala, central Africa

Yannick Cedric Ngangmo[1,], Cyrille Mezoue Adiang[1,2], Arti Choudhary[3], David Monkam[1,2]*

[1] Laboratory of Fundamental Physics, Faculty of Science, University of Douala, Douala, Cameroon
[2] National Higher Polytechnic School of Douala, University of Douala, Douala, Cameroon
[3] Centre of Environment Climate Change and Public Health, Utkal University Bhubaneswar Odisha, India

ARTICLE INFORMATION

Article Chronology:
Received 27 December 2022
Revised 28 January 2023
Accepted 28 March 2023
Published 29 March 2023

Keywords:
Particulate matters (PM); Pollution in central Africa; Calm wind; Re-suspension phenomenon

CORRESPONDING AUTHOR:

yannickngangmo91@yahoo.com
Tel: (+237) 694454411
Fax: (+237) 694454411

ABSTRACT

Introduction: Road traffic emissions are among the most significant sources of pollution in Douala, Cameroon's economic town, alongside industrial operations. The morning and the evening are two times of the day when traffic is heavier and the winds are also at their calmest. The majority of the non-exhaust Particulate Matters (PMs) produced by autos is re-suspended road contaminants. The purpose of this research is to estimate fine particle dispersion in conditions of calm winds.

Materials and methods: In one of Douala's roundabouts, the Gaussian Plume model is employed to calculate the PM concentration under calm winds conditions. Different vehicle classes (HDV: Heavy Duty Vehicles, LDV: Light Duty Vehicles, PC: Passenger Cars) are used to figure out the amount of PMs they produce. Measurements of ambient fine particle concentrations are made with the OC-300 laser dust particle detector.

Results: The results made it possible to compare actual measurements of $PM_{2.5}$, PM_{10} (300±150 µg/m^3 and 650±150 µg/m^3, respectively) with simulated values ($PM_{2.5}$, PM_{10}: 310 µg/m^3 and 631 µg/m^3, respectively). The difference between in-situ and computed values can range from 10 to 132 µg/m^3. From 6 to 10 AM, the population's exposure to PM pollution is more severe. It has also been demonstrated that there is a significant association between traffic flow and PM Concentration during the dry season (R^2=0.921). With increased traffic flow intensity, particle concentration levels rise.

Conclusion: The concentration threshold stays above the World Health Organization (WHO) limits regardless of the approach. Furthermore, this paper provides important information about Douala's pollution levels.

Introduction

Particulate Matter (PM) is a complex mixture of solid and liquid particles, including dust, dirt, soot, smoke and liquid droplets [1]. The World Health Organization (WHO) has documented the negative effects of air pollution, particularly in metropolitan areas, on human health, and other researchers have documented the regional and

Please cite this article as: Ngangmo YC, Adiang CM , Choudhary A, Monkam D. Road traffic-induced particle matter dispersion in a calm wind environment at the main roundabout in Douala, central Africa. Journal of Air Pollution and Health. 2023;8(1): 59-76.

Copyright © 2023 Tehran University of Medical Sciences. Published by Tehran University of Medical Sciences.
This work is licensed under a Creative Commons Attribution-NonCommercial 4.0 International license (https://creativecommons.org/licenses/by-nc/4.0/). Noncommercial uses of the work are permitted, provided the original work is properly cited.

worldwide repercussions of poor air quality [2, 3]. This collection of data serves as a guide for policymakers who want to take steps to clean up the environment. The majority of these research looked at background pollution levels, or levels of pollutants measured at locations far from any known sources (industrial or automotive). This background pollution also results from long distance transports from the dispersion of pollutants emitted locally heating, road traffic,... [4–6].

In West African countries, Saharan dust is a major contributor to local background pollution. However, the source is unrelated to local economic activity, and the consequences for air quality and human health have received far less attention [7, 8]. Cities in Sub-Saharan Africa (SSA) and other emerging regions have the highest fine particle concentrations on the planet [9]. The dearth of studies in SSA could be explained mostly by the limited data emanating from the region.

In terms of health effects, several epidemiological studies have found that an increase in bient levels of atmospheric particles is linked to both short-term (acute punctual exposure) and long-term (chronic exposure) effects on morbidity and mortality, particularly fine particles (i.e. $PM_{2.5}$), which can more easily enter the lungs and thus are more likely to increase the incidence of respiratory and cardiovascular disease [10, 11]. These small particles can transport hazardous and carcinogenic substances, such as Polycyclic Aromatic Hydrocarbons (PAHs), metals, and soot carbon, that can overcome the physiological barrier and reach the blood vessels and important organs, even at low quantities [12]. In terms of health effects, several epidemiological studies have found that an increase in ambient levels of atmospheric particles is linked to both short-term (acute punctual exposure) and long-term (chronic exposure) effects on morbidity and mortality, particularly fine particles (i.e. $PM_{2.5}$), which can more easily enter the lungs and thus are more likely to increase the incidence of respiratory and cardiovascular disease [10, 11]. These negative effects of PM on human health are particularly pronounced in urban areas because of the high population density, intense anthropogenic activities, and the proximity of local sources of combustion (e.g. road traffic) [13].

There is an urgent need for the comprehensive studies on this scourge. Till date, several reported research works are focused on identification and categorization of pollutants sources, determination of pollutants concentrations and their mode of dispersion in the air. Therefore, with the aim of assessing the effect of these pollutants on the population, in respect of World Health Organization (WHO) guides values, the steady state Gaussian plume dispersion models are applied with calm wind condition to assess air pollution concentrations in Douala city. The Gaussian plume dispersion model is utilized to come up with a realistic description of dispersion because of its simplicity, ease of usage, and reliability. The model represents an analytical solution to the diffusion equation for concentrations of non-reactive contaminants moving through wind-induced advection [14]. The meteorological circumstances (values of wind speed and direction, temperature, and atmospheric stability) fed into the Gaussian plume as inputs are connected to the emission description within the study area.

Due to higher traffic activity, which occurs generally in morning and evening, and calm meteorology made the surrounding air quality worst. The calm wind condition in association with cool air, limit the dispersion of traffic emission during morning rush hour [15, 16]. Using models, different scenarios can be tested in order to reduce or optimize pollutants emissions. These modeling studies can then provide the base to the scientists, needed to develop effective environmental public policies. For a good modeling of the atmospheric dispersion of PMs, it is important to distinguish the spatio-temporal scales in which the consequences of this phenomenon are manifested. It's especially

about the scale: the global scale (global) with global warming and the destruction of the ozone layer, the regional (continental) scale with hurricanes and cyclones, the local scale (country) with the degradation of the air quality which is the root cause of public health problems [3, 17].

The objective of this study is to compute PM concentration due to road traffic under calm wind conditions. Based on the main source of fine particles (traffic flow), the PM's emission factor estimation was estimated, for all categories of vehicles. Secondly, to estimate the PMs concentration for the calm wind condition of the city of Douala, in the tropics, which occurs frequently in the morning and evening [18]. Further, to calculate the emissions load of PMs by taking into account parameters of influences.

Materials and methods

Study area

Douala, the economic capital of Cameroon is a city recognized for its growth. This city listed among the most popular cities in Central Africa, with several activities carried out within it, one of the main economic activity is road traffic and maritime. Further, the transfer of goods to other countries of the sub-regions (Chad, Central African Republic, and Republic of the Congo) with its innumerable heavy-duty trucks significantly increases the vehicular emission in the local vicinity. Douala is a coastal city located at the bottom of the Gulf of Guinea which shares almost 65 km of coastline with the Atlantic Ocean. It is located 19m altitude at sea level and has geographic coordinates, 4°02'53''N and 9°42'15''E. It has a hot and humid climate base of the active Mount Cameroon volcano at an altitude of 4100 m. Douala city is covers around 210 km^2 and has a population of around 4.0 million in 2020 [19]. The Deido roundabout is one of the most used intersections for road traffic in the city of Douala (Fig. 1), it is the crossroad connecting several districts of the city, indicating high density and emission intensive intersection.

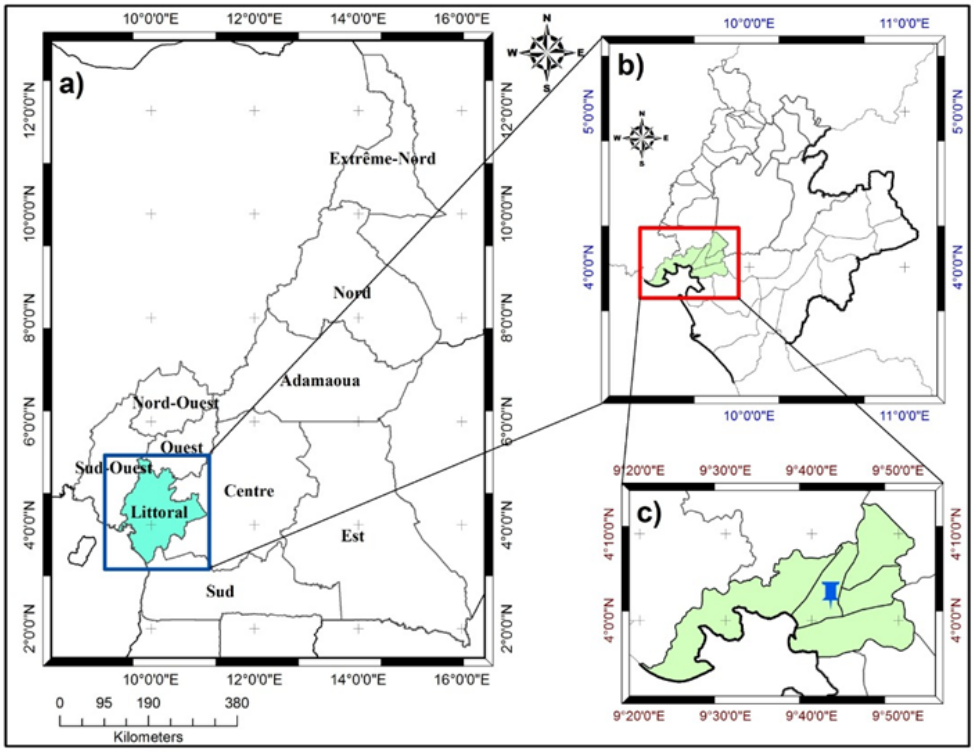

Fig. 1. Map of Cameroon illustrating the Deido roundabout in the city of Douala, Cameroon

Therefore, road traffic at this intersection was considered for estimation of dispersion of fine particles due to road traffic turbulence created by the movement of vehicles in calm wind conditions (wind speed lower than 1 m/s). Real-time air quality monitoring instruments was used in this study, for analysis of air quality in the study area, which is the case more developing countries [20, 21]. PM_{10} and $PM_{2.5}$ ground level concentration (at 1.5 m from the ground) were monitored at the Deido roundabout, a highly circulated square roads in the city (4°3'52''N and 9°42'25''E). In order to estimate the level of pollution during this season, a fixed point of data monitoring at the intersection road was suggested all across the dry season, specifically in March 2021, for two consecutive days. Public and private transport both cars and two wheelers, may directly influence the automatic PM measurements using OC-300. The OC-300 Laser dust particle detector is a direct reading and mobile, aerosol monitoring device, which allows simultaneously measurement of four different sizes fine particles concentrations 10µm, 5 µm, 2.5 µm and 1.0 µm, respectively [22]. These types of instruments are also developed to have low cost devices that can measure air quality data with acceptable accuracy. From this point of view, a hybrid measurement kit for Real-time air quality monitoring was constructed in Dakar, Senegal [21]. Concerning PM detectors, it has been found that the laser scattering is the best technique for the precise detection of PMs [23].

Meteorology and traffic flow

Douala is a city on Cameroon's coast that is about 5 meters above sea level and close to the Atlantic ocean. Weather data for the Douala P30 Airport station (WMO station number 64910, latitude 04° 03'16" N, longitude 09° 43'53" E, altitude 5 m above sea level) were received from the Cameroon Meteorological Department. The temperature ranged from 20 to 40 °C, with an average of 29 °C and an 85% relative humidity. Between 06-10 a.m., the calm wind was seen by roughly 29.70 percent, as shown in Fig. 2a (because adequate data was available for the selected period 2004-2009) [18]. The prevailing wind direction was south-west, most likely due to the Atlantic's closeness. In Douala, the plotted wind rose during the month of May, 2020, showing more than 50% quiet wind. Fig. 2b shows a view of the wind direction and speed in the city.

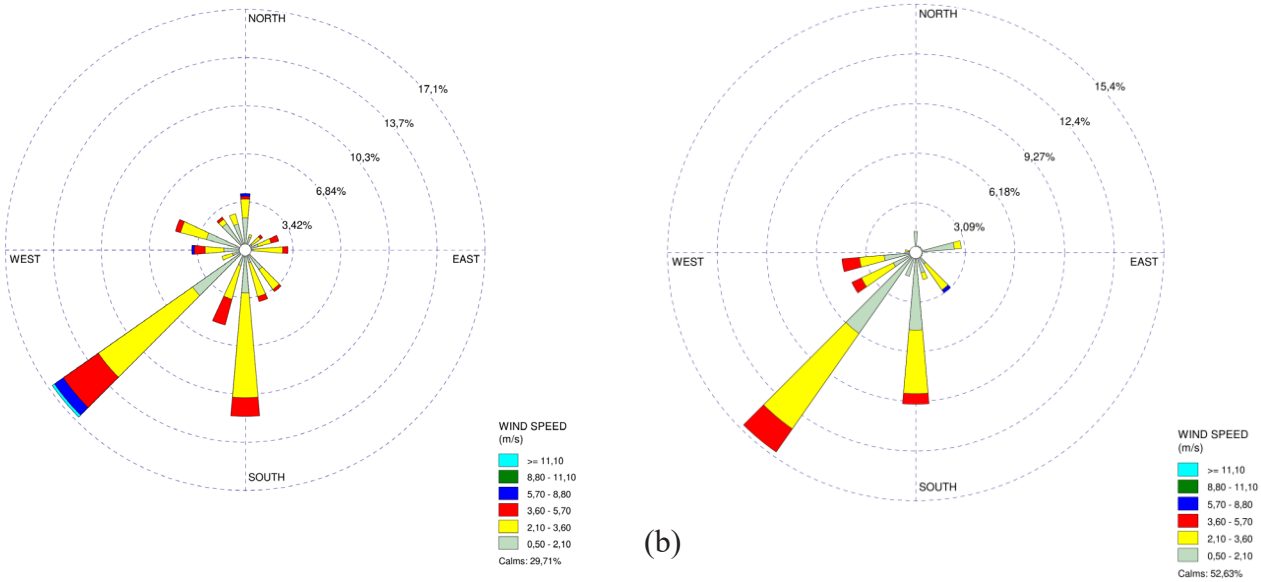

Fig. 2. a) Wind rose at Douala 2004-2009, and b) wind rose at Douala May 2020

The city of Douala's road traffic is diverse, with trucks, tanks, vans, taxis, buses, two- and three-wheel vehicles, and other types of vehicles sharing the road. Vehicles are divided into three categories for our research: Heavy Duty Vehicles (HDV), Light Duty Vehicles (LDV), and Passenger Cars (PC). The volume, form, and weight of vehicles are used to classify them. Vehicles weighing more than 7.5 tons are classified as HDV, 2.5 tons are classified as LDV, and less than 1.4 tons are classified as PC.

The different categories of cars were counted at the Deido roundabout crossroads by taking into account all vehicles crossing the intersection in all directions. The traffic figure is based on a 2008 research of mobility in Douala, which was published in the literature [24]. Fig. 3 shows a diagram of this intersection. The traffic counts were done in both directions for each lane. The traffic count was conducted from 6 to 10 a.m., when the wind is typically calm and traffic density is at its highest.

The traffic flow in Deido roundabout resembling other cities of Douala is heterogeneous in nature, having different type of vehicles present at the same time in the road. Table1 summarizes the traffic flow during four hours: 6-10 AM. Bicycles and other non-engine locomotives are included under "Others". The histogram (Fig. 4) shown that road traffic is dominated by PCs. The higher share of PCs indicating that peak period (6-10 AM) of traffic flow, PCs (taxi, two-wheeled motorcycles) are the main transport mode used by Douala community. The highest traffic count was observed for period of 7-8 AM, which is time of office, school and workers to move for their respective work place (Fig. 5). All vehicle groups taken together, the average daily traffic can be calculated to be roughly 2,422 vehicles. This number falls under the Low-ADT category (Low Average Daily Traffic) [25].

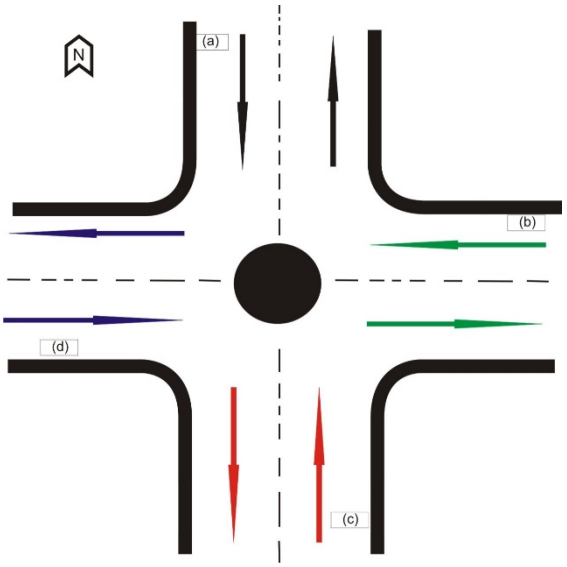

(a) Deido roundabout towards Bessengue / Bessengue towards the Deido

(b) Deido roundabout towards Akwa / Akwa towards Deido roundabout

(c) Deido roundabout towards Bonaberie / Bonaberie to the Deido roundabout

(d) Deido roundabout towards Akwa Nord / Akwa Nord to the Deido roundabout

Fig. 3. Simplified image of the Deido roundabout

Table 1. Summary of the different categories of vehicle counts corresponding to the hours of the day based on CUD data, 2008

	Categories of vehicles			
Time (h)	LDV	PC	HDV	Others
6 - 7 AM	1407	7498	209	80
7- 8 AM	2852	10616	266	90
8 - 9 AM	3034	8611	311	32
9 - 10 AM	2369	7641	358	31

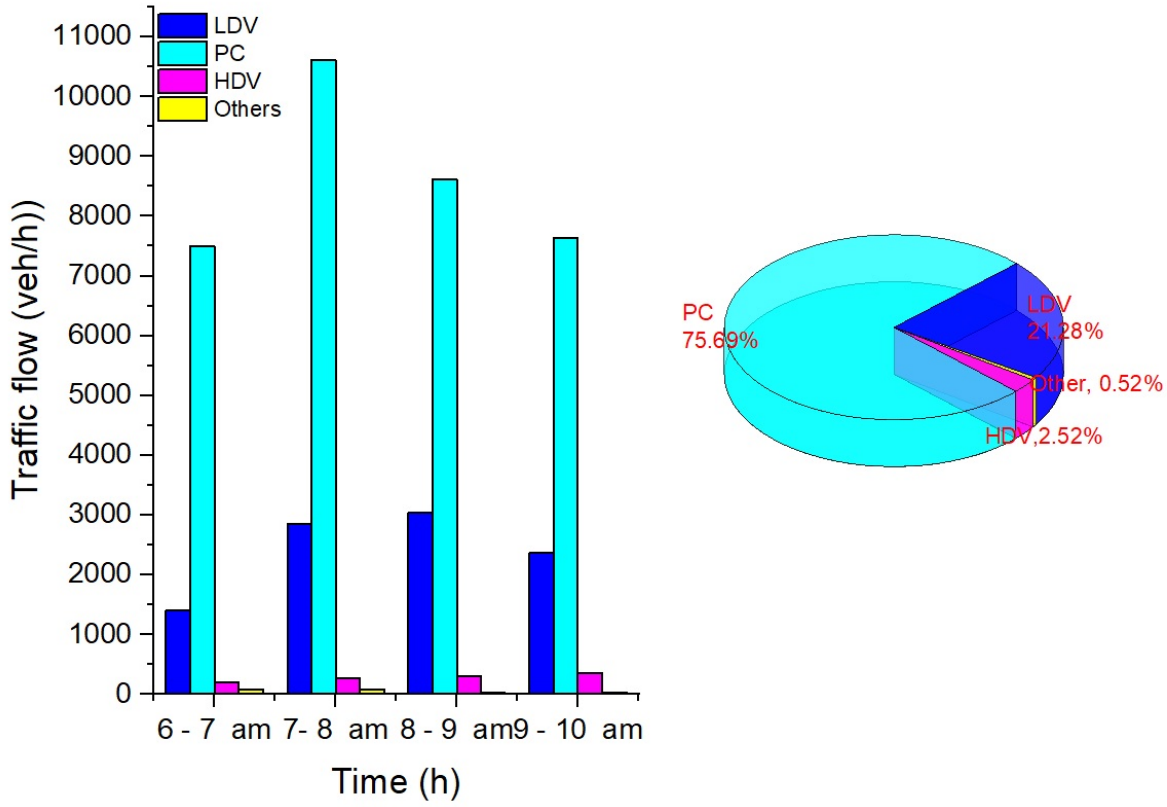

Fig. 4. Traffic flow of the different categories of vehicles at the roundabout Deido between 6-10 AM

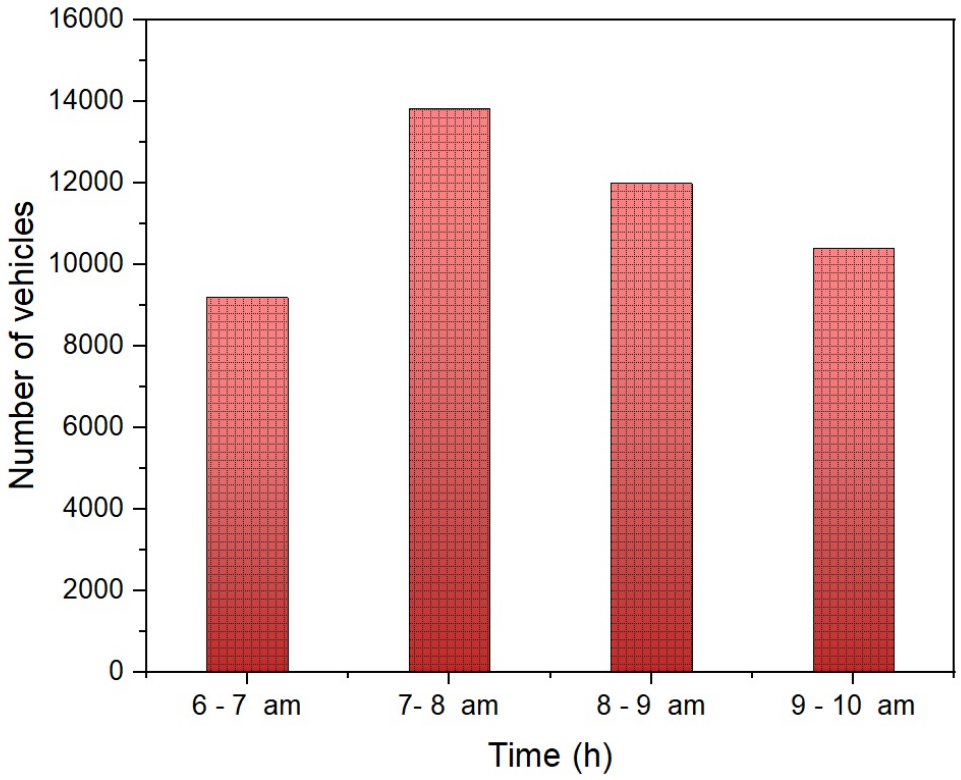

Fig. 5. Vehicle counts at the Deido roundabout between 6–10 AM

Traffic activity and emission

A number of studies, in developed and developing countries, apportioning the sources of air pollution put the transport sector atop, both from direct exhaust and indirect road dust [5, 26–28]. The growing number of vehicles on the road (two and three wheelers, passenger cars, buses, and lorries) increases the amount of pollution produced. Vehicle travels are considered per mode or category in this activity. The histogram in Fig. 5 depicts the activity trends of the various groups of vehicles. A surge of traffic was noted between the hours of 7 and 8 a.m., indicating high road traffic. In general, the higher the traffic density, the more fine particles in suspension, which adversely raises pollution levels [29].

The general methodological principle for calculating emissions is based on the basic Eq. 1.

$$Q = EF \times A \quad (1)$$

Where Q is the emission, generally expressed in mass (g), A is the activity of the transmitters (generally expressed in vehicles.km), EF is the emission factor (g.(veh,km)$^{-1}$). For the estimation of emission factor from the re-suspension of PMs due to road traffic several variables required, vehicle size or category is one of the main parameters that consider in the equation of emission factor (the emission factor is proportional to the category of the vehicle even if it is assumed that the vehicles will have the same travel speed). Several empirical expressions are reported in the literature. For example, researchers of two study applied Eq. 2 and Eq. 3 to estimate emission factor, it consider specific parameters such as vehicle weight and silt loading, respectively.

$$EF_i = k_\alpha (sL)^{0.91} (W_i)^{1.02} \quad (2)$$

$$EF_i = k_\alpha (sL)^{0.91} (W_i)^{1.02} \left(1 - \frac{P}{4N}\right) \quad (3)$$

Eq. 2 and 3 are almost identical, the only difference is that, Eq. 3 accounts the rainfall, greatly influences the emission load.

Where: α represents the different types of particles according to their aerodynamic radius ($PM_{10}, PM_{2.5}\ etc$....).

EF_i represents the emission factor of the particle, k_α represents the default size of the particle α. Generally, the size of particles was $k_{PM_{10}} = 0.62\mu g.(veh.km)^{-1}$ and $k_{PM_{2.5}} = 0.15\ \mu g.(veh.km)^{-1}$ [30], sL: is the silt loading and according to the report by the US EPA (United States Environmental Protection Agency, 2011,Chap.5), this term refers to the mass of sedimentary material of size equal to or less than 75 micrometers of physical diameter per unit area of a route considered. The total amount of the dust on the road surface is made up of different loose materials which can be collected through a sweep and vacuum system. W represents the weight of each vehicle category, P is the number of days during which the precipitation was greater than 0.254 mm over a given period (months, days, hours), N is the number of days in the period considered (year, season, month),$\boldsymbol{i}$ represents vehicle category (HDV,LDV and PC).

Air quality modeling

Air quality modeling is a complex phenomenon which involves studying any parameters that can influence the dispersion of fine particles (wind speed, precipitation, and the temperature inversion phenomenon). In this study a Gaussian model adapted for the calm wind conditions. Several studies have already been carried out as part of the dispersion of particles in low wind conditions [31, 32]. Assuming that the average wind speed is less than a certain threshold (0.1 m/s), the horizontal spread of the plume covers 360°; thus proposed empirical Eq. 4. It takes into account the contribution of the vertical and horizontal component of the plume of the linear source [33].

$$C_{lw}(x,y,z) = \sqrt{\frac{2}{\pi}}\frac{Q\times F(z)\times\theta_s}{2\pi u\sigma_z} \quad (4)$$

Where: $F(z) = \exp\left(-\frac{(h_s - z)}{2\sigma_z^2}\right) + \exp\left(-\frac{(h_s + z)}{2\sigma_z^2}\right)$]and $\theta_s = \tan^{-1}\left(\frac{y_2 - y_1}{x}\right) + \tan^{-1}\left(\frac{y - y_1}{x}\right)$.

Where C_{lw} (x,y,z) is the concentration of pollutants at the location of the receptor (x, y, z) in µg/m^3, x is the distance from the source along the wind direction in m, y and z are the wind distances along of the transversal with respect to the midline of the plume in m, Q is the amount of emission of fine particles in (g or μg), θ_s is the angle which connects the linear source from the receiver in degree, u is the wind speed in m/s, σ_z is the standard deviation representing the dispersion of pollutants in the wind direction in urban area. The present study considers only the standard deviations that belong to the interval corresponding to calm winds (class A or A-B), it is calculated here with the setting of Briggs with the mathematical expression [34]:

$$\sigma_z(z) = \alpha x(1+\beta x)^{\gamma} = 0.24x\sqrt{1+0.001x} \quad (5)$$

Where α, β and γare constants which depend on the Pasquill stability class.

Results and discussion

Emission factor

Using Eq. 3, which is an adapted equation proposed by someresearchers used to estimate the emission factors of particles as a function of the different vehicle categories and also according to the season in our case study. The $PM_{2.5}$ and PM_{10} emission factors for each vehicle type are calculated using Eq. 3 and reported in Table 2. The analysis shows that the emission factor is proportional to the vehicle's weight, hence the emission factor is higher when the particle size is larger.

Table 2. The emission factors by vehicle category and by particle size µg/veh.km

Vehicle categories	PM_{10}	$PM_{2.5}$
PC	0.038	0.009
LDV	0.046	0.015
HDV	0.19	0.049

Table 3. Emission load of PM_{10} and $PM_{2.5}$ as a function of the particle size (μg)

Vehicle categories	PM_{10}	$PM_{2.5}$
PC	1305.56	309.21
LDV	618.36	144.93
HDV	217.36	56.05

Estimation of fine particulate matters emission load

By combining the Eqs. 1 and 3, Eq. 6 was obtained.

$$Q_i = A_i \times k_\alpha \left(sL\right)^{0.91} \left(W_i\right)^{1.02} \left(1 - \frac{P}{4N}\right) \quad (6)$$

Where, i represent the different categories of vehicles. More explicitly according to the vehicle category emission load was estimated by applying Eqs. 7, 8 and 9.

$$Q_{HDV} = A_{HDV} \times k_\alpha \left(sL\right)^{0.91} \left(W_{HDV}\right)^{1.02} \left(1 - \frac{P}{4N}\right) \quad (7)$$

$$Q_{LDV} = A_{LDV} \times k_\alpha \left(sL\right)^{0.91} \left(W_{LDV}\right)^{1.02} \left(1 - \frac{P}{4N}\right) \quad (8)$$

$$Q_{PC} = A_{PC} \times k_\alpha \left(sL\right)^{0.91} \left(W_{PC}\right)^{1.02} \left(1 - \frac{P}{4N}\right) \quad (9)$$

The parameter α, depend on the size of the particle that is considered (PM_{10} or $PM_{2.5}$).

For the purposes of this study, a period of 6 months, or 181 days, will be taken into account, which corresponds to the dry season from January 2008 to June 2008. This is based on information provided by the Douala P30 Airport station (WMO station number 64910, latitude 04° 03'16" N, longitude 09° 43'53" E, altitude 5m above sea level). We notice that during the period of the six months, there are approximately 32 days with precipitation totaling more than 0.254 mm: P=32 days and N=181 days. One of the key variables used to compute dust re-suspension is the silt load (sL). The default setting for the parameter sL corresponds to a daily traffic density of roughly 0.40 g/m^2 . From Eqs. 8, 9, 10 emission load was estimated for $PM_{2.5}$ and PM_{10}, reported in the Table 3.

As shown in Table 3, the emission load is directly proportional to the vehicle activity. Because the activity of HDV is very low compared to PC, the emission load is inversely related to the vehicle weight. As a result, the emission load falls even though the overall emission is proportionate to the vehicle category (Fig. 4). HDV traffic is lower between 6 and 10 a.m. (morning hours), whereas PC (taxis, motorbikes with two wheels) traffic is highest between 6 and 10 a.m., because it is the most convenient mode of transportation in Douala. This justifies the fact that PC has a much higher emission load than other categories. Other categories such as: LDV (large bus, minibus); HDV (two-axle trucks, trucks with more than two axles, semi-trailer) are less in count during this period, which justifies the various results in Table 3. Fig. 6 shows the particle emission load of PM_{10} and $PM_{2.5}$ depending on the vehicular activity in study area.

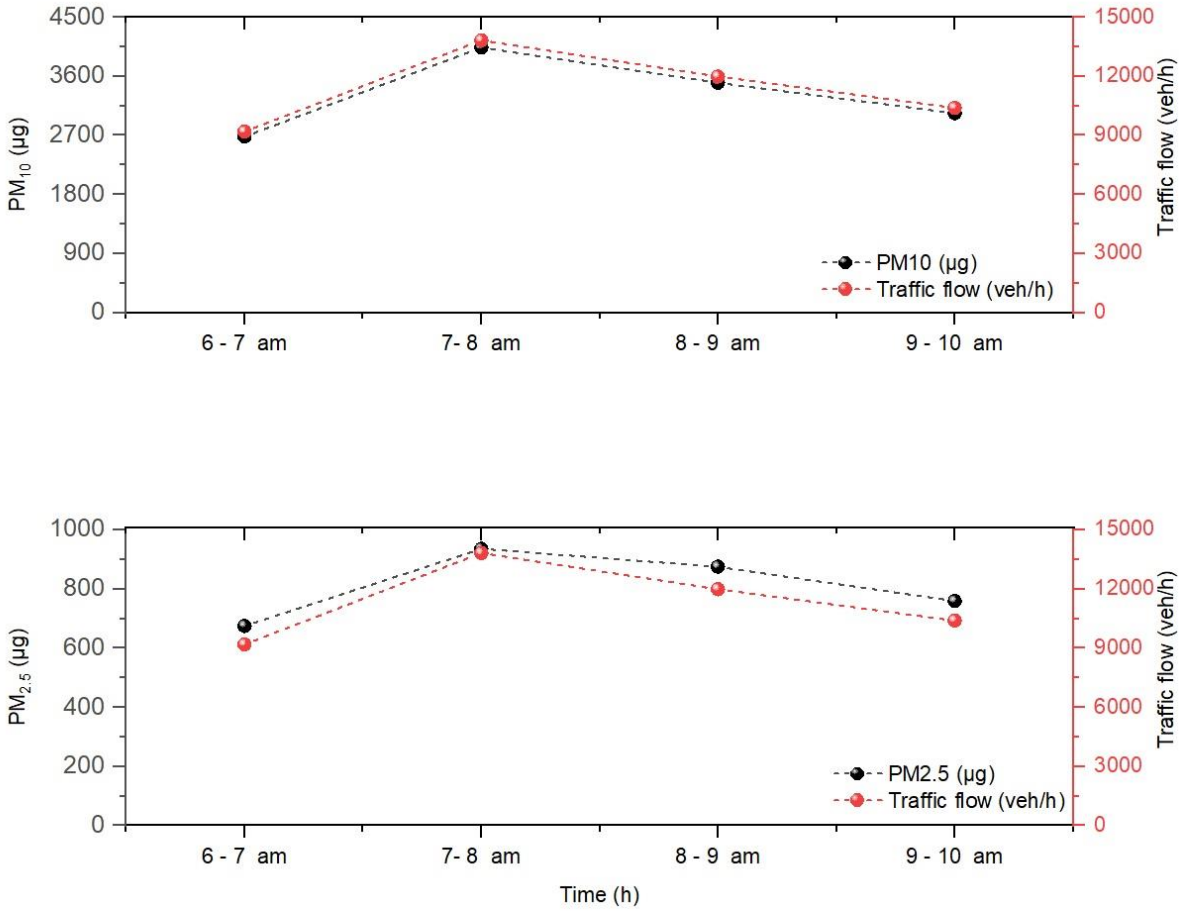

Fig. 6. Traffic flow and emission load of $PM_{2.5}$ and PM_{10} at the Deido roundabout during 6–10 AM

Computation of fine particulate matter concentration

The PM concentration was estimated in the study using the Gaussian plume model under calm wind conditions (Eq. 5) and considered traffic flow as the principal source contributing to the emission burden. Fig. 7 shows the $PM_{2.5}$ concentration trend from 6 to 10 a.m. under a calm wind situation. High $PM_{2.5}$ concentrations are displayed in orange coloration in Fig. 7 (a-d), with a threshold of 257.20 $\mu g/m^3$. It was observed that a minor dispersion of $PM_{2.5}$ exceeding the radius of the roadway set at 10 m.

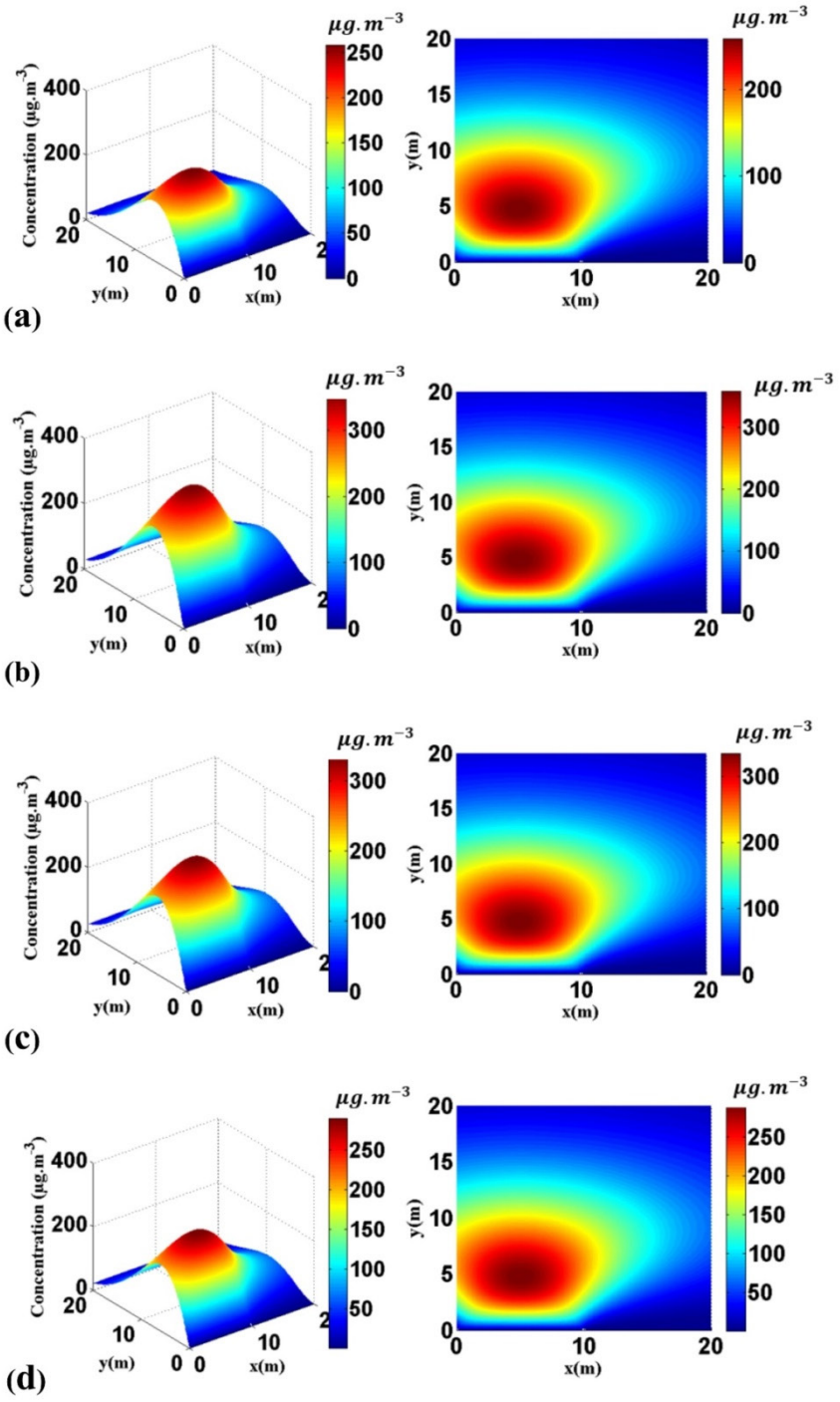

Fig. 7. Dispersion of $PM_{2.5}$ between 6-10 AM (a-d) at the Deido roundabout

During 7-8 AM $PM_{2.5}$ threshold was found around 358.10 $\mu g/m^3$ (Fig. 7b). The sharp increase in concentration during this period is due to the increase in vehicle activity, more specifically passenger's cars (taxi, motorbikes two or three wheels), which is the most commonly used mode of travel at this time. During 8-9 AM $PM_{2.5}$ threshold was found 332.60 $\mu g/m^3$ (Fig. 7c). It is observed that a considerable decrease in concentration at this time is due to decrease in vehicular activity, especially among PCs, because at this time most of the users reached to their respective work place. The pollution threshold during 9-10 AM is estimated 290.10 $\mu g/m^3$ (Fig. 7d). Alike to $PM_{2.5}$, PM_{10} depicting similar dispersion trend in calm wind condition during 6-10 AM at roundabout, the only difference in magnitude is observed (Fig. 8 a-d). Such as during 6-7 AM, 7-8 AM,8-9 AM and 9-10 AM PM_{10} emission threshold value was 513.00 $\mu g/m^3$, 771.50 $\mu g/m^3$, 668.90 $\mu g/m^3$, and 572.30 $\mu g/m^3$, respectively (Fig. 8a, b, c and d, respectively).

As a summary on the modeling of PMs at the Deido roundabout the average concentrations of the PMs (PM_{10}, $PM_{2.5}$) was around CM_PM_{10} 631.42 $\mu g/m^3$ and $CM\_PM_{2.5}$ 310.00 $\mu g/m^3$, respectively which is much higher from the values set by the World Health Organization (WHO) which are 60 $\mu g/m^3$ for PM_{10} and 20 $\mu g/m^3$ for $PM_{2.5}$.

Table 4. Summary of traffic flow, PM concentrations (PM_{10}, $PM_{2.5}$) during 6-10 AM

Time (h)	Traffic flow (veh/h)	Concentration ($\mu g/m^3$)	
		PM_{10}	$PM_{2.5}$
6-7 AM	9.185	513.00	257.20
7-8 AM	13.811	771.50	358.10
8-9 AM	11.988	668.90	332.60
9-10 AM	10.399	527.30	290.10

It can be concluded from the Table 4, summarizes the results of study that concentration of fine particles increases with the traffic flow. The concentration levels of PMs are higher with higher traffic activity (Fig. 9). The highest PM concentrations is observed between 7-9 AM, similar findings are reported by other researchers. The exposure of the population to air pollution on the roads is more intense during 6-10 AM, since the level of particles concentration is higher for highest traffic flow as compared to the lower traffic flow condition.

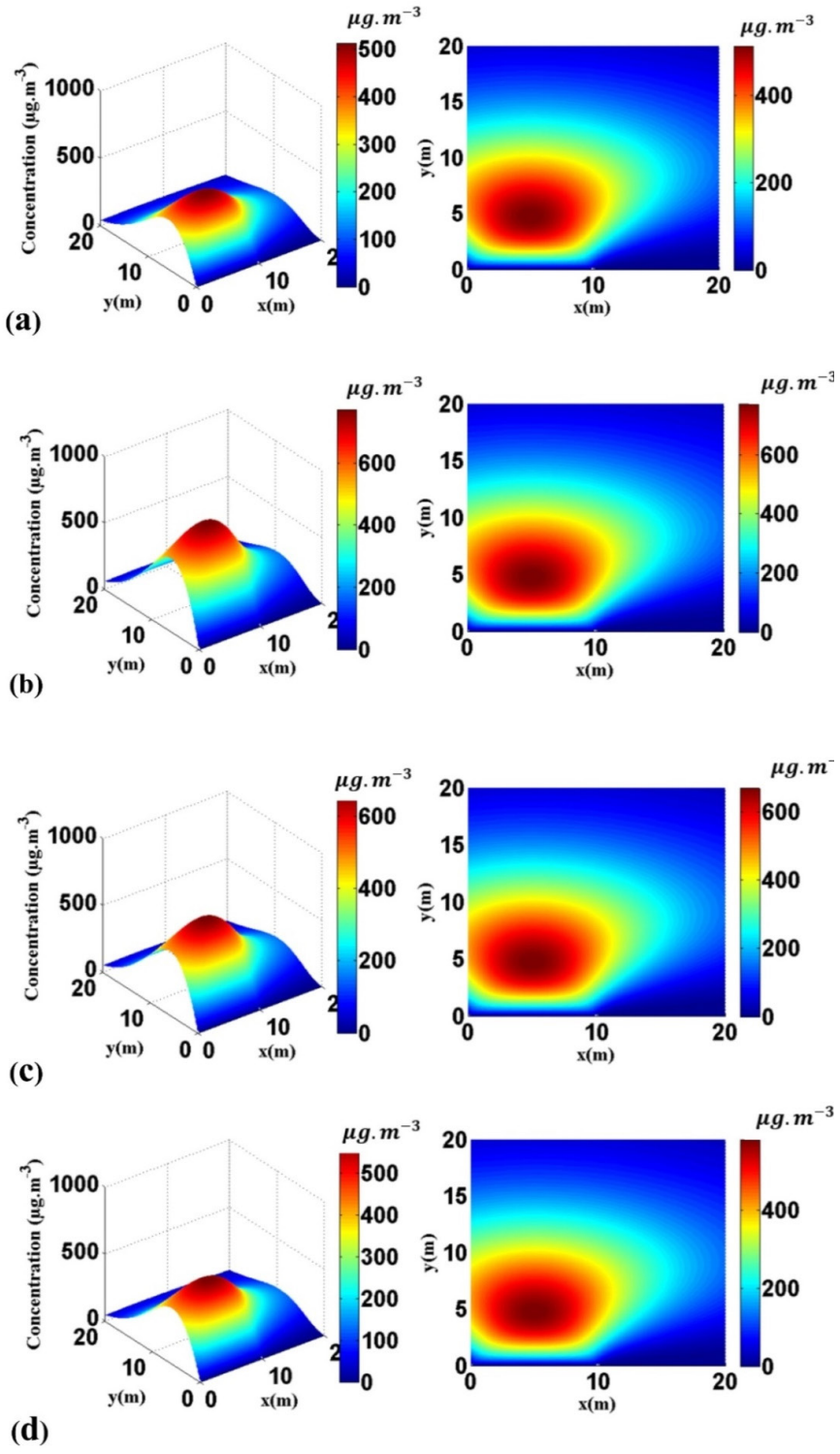

Fig. 8. Dispersion of PM_{10} during 6–10 AM (a-d) at the Deido roundabout

Evolution and prediction

It is well known that most of the developing countries having the higher traffic flow rate and consequently higher traffic activity, roadway transportation is the 24 h mobile and most dynamic sector, particularly in large cities. Furthermore, the quantity of vehicles (passenger cars, light commercial vehicles, heavy goods vehicles) increases by 10% each year [18]. By considering the fact of 10% annual growth of all categories of vehicles, the present study extrapolated the data of average concentrations, which is used to estimate the possible thresholds pollution up to 2021 (Fig. 10).

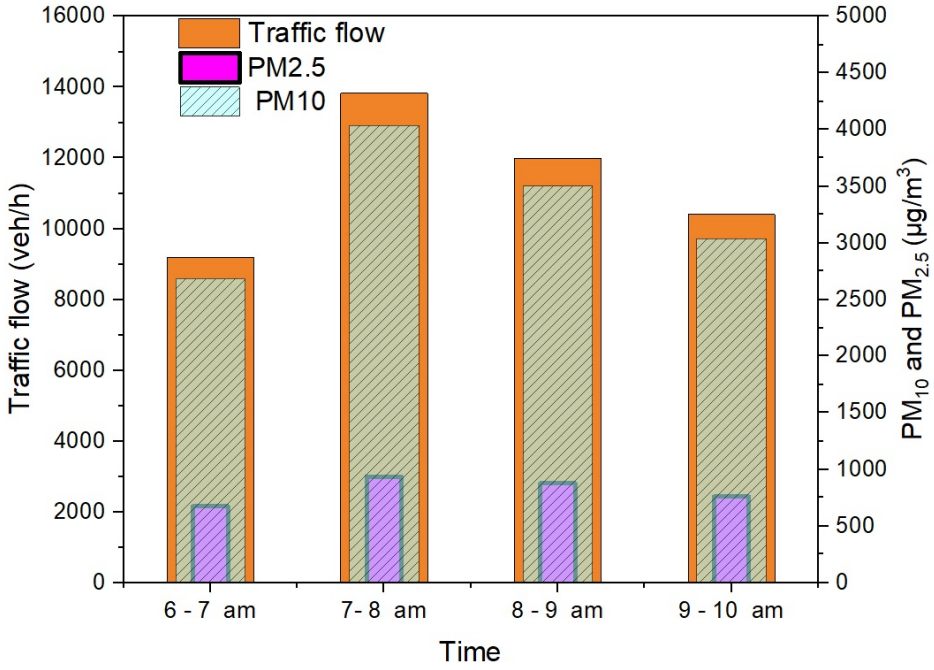

Fig. 9. Hourly variations of $PM_{2.5}$ and PM_{10} concentrations according to Traffic flow

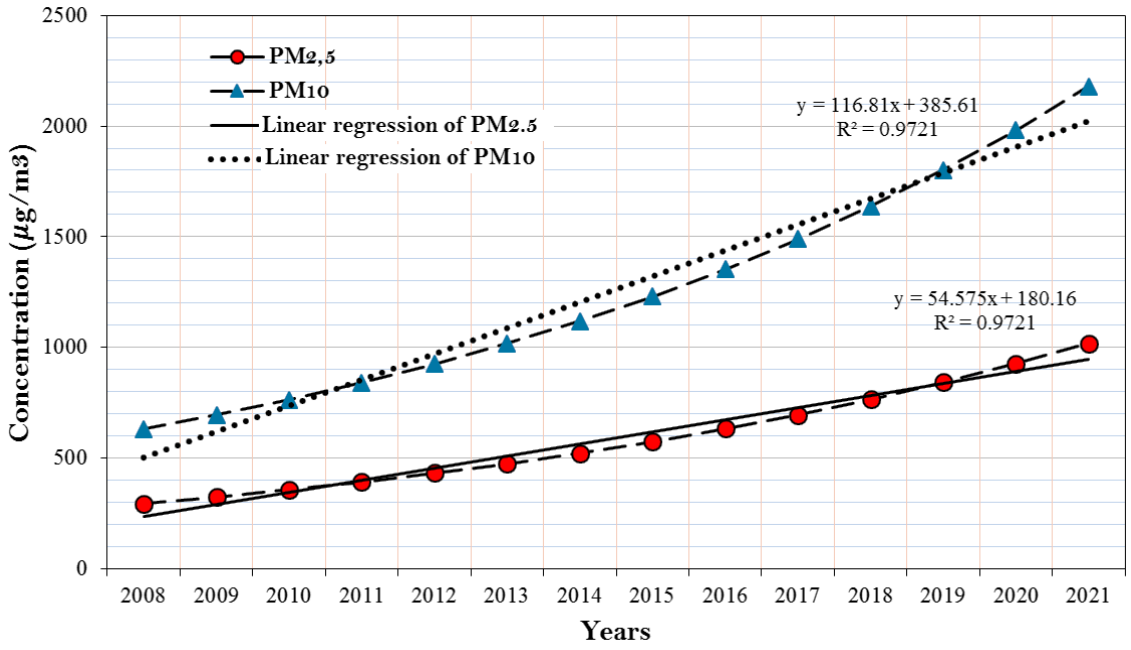

Fig. 10. Evaluation and prediction of PMs based on an annual increase of 10% in the number of vehicles

Discussion

In practically every country on the planet, road transportation contributes significantly to rising levels of air pollution. This study modelled the dispersion of PMs from the re-suspension of particles from vehicle movement or the re-suspension of PMs previously deposited on the roadway and re-suspension by vehicle movement in calm wind conditions to understand the current time contribution of PMs in Douala, Central Africa. Further, proposed equation used to estimate the amount of specific emission to each category of vehicles (HDV, LDV, and PC) and by particles size (PM_{10} and $PM_{2.5}$) with the known input of the traffic flow. The present study only account emission load by re-suspension, and assumes that presence of background pollution, and modeling the dispersion of PMs concentration during calm wind conditions. Thus, results will be suggestive about the risks in-linked to PM exposure, to the society. Using Dust track real time analyzer, the daily average concentration of PM_{10} and $PM_{2.5}$ is obtained 391.81 $\mu g/m^3$ and 183 $\mu g/m^3$ in dry season, respectively [35].

This study performed a numerical simulation in calm wind conditions using traffic data of year 2008. It is found that simulated concentrations are twice of the measured value. The measurement PMs concentration using the OC 300 Laser dust particle detector in 2021 during 6-10 AM for calm wind condition, was found around 650±150 µg/m^3 and 300±150 µg/m^3 for PM_{10}, $PM_{2.5}$ respectively (Table 5). The prediction for the city of Douala up to 2021 is based on 2008 traffic flow statistics, with a 10% annual increase in vehicle fleet. The expected results are higher than those obtained during the measuring campaign, according to the study (Fig. 10). The study also emphasizes the significance of weather variables on PM dispersion. It is obvious that when a strong wind blows, particles disperse over a vast area, lowering the pollutant concentration threshold in the area under consideration. In contrast, in calm wind conditions, particles disperse less and are very dense on a small area, magnifying the concentration of fine particulate pollutants, while higher traffic flow periods amplify the concentration of fine particulate pollutants. The conclusion drawn from the results is consistent with study in Libya, which shows that emissions, especially those produced at low and moderate wind speeds, cause a dispersion with high concentration levels in the vicinity of the emission source [36]. The findings also demonstrate that the confidence interval widens as air pollution concentration increases; the observation error significantly affects the confidence interval [37].

Table 5. The average concentrations of measured and simulated PMs at the Deido roundabout in dry weather conditions

Average concentration	Daily measurement 2018	Calm wind period measurement 2021	simulated	Relative error
CM_PM_{10}	391.81 µg/m^3	650 ± 150µg/m^3	631.42 µg/m^3	2.94 %
CM_$PM_{2.5}$	183.43 µg/m^3	300 ± 150µg/m^3	310.0 µg/m^3	3.23%

Conclusion

In metropolitan areas, particles re-suspended by autos account for half of the pollution limitations. The study's average concentrations were discovered to be higher above the WHO's threshold limits. The increased pollutant concentrations calculated by numerical simulation are also due to the calm wind conditions, as particles scatter less in a calm wind, resulting in higher pollutant concentrations. The particles matters seen in an isotropic medium with no preferential dispersion direction plainly justify a higher particle concentration in one region (demonstrated with strong orange color). This research shows how wind speeds affect fine particle dispersion in the atmosphere. Particles matters, molecules, and other chemicals are transported more easily by the wind, which might change pollutant concentration thresholds.

Financial supports

No funding was obtained for this study

Competing interests

The authors declared no conflicts of interest with respect to concerning the authorship and/or publication of this article.

Acknowledgements

The authors would like to acknowledge to Douala Council for providing the necessary data on traffic. However, Yannick Cedric Ngangmo would like to acknowledge Dr. Mezoue Adiang Cyrille to provide a device (OC-300 Laser dust particle detector) to collect data concentration in this work.

Ethical considerations

Ethical issues (Including plagiarism, Informed Consent, misconduct, data fabrication and/or falsification, double publication and/or submission, redundancy, etc) have been completely observed by the authors.

References

1. Koelemeijer RB, Homan CD, Matthijsen J. Comparison of spatial and temporal variations of aerosol optical thickness and particulate matter over Europe. Atmospheric Environment. 2006 Sep 1;40(27):5304-15.

2. Andersen ZJ, Kristiansen LC, Andersen KK, Olsen TS, Hvidberg M, Jensen SS, Ketzel M, Loft S, Sørensen M, Tjønneland A, Overvad K. Stroke and long-term exposure to outdoor air pollution from nitrogen dioxide: a cohort study. Stroke. 2012 Feb;43(2):320-5. Available from: https://www.ahajournals.org/doi/abs/10.1161/STROKEAHA.111.629246

3. Snow SJ, Cheng W, Wolberg AS, Carraway MS. Air Pollution Upregulates Endothelial Cell Procoagulant Activity via Ultrafine Particle-Induced Oxidant Signaling and Tissue Factor Expression. Toxicol Sci [Internet]. 2014 Jul 1 [cited 2021 Nov 15];140(1):83–93. Available from: https://academic.oup.com/toxsci/article/140/1/83/1675677

4. Ratsombath PN, Morel G, Martell-Flores H, Berton M. Modélisation de la pollution particulaire liée au trafic routier à l'échelle de la rue et étude des leviers d'atténuation. Cybergeo: European Journal of Geography. 2017 Jan 6. Available from: http://journals.openedition.org/cybergeo/27882

5. Choudhary A, Gokhale S. On-road measurements and modelling of vehicular emissions during traffic interruption and congestion events in an urban traffic corridor. Atmospheric Pollution Research. 2019 Mar 1;10(2):480-92.

6. Choudhary A, Gokhale S. Evaluation of emission reduction benefits of traffic flow management and technology upgrade in a congested urban traffic corridor. Clean Technologies and Environmental Policy. 2019

Mar 15;21:257-73.

7. Heft-Neal S, Burney J, Bendavid E, Voss KK, Burke M. Dust pollution from the Sahara and African infant mortality. Nature Sustainability. 2020 Oct;3(10):863-71. Available from: https://www.nature.com/articles/s41893-020-0562-1

8. De Longueville F, Hountondji YC, Ozer P, Marticorena B, Chatenet B, Henry S. Saharan dust impacts on air quality: what are the potential health risks in West Africa?. Human and Ecological Risk Assessment: An International Journal. 2013 Nov 2;19(6):1595-617.

9. Amegah AK, Agyei-Mensah S. Urban air pollution in Sub-Saharan Africa: Time for action. Environmental Pollution. 2017 Jan 1;220:738-43.

10. Bell ML, Davis DL, Fletcher T. A retrospective assessment of mortality from the London smog episode of 1952: the role of influenza and pollution. Environmental health perspectives. 2004 Jan;112(1):6-8.

11. Sahu SK, Sharma S, Zhang H, Chejarla V, Guo H, Hu J, Ying Q, Xing J, Kota SH. Estimating ground level $PM_{2.5}$ concentrations and associated health risk in India using satellite based AOD and WRF predicted meteorological parameters. Chemosphere. 2020 Sep 1;255:126969.

12. Yim SH, Barrett SR. Public health impacts of combustion emissions in the United Kingdom. Environmental science & technology. 2012 Apr 17;46(8):4291-6. Available from: https://pubs.acs.org/doi/full/10.1021/es2040416

13. Mbiaké R, Mfoumou E, Wakata AB, Ndjeuna E, Djamen JK, Leduc R, Bobda C. Atmospheric dispersion modeling of the emissions from the logbaba thermal power plant, Douala-Cameroon. Open Journal of Air Pollution. 2017 Nov 9;6(4):117-34. Available from: http://www.scirp.org/journal/PaperInformation.aspx?PaperID=80227

14. Lotrecchiano N, Sofia D, Giuliano A, Barletta D, Poletto M. Pollution dispersion from a fire using a Gaussian plume model. International Journal of Safety and Security Engineering. 2020;10(4):431-9.

15. Kinney PL. Climate change, air quality, and human health. American journal of preventive medicine. 2008 Nov 1;35(5):459-67.

16. Cuesta-Mosquera AP, Wahl M, Acosta-López JG, García-Reynoso JA, Aristizábal-Zuluaga BH. Mixing layer height and slope wind oscillation: Factors that control ambient air SO2 in a tropical mountain city. Sustainable cities and society. 2020 Jan 1;52:101852.

17. Salam A, Hossain T, Siddique MN, Alam AS. Characteristics of atmospheric trace gases, particulate matter, and heavy metal pollution in Dhaka, Bangladesh. Air Quality, Atmosphere & Health. 2008 Oct;1:101-9. Available from: https://link.springer.com/article/10.1007/s11869-008-0017-8

18. Adiang CM, Monkam D, Njeugna E, Gokhale S. Projecting impacts of two-wheelers on urban air quality of Douala, Cameroon. Transportation Research Part D: Transport and Environment. 2017 May 1;52:49-63.

19. CUD. CUD | Ma Ville [Internet]. [cited 2023 Jan 23]. Available from: https://douala.cm/maville/region

20. Liousse C, Galy-Lacaux C, Ndiaye SA, Diop B, Ouafo M, Assamoi EM, Gardrat E, Castera P, Rosset R, Akpo A, Sigha L. Real time black carbon measurements in West and Central Africa urban sites. Atmospheric Environment. 2012 Jul 1;54:529-37.

21. Ngom B, Seye MR, Diallo M, Gueye B, Drame MS. A hybrid measurement kit for real-time air quality monitoring across senegal cities. In2018 1st International Conference on Smart Cities and Communities (SCCIC) 2018 Jul 24 (pp. 1-6). IEEE.

22. Oceanus. Handheld Laser particle counter

with optical sensor [Internet]. 2016 [cited 2021 Nov 27]. Available from: https://www.ocgasdetector.com/en/product/Handheld-Laser-particle-counter-with-optical-sensor.html

23. Carminati M, Sampietro M, Carminati G. Analysis of instrumentation performance for distributed real-time air quality monitoring. In2011 IEEE Workshop on Environmental Energy and Structural Monitoring Systems 2011 Sep 28 (pp. 1-6). IEEE.

24. Douala Urban Council. Douala infrastructure project : elaboration of a transport and mobility plan in Douala city. Douala; 2008.

25. Etyemezian V, Kuhns H, Gillies J, Chow J, Hendrickson K, McGown M, Pitchford M. Vehicle-based road dust emission measurement (III):: effect of speed, traffic volume, location, and season on PM_{10} road dust emissions in the Treasure Valley, ID. Atmospheric Environment. 2003 Oct 1;37(32):4583-93.

26. Guttikunda S. Four Simple Equations for Vehicular Emissions Inventory. SIM-air Working Paper Series. 2008 Jul;2.

27. Adiang CM, Monkam D, Lenouo A, Njeugna E, Gokhale S. Evaluating impacts of two-wheeler emissions on roadside air quality in the vicinity of a busy traffic intersection in Douala, Cameroon. Air Quality, Atmosphere & Health. 2017 May;10:521-32.

28. Choudhary A, Gokhale S. Urban real-world driving traffic emissions during interruption and congestion. Transportation Research Part D: Transport and Environment. 2016 Mar 1;43:59-70.

29. Houngbégnon P, Ayivi-Vinz G, Lawin H, Houessionon K, Tanimomon F, Kêdoté M, Fayomi B, Dossou-Gbété S, Agueh V. Exposure to $PM_{2.5}$ related to road traffic: comparison between crossroads and outside of crossroads at Cotonou, Benin.

30. Gulia S, Nagendra SS, Khare M, Khanna I. Urban air quality management-A review. Atmospheric Pollution Research. 2015 Mar 1;6(2):286-304.

31. C Cimorelli AJ, Perry SG, Venkatram A, Weil JC, Paine RJ, Wilson RB, Lee RF, Peters WD, Brode RW. AERMOD: A dispersion model for industrial source applications. Part I: General model formulation and boundary layer characterization. Journal of Applied Meteorology and Climatology. 2005 May 1;44(5):682-93. Available from: https://journals.ametsoc.org/view/journals/apme/44/5/jam2227.1.xml

32. Carruthers DJ, Holroyd RJ, Hunt JC, Weng WS, Robins AG, Apsley DD, Thompson DJ, Smith FB. UK-ADMS: A new approach to modelling dispersion in the earth's atmospheric boundary layer. Journal of wind engineering and industrial aerodynamics. 1994 May 1;52:139-53.

33. Venkatram A, Snyder MG, Heist DK, Perry SG, Petersen WB, Isakov V. Re-formulation of plume spread for near-surface dispersion. Atmospheric environment. 2013 Oct 1;77:846-55.

34. Briant R, Korsakissok I, Seigneur C. An improved line source model for air pollutant dispersion from roadway traffic. Atmospheric Environment. 2011 Aug 1;45(24):4099-107.

35. Ngam'nye Fotso L, Mbiaké R. Challenges of assessing, air pollution data in a developing region: case of cameroon, Douala. University of Douala; 2018.

36. Haddar M, Djemel H, Kallel A, Baccar M. Preliminary Assessment of Volatile Organic Compounds (Vocs) and Hazardous Gases Dispersion at Low Winds: Case of Mellitah Gas Complex, Libya.

37. Cao B, Cui W, Chen C, Chen Y. Development and uncertainty analysis of radionuclide atmospheric dispersion modeling codes based on Gaussian plume model. Energy. 2020 Mar 1;194:116925.

Journal of Air Pollution and Health (Winter 2023); 8(1): 77-86

Original Article

Available online at http://japh.tums.ac.ir

Evaluation of oxidative stress biomarkers and liver enzyme activity in workers occupationally exposed to respirable free crystalline silica

Ali Poormohammadi[1], Elaheh Talebi Ghane[2], Effat Sadat Mir Moeini[1], Saeed Bashirian[3], Seyedmousa Motavallihaghi[4], Fereshteh Mehri[5,]*

[1] Center of Excellence for Occupational Health, Research Center for Health Sciences, School of Public Health, Hamadan University of Medical Sciences, Hamadan, Iran
[2] Modeling of Noncommunicable Diseases Research Center, Hamadan University of Medical Sciences, Hamadan, Iran
[3] Research Center for Health Sciences, School of Public Health, Hamadan University of Medical Sciences, Hamadan, Iran
[4] Department of Medical Parasitology and Mycology, Faculty of Medicine, Hamadan University of Medical Sciences, Hamadan, Iran
[5] Nutrition Health Research Center, Center of Excellence for Occupational Health, Hamadan University of Medical Sciences, Hamadan, Iran

ARTICLE INFORMATION

Article Chronology:
Received 18 October 2022
Revised 05 February 2023
Accepted 03 March 2023
Published 29 March 2023

Keywords:
Crystalline silica; Oxidative stress; Serum; Liver

CORRESPONDING AUTHOR:

freshteh_mehri@yahoo.com
Tel: (+98 81) 38380016
Fax: (+98 81) 38380016

ABSTRACT

Introduction: In various mining activities, workers are exposed to free Crystalline Silica (CS), which can cause the constant production of reactive oxygen species and silicosis. This research was conducted to evaluate oxidative stress biomarkers and liver tissue function in workers occupationally exposed to CS during their activities.

Materials and methods: In this study, the biomarkers of oxidative stress were evaluated in 40 workers in silica mines of Azandarian region (Hamadan province, Iran) with occupational exposure to CS, as the case group and 40 workers without any silica-exposure as controls.

Results: A significant higher serum levels of Malondialdehyde (MDA), Reactive Oxygen Species (ROS) and Alanine Transaminase (ALT) were observed in the silica-exposed group compared to the controls. Moreover, in the serum of the silica-exposed cases, the total antioxidant capacity was lower than that of the control group. Based on findings chronic exposure to CS can obviously affect the serum levels of oxidative stress biomarker and liver tissue function in the exposed workers.

Conclusion: Therefore, the use of suitable face mask and different dietary antioxidants are recommended in the silica-exposed workers for the reduction of oxidative stress production and prevention of liver tissue disorders.

Introduction

Repairable Crystalline Silica (RCS) as a common mineral found in the earth's crust can be considered an environmental and occupational pollutant. RCS exposure may occur in industrial and non-industrial sources [1]. From non-industrial sources exposures can point to mining and grinding of sandstone, ceramic, silica grinding, granite and quartz crushing that have many effects the human health [2]. The non-industrial source exposures are naturally occurred in the environment such as sandstorms in deserts, which are harmful to health

Please cite this article as: Poormohammadi A, Talebi Ghane E, Mir Moeini ES, Bashirian S, Motavallihaghi S, Mehri F. Evaluation of oxidative stress biomarkers and liver enzyme activity in workers occupationally exposed to respirable free crystalline silica. Journal of Air Pollution and Health. 2023;8(1): 77-86.

Copyright © 2023 Tehran University of Medical Sciences. Published by Tehran University of Medical Sciences.
This work is licensed under a Creative Commons Attribution-NonCommercial 4.0 International license (https://creativecommons.org/licenses/by-nc/4.0/). Noncommercial uses of the work are permitted, provided the original work is properly cited.

[3]. In developing countries, there are active silica crushing units that cause chronic exposure to RCS in the workplaces [4]. Although many efforts accomplished to control the exposure of workers to RCS, millions of workers in various industries are occupationally exposed to RCS at their workplaces [5].

It has been reported that occupational exposure to RCS is associated with a wide range of disorders such as pulmonary obstructive, silicosis, pulmonary fibrosis, chronic bronchitis, kidney diseases and Systemic Autoimmune Rheumatic Disease (SARD) [6]. The International Agency for Research on Cancer (IARC) and the World Health Organization (WHO) have reported that 3.2 million workers are exposed to RCS in the European Union and have classified this compound as carcinogenic to humans [3, 7] Although the lung is the main target of damage due to chronic exposure to silica dusts (RCS), many studies have shown that prolong exposure to this compound is associated with a wide range of adverse effects on other organs [6]. Although the molecular mechanisms in the pathogenesis of silicosis are still not entirely known, accumulating evidence suggested that the phagocytosis of RCS causes an active inflammation and oxidative stress that plays an important role in the various diseases in the exposed individuals.

Depending on the duration and exposure concentration of silica dusts, silicosis can occur as acute, progressive, chronic, and conglomerate silicosis (advanced progressive silicosis or complex silicosis) [8]. After exposure to RCS, the dusts are able to reach the alveoli, inducing oxidative stress by the formation of Reactive Oxygen (ROS) and Nitrogen Species (RNS) [9]. As mentioned abundantly excess generation of free radicals can eventually lead to the damage of cellular lipids, proteins, and DNA, inhibiting their functions and also decrease of antioxidant enzymes such as Glutathione S-Transferase (GST), Catalase (CAT), Superoxide Dismutase (SOD) as first line of defense against free radical [10].

The many studies have conducted on the assessment of health risk of exposure to RCS in workers of various occupations, including coal miners, pottery, cement, stone crushers and granite foundry [3, 10, 11]. For example, some researchers indicated the workers working in high-risk units such as stamping machine operator and stone separation operator are more likely to suffer from adverse health complications such as silicosis, lung cancer and other respiratory complications [3]. Other researchers concluded exposure of humans to cement dust is capable of inducing free radicals, marked hazardous alterations in some enzymatic activities, liver functions and some biochemical parameters [10]. Therefore, given the actual exposure of workers to RCS in silica mines of Azandarian region (Hamadan province, Iran) and the lack of a determined method for early detection and screening of high risk workers before occurring silicosis, the present study aimed to evaluate the biochemical parameters of liver enzyme activity and oxidative stress as potential early peripheral biomarkers for investigating the health status of the silica-exposed workers in silica mines.

Materials and methods

Human subjects

The current case–control study was performed in different parts of industrial production units of silica in Azandrian region, Hamadan province in West of Iran, during spring, 2021. In this study, in the first step, all workers in various units of silica production agreed to participate in the study and were asked to sign a consent form. Next, all workers were asked to complete a questionnaire containing health status and demographic information including income, education, lifestyle, smoking, alcohol consumption, intake of drug, or/and supplement and diet. Moreover,

to identify any type of chronic diseases include (diabetes, blood pressure, cardiovascular diseases, chronic kidney disease, immune system disorders, cancer, respiratory diseases including bronchitis, epilepsy, hearing loss, digestive diseases, asthma, etc.) all the participants were asked to complete clinical examination. All subject with alcohol, chronic diseases and antioxidants less than six months in silica production units were excluded from the study. Therefore, eighty participants were included in the study and classified into two groups, including 40 workers exposed to RCS working in various units of silica production as the case group (or exposed group) and 40 well-matched workers whiteout any exposer to silica dusts who were working in food distribution industry. Current study was approved by the Research Ethics Committee of Hamadan University of Medical Sciences (IR.UMSHA.REC.1400.384). All volunteers provided informed consent prior to participation in this study.

Sample collection

Blood samples from study subjects were drawn by venipuncture. Samples were centrifuged immediately at 800 g for 15 min to obtain plasma and kept in −80 °C for further analyses. All the participants were sampled on the same day. Complete blood analysis was done to determine Alanine Transaminase (ALT), Aspartate aminotransferase (AST) and Alkaline Phosphatase (ALP).

Biochemical analysis

Analysis of chemical biomarkers of liver enzyme activity such as (ALT), (AST) and (ALP) was done using Pars Azmun commerical kits (Tehran,Iran, Cat. No: KSOD91).

Measurement of oxidative and anti-oxidative stress markers in serum

Measurement of malondialdehyde level (MDA) and ROS in serum

The lipid peroxidation was evaluated using spectrofluorometrically as Thiobarbituric Acid (TBA) reactive substances. The reaction of TBA with MDA led to the formation of TBA reactant substances, which can be considered as biomarkers of oxidative at acidic pH and high temperature. The maximum absorbance measurement at 532 nm indicated the MDA level. MDA content was considered as (nmol/L) [12]. Kiazist kit (KTOS96), which works based on oxidation of ferrous iron to ferric iron in the presence of oxidant factors, was used for detecting ROS in serum as another indicator of oxidative stress by. ROS levels were expressed as (mM/L).

Evaluation of total antioxidant capacity (TAC) and CAT in serum

TAC measurement was done manually using ferric-reducing ability of serum (FRAP) method. The method is based on the capacity of sample to reduce Fe^{3+} (Ferric) ions to Fe^{2+} (Ferrule) in the presence of TPTZ (Tripyridyl-s-triazin). The interaction of Fe^{2+} - TPTZ complex produces a blue color. Maximum absorption of optical density was measured at 593 nm [13]. Catalase (CAT) is important antioxidant enzymes. The activities of this enzyme are measured by kiazist kits of KSOD94.

Statistical analysis

To compare qualitative data from the Kolmogorov–Smirnov test was used. For determining normal distribution from Independent t-test and Mann- Whitney were used to compare the mean difference between the RCS exposed and control groups in quantitative data. All data were analyzed using SPSS software (Version 20). The results were presented as mean ± SD and $p<0.05$ was considered as statistically significant.

Results and discussion

Table 1 presents the demographic data of the subjects. Based on findings, there were no statistically significant difference between the case and control groups in term of age, duration of work, weight, place of residence ($p>0.05$).

Table 1. Comparison of demographical data between case and control groups

Demographical data	Case	Control	
	Mean±SD	Mean±SD	p-value
age	30.53 ±7.74	33.32 ±8.64	0.076[a]
weight	78.66 ±8.22	78.53 ±9.06	0.927[b]
	N (%)	N (%)	P-value [c]
Residence			
City	55 (69.6)	54 (68.4)	0.863
Village	24 (30.4)	25 (31.6)	
Work experience			
1-5 years	9 (11.4)	16 (20.3)	0.060
6-10 years	15 (19.0)	20 (25.3)	
11-15 years	27 (34.2)	29 (36.7)	
>15 years	28 (35.4)	14. (17.7)	

a. Mann-Whitney, b. Independent t-test, c. Chi-square

Table 2. Comparison of blood factors analyses between exposed workers and controls

	Number	Mean ±SD of Case	Mean ±SD of Control	P-value[a]
AST[b]	80	19.27 ± 7.85	19.27 ± 9.23	0.798
ALT[c]	80	18.82 ± 7.02	16.71 ± 6.05	0.041
Alp[d]	80	221.77 ± 57.13	237.04 ± 53.37	0.125

a.Mann- Whitney, d. Aspartate aminotransferase, c. Alanine aminotransferase,

d. Alkaline phosphatase

The concentration of ALP, ALT and AST in serum

As shown in Table 2, blood factors analyses showed a significant difference (increasing trend) in the ALT levels between the exposed cases and controls ($p<0.001$), while no significant difference was observed in term of other blood factors (e.g. ALP and AST) ($p>0.05$).

Concentration of MDA and ROS in serum of the exposed worker

In this step, the serum levels of MDA (nmol/L) and ROS (mM/L), as an oxidative stress biomarkers were measured and compared between the exposed and non-exposed workers. As shown in Fig. 1, there were significant increases in the ROS and MDA levels in the exposed workers compared to the control group ($p<0.01$ and $p<0.001$, respectively).

Concentration of TAC and CAT in serum of the study groups

As shown in Fig. 2 concentrations of TAC (mmol/L) in serum were statistically significantly lower in the case group when compared to that of the control group ($P<0.05$). However, no statistical difference was found in the CAT level in serum samples of groups ($P>0.05$).

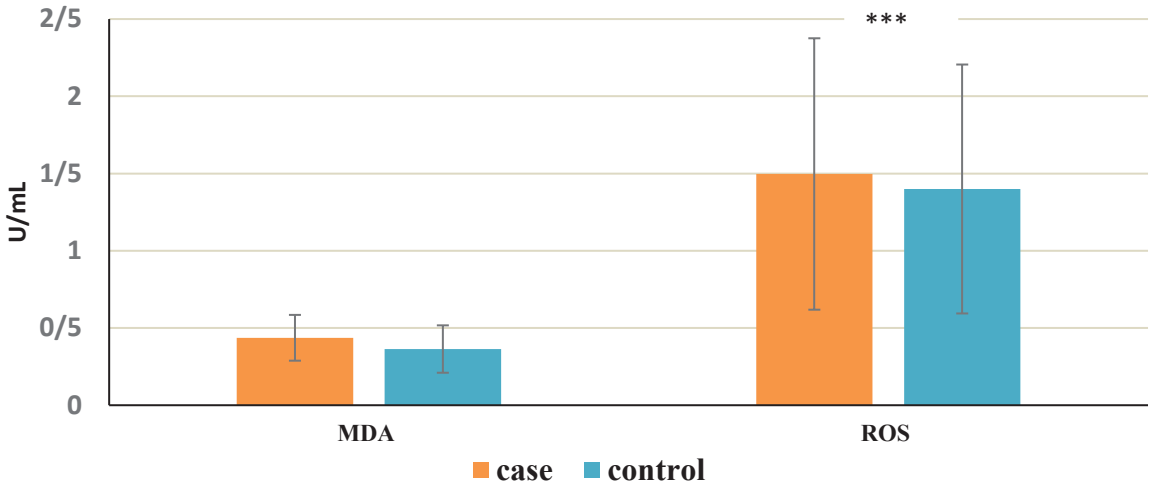

Fig. 1. Serum levels of MDA and ROS in the exposed workers and controls (as mean±standard deviation). Difference between exposed and control groups was considered significant at p-value<0.001 (***), p<0.01(**)

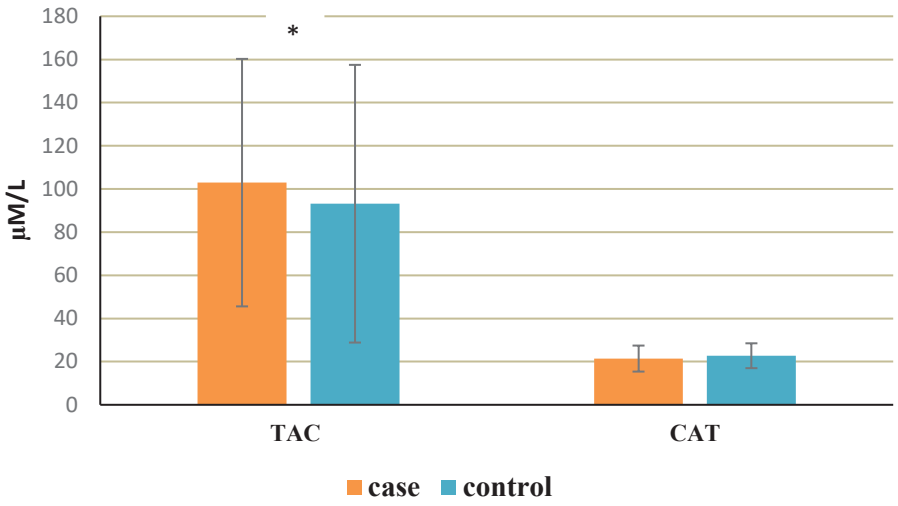

Fig. 2. Concentration of TAC and CAT in serum of case and control groups, Results is represented as mean±standard. Difference between control and other groups is significant at p-value<0.05 (*)

RCS is an important material that is widely used in a wide range of industries and is associated with many health problems in different organs. In this study, we focused on biomarkers of oxidative stress and liver function in serum of the exposed-workers in various units of silica mines of Azandarian region (Hamadan province, Iran) and their results were compared with non-exposed group as controls. Silicosis as an occupational respiratory disorder is generally occurred due to chronic exposure (occupational exposure) RCS.

It is noteworthy that several studies in recent years have reported several silicosis cases with non-occupational exposure. It is described chiefly by huge pulmonary fibrosis due to proliferation and progressive increase in connective tissue, which is substituted for normal functional parenchyma [14]. Although the main target tissue in toxicity with silica crystalline is the lung, but abnormal of blood cells, hematologic injury, breakage of chromosomal, complications including liver dysfunction, cancer and reduced in mitotic index are still the topic of various studies [15, 16]. RCS particles penetrate the worker's organs mainly through the respiratory and skin routes and rarely through ingestion. [17]. Until now, the mechanism underlying the induction of fibrosis and silicosis of lung tissue has been severally studied.

Evidence shows that stress oxidative damage plays a key role in developing fibrotic lung disease, and hence maybe used as an indicator [18]. Our study clearly indicated the function of liver enzyme (ATL level) was significantly decreased in the silica-exposed group compared to the control, while no significant changes were observed in other liver enzymes (ALP and AST) (as can be seen in Table 2). Liver tissue is one of the most important organs that play an important role in the detoxification of endogenous and exogenous compounds in the body. Serum levels of liver enzymes are identified as an estimation of liver function [19]. ALT enzyme is known as a serum dysfunctional enzyme due to the hepatic cell injury [20], while AST enzyme is biomarker of liver tissue damage and is abundantly found in heart, kidney, skeletal muscle and liver [21]. Moreover, ALP is typically concentrated in liver and plays a key role in the detoxification, metabolism and biosynthesis of energetic macromolecules for various essential functions [22]. During cellular degeneration or destruction of liver, these enzymes are released from the cytosol into the bloodstream [10]. Consistent with our results, many researchers, indicated that in silica-exposed workers (in cement factories), there was an association between the level of liver enzymes and the duration of exposure [15]. Other researchers stated that ALT level was higher among cement exposed workers compared with the control group, but no statistically significant [17]. In a study, it was showed that the activities of AST , ALP and ALT in plasma of exposed workers in cement factory had an increase compared to the control group [10]. Moreover, a significant increase can occur in the activity of ALP in plasma due to the change in permeability of plasma membrane or cellular necrosis [23].

According to published studies, oxidative stress occurs due to the imbalance between oxidant and antioxidant status in the body [24]. A large body of experimental work indicated exposure with RCS can induce ROS on epithelial cells and extracellular components (macrophages) and lead to activation of cell signaling pathways, specific transcription factors and increased oxidative stress biomarkers [25]. ROS are active molecular species containing oxygen, such as superoxide anion (O^{2-}), Hydroxyl radical ($HO^{\bullet}$) and Hydrogen peroxide (H_2O_2), which offer a higher chemical activity compared with molecular oxygen [26]. Various antioxidant systems are present in the human body to protect against destructive effects from activated

Reactive Oxygen Species (ROS). As mentioned in previous studies, O^{2-} generation can convert to H_2O_2 by SOD and then by CAT enzymes alter to oxygen and water [27].

Considering the important role of oxidative stress, evaluation of biomarkers of oxidative stress and its relationship with liver function in RCS-exposed workers can help in early diagnosis of silicosis. In our study, an increase was observed in oxidant stress biomarkers (MDA and ROS) and a decrease in the antioxidant system parameters (TAC) in the exposed workers, while there was no significant difference in serum level of CAT in the silica-exposed workers. Prolonged exposure with silica crystals might cause ROS production and membrane lipid peroxidation. Corroborating our results, several studies reported the involvement of lipid peroxidation in plasma, after crystalline silica exposure. In two studies, it was indicated an significant increase in MDA plasma levels of workers in the field of ceramics and glass sandblasters exposed to RCS compared to the non-exposed workers, respectively [28, 29]. Other researchers indicated statistical change in plasma MDA levels cement-exposed workers than control group [30]. In a study, it was found that plasma concentration of MDA were much higher in asbestos-exposed workers compared to non-exposed individuals [31].

CAT enzymes have important role in the detoxification of superoxide anion and hydrogen peroxide (H_2O_2), which protect the cell against ROS-induced injury [30]. This enzyme, along with Total Antioxidant Capacity (TAC) constitutes a major defense against oxidative damage. TAC as valuable antioxidant can be useful as an early marker of oxidative stress to monitor antioxidant status in body. TAC indicate an important index of the total amounts of enzymatic and non-enzymatic antioxidants in body which can the activity of one or two enzymes, and also be various dietary antioxidants such as ascorbic acid and a-tocopherol [32]. Our research indicated a statistical significant reduction in serum levels of TAC in RCS-exposed workers that can be attributed to the production of reactive oxygen species caused by the exposure to RCS in their workplaces. Free radicals produced can be eliminated by TAC and the decrease in the activity of this antioxidant show that exposure to crystalline silica can increase oxidative stress in body [33]. In line with our results, a previous study reported a reduction in TAC content in workers with direct exposure to cement [11]. In another study, it was showed a slight increase in levels of TAC among the exposed-workers compared to controls [17]. Unlike in other studies, it was reported that there was no significant difference in the level of TAC between the groups [34] .The conflicting findings mentioned in this study in levels TAC can be related to intensity of exposure, protective equipment, and nutritional status [17]. In general, there were some limitations in this study; for instance, the levels of RCS dusts did not measured in different parts of the workplace. Moreover, other enzymatic antioxidants such as superoxide dismutase, glutathione peroxidase and other non-enzymatic antioxidants (e.g. ascorbic acid and tocopherol) did not determined. However, of the evaluation of the studied parameters in several exposed workers in different work units with various exposure levels can be mentioned as strength of the study.

Conclusion

The present study showed that occupational exposure to RCS dusts can lead to damage to liver enzyme activity and oxidative stress as evidenced by increased serum levels of MDA, ROS and ALT and reduction in the level of TAC. To overcome these oxidative stresses, supplementation with dietary antioxidants, including ascorbic acid and A-tocopherol may suggestion beneficial health effects in the exposed workers. However, it is recommended to protect the health of workers

against silica dust they be use from industrial masks and proper ventilation system should be installed in the environment.

Financial supports

The authors would like to acknowledge the Deputy of Research and Technology, Hamadan University of Medical Sciences for their financial support (Project NO. 140008257172).

Competing interests

All authors declared no conflict of interest regarding this paper.

Acknowledgements

This study (Evaluation of Oxidative stress biomarkers and liver enzyme activity in workers occupationally exposed to respirable free crystalline silica) was reviewed and approved Research Ethics Committee of Hamadan University of Medical Sciences (IR.UMSHA.REC.1400.384).All volunteers provided informed consent prior to participation in this study.

Ethical considerations

Ethical issues (Including plagiarism, Informed Consent, misconduct, data fabrication and/or falsification, double publication and/or submission, redundancy, etc) have been completely ob-served by the authors.

References

1. Mehri F, Jenabi E, Bashirian S, Shahna FG, Khazaei S. The association between occupational exposure to silica and risk of developing rheumatoid arthritis: a meta-analysis. Safety and Health at Work. 2020 Jun 1;11(2):136-42.

2. Esfahani M, Bashirian S, Mehri F, Khazaei S. Association between Silica Exposure and Cardiovascular Disease Mortality: A Meta-Analysis. The Journal of Tehran University Heart Center. 2020 Oct;15(4):151.

3. Poormohammadi A, Moeini ES, Assari MJ, Khazaei S, Bashirian S, Abdulahi M, Azarian G, Mehri F. Risk assessment of workers exposed to respirable crystalline silica in silica crushing units in Azandarian industrial zone, Hamadan, Iran. Journal of Air Pollution and Health. 2021;6(3):225-32.

4. Huang X. Iron, oxidative stress, and cell signaling in the pathogeneses of coal workers' pneumoconiosis, silicosis, and asbestosis. Am J Biomed Sci. 2011 Apr 1;3(2):95-106.

5. Farokhzad M, Ranjbar A, Kheiripour N, Soltanian A, Assari MJ. Potential in the diagnosis of oxidative stress biomarkers in noninvasive samples of urine and saliva and comparison with serum of persons exposed to crystalline silica. International Archives of Health Sciences. 2020 Apr 1;7(2):84.

6. Peruzzi C, Nascimento S, Gauer B, Nardi J, Sauer E, Göethel G, Cestonaro L, Fão N, Cattani S, Paim C, Souza J. Inflammatory and oxidative stress biomarkers at protein and molecular levels in workers occupationally exposed to crystalline silica. Environmental Science and Pollution Research. 2019 Jan 21;26:1394-405.

7. Steenland K, Mannetje A, Boffetta P, Stayner L, Attfield M, Chen J, Dosemeci M, DeKlerk N, Hnizdo E, Koskela R, Checkoway H. Pooled exposure–response analyses and risk assessment for lung cancer in 10 cohorts of silica-exposed workers: an IARC multicentre study. Cancer Causes & Control. 2001 Nov;12:773-84.

8. Bakhshandeh E, Jannesari A, Ranjbar Z, Sobhani S, Saeb MR. Anti-corrosion hybrid coatings based on epoxy–silica nano-composites: Toward relationship between the morphology and EIS data. Progress in Organic Coatings. 2014 Jul 1;77(7):1169-83.

9. Nardi J, Nascimento S, Göethel G, Gauer B, Sauer E, Fao N, Cestonaro L, Peruzzi C, Souza

J, Garcia SC. Inflammatory and oxidative stress parameters as potential early biomarkers for silicosis. Clinica Chimica Acta. 2018 Sep 1;484:305-13.

10. Al Salhen KS. Assessment of oxidative stress, haematological, kidney and liver function parameters of Libyan cement factory workers. Journal of American science. 2014;10(5):58-65..

11. Pournourmohammadi S, Khazaeli P, Eslamizad S, Tajvar A, Mohammadirad A, Abdollahi M. Study on the oxidative stress status among cement plant workers. Human & experimental toxicology. 2008 Jun;27(6):463-9.

12. Mehri F, Ranjbar A, Shirafkan N, Asl SS, Esfahani M. The protective effect of resveratrol on diazinon-induced oxidative stress and glucose hemostasis disorder in rats' liver. Journal of Biochemical and Molecular Toxicology. 2022 Jul;36(7):e23063.

13. Esfahani M, Rahbar AH, Soleimani Asl S, Mehri F. Resveratrol: a panacea compound for diazinon-induced renal toxicity. Toxin Reviews. 2021 Nov 19:1-1.

14. Hamilton Jr RF, Thakur SA, Holian A. Silica binding and toxicity in alveolar macrophages. Free Radical Biology and Medicine. 2008 Apr 1;44(7):1246-58.

15. Mojiminiyi FB, Merenu IA, Ibrahim MT, Njoku CH. The effect of cement dust exposure on haematological and liver function parameters of cement factory workers in Sokoto, Nigeria. Nigerian journal of physiological sciences. 2008;23(1-2).

16. Cohen SS, Sadoff MM, Jiang X, Fryzek JP, Garabrant DH. A review and meta-analysis of cancer risks in relation to Portland cement exposure. Occupational and environmental medicine. 2014 Nov 1;71(11):796-802.

17. Malekirad AA, Rahzani K, Ahmadi M, Rezaei M, Abdollahi M, Shahrjerdi S, Roostaie A, Mohajerani HR, Boland Nazar NS, Torfi F, Mousavi Khaneghah A. Evaluation of oxidative stress, blood parameters, and neurocognitive status in cement factory workers. Toxin Reviews. 2021 Oct 2;40(4):1128-34.

18. Hemmati AA, Nazari Z, Samei M. A comparative study of grape seed extract and vitamin E effects on silica-induced pulmonary fibrosis in rats. Pulmonary pharmacology & therapeutics. 2008 Aug 1;21(4):668-74.

19. Oberdörster G, Oberdörster E, Oberdörster J. Nanotoxicology: an emerging discipline evolving from studies of ultrafine particles. Environmental health perspectives. 2005 Jul;113(7):823-39.

20. Kim WR, Flamm SL, Di Bisceglie AM, Bodenheimer HC. Serum activity of alanine aminotransferase (ALT) as an indicator of health and disease. Hepatology. 2008 Apr 1;47(4):1363-70.

21. Thapa BR, Walia A. Liver function tests and their interpretation. The Indian Journal of Pediatrics. 2007 Jul;74:663-71.

22. Torkadi PP, Apte IC, Bhute AK. Biochemical evaluation of patients of alcoholic liver disease and non-alcoholic liver disease. Indian journal of clinical biochemistry. 2014 Jan;29:79-83.

23. Rahman K. Studies on free radicals, antioxidants, and co-factors. Clinical interventions in aging. 2007 Jan 1;2(2):219-36.

24. Mehri F, Faizi M, Salimi A, Seydi E, Pourahmad J. Toxicity of 4-methylimidazole on isolated brain mitochondria: using both in vivo and in vitro methods. Toxicological & Environmental Chemistry. 2015 May 28;97(5):663-73.

25. Mossman BT. Serial review: Role of reactive oxygen and nitrogen species (ROS/RNS) in lung injury and diseases. Free Radical Biology and Medicine. 2003;34:1130-5.

26. Akhtar MJ, Ahamed M, Kumar S, Siddiqui H, Patil G, Ashquin M, Ahmad I. Nanotoxicity of

pure silica mediated through oxidant generation rather than glutathione depletion in human lung epithelial cells. Toxicology. 2010 Oct 9;276(2):95-102.

27. Pi J, Zhang Q, Fu J, Woods CG, Hou Y, Corkey BE, Collins S, Andersen ME. ROS signaling, oxidative stress and Nrf2 in pancreatic beta-cell function. Toxicology and applied pharmacology. 2010 Apr 1;244(1):77-83.

28. Anlar HG, Bacanli M, İritaş S, Bal C, Kurt T, Tutkun E, Hinc Yilmaz O, Basaran N. Effects of occupational silica exposure on oxidative stress and immune system parameters in ceramic workers in Turkey. Journal of Toxicology and Environmental Health, Part A. 2017 Aug 3;80(13-15):688-96.

29. Azari MR, Ramazani B, Mosavian MA, Movahadi M, Salehpour S. Serum malondialdehyde and urinary neopterin levels in glass sandblasters exposed to crystalline silica aerosols. International Journal of Occupational Hygiene. 2011;3(1):29-32.

30. Aydin S, Aral I, Kilic N, Bakan I, Aydin S, Erman F. The level of antioxidant enzymes, plasma vitamins C and E in cement plant workers. Clinica chimica acta. 2004 Mar 1;341(1-2):193-8.

31. Kamal AA, Khafif ME, Koraah S, Massoud A, Caillard JF. Blood superoxide dismutase and plasma malondialdehyde among workers exposed to asbestos. American journal of industrial medicine. 1992;21(3):353-61.

32. Chatterjee IB, Nandi A. Ascorbic acid: a scavenger of oxyradicals. Indian journal of biochemistry & biophysics. 1991 Aug;28(4):233-6.

33. Khan IA, Reddy BV, Mahboob M, Rahman MF, Jamil K. Effects of phosphorothionate on the reproductive system of male rats. Journal of Environmental Science and Health, Part B. 2001 Jun 30;36(4):445-56.

34. Afaghi A, Oryan S, Rahzani K, Abdollahi M. Study on genotoxicity, oxidative stress biomarkers and clinical symptoms in workers of an asbestos-cement factory. EXCLI journal. 2015;14:1067.

Journal of Air Pollution and Health (Winter 2023); 8(1): 87-102

Original Article

Available online at http://japh.tums.ac.ir

A study to access and estimation of air pollution using a multivariate statistical model in Chennai, India

Yuvaraj Ramachandran Muthulakshmi[1,*], *Sakthivel Mathivanan*[1], *Marangattu Raghavan Sindhumol*[2]

[1] Department of Geography, University of Madras, Chennai, Tamil Nadu, India
[2] Department of Statistics, University of Madras, Chennai, Tamil Nadu, India

ARTICLE INFORMATION

Article Chronology:
Received 05 December 2022
Revised 30 January 2023
Accepted 20 February 2023
Published 29 March 2023

Keywords:
Air pollution; Particulate matter; Particulate matters less than 2.5 µm ($PM_{2.5}$); Particulate matters less than 10 µm (PM_{10}); Multivariate statistical model

CORRESPONDING AUTHOR:

yuvaraj1023@gmail.com
Tel: (044) 24866001
Fax: (044) 24866001

ABSTRACT

Introduction: Rapid urbanization and industrial growth are the primary causes of deteriorating urban air quality in developing countries, including India. Vehicular emission is a significant cause of the degradation of air quality. It includes Air Pollution like carbon monoxide, hydrocarbons, oxides of nitrogen, oxides of sulfur, Suspended Particulate Matter (SPM), respiratory Particulate Matters ($PM_{2.5}$ and PM_{10}), and lead.

Materials and methods: The study has considered land use,land cover, land surface temperature, vegetation, literacy rate, vehicle population, population density, and households, finding the responsible causes of air pollutionfor the analysis. Supervised classification using ArcGIS for extracting land use and land cover, Least Slack Time (LST) algorithms have used to extract land surface temperature, spatial interpolation methods like Inverse Distance Weighting (IDW) using ArcGIS for identifying the spatial distribution of Literacy rate, vehicle population, population density and households and finally the multivariate statistical model applied to identify the major responsible factor for air pollution using SPSS.

Results: The study reveals that the particulate matter is below the standard value prescribed by the central pollution control board. The Highest air pollution is primarily responsible for vehicle population and industries. Wednesday and Thursday are the maximum pollution in Chennai, whereas it was recorded as very low on Sunday as compared to other days.

Conclusion: Regression shows that the vehicle population is responsible for air pollution, followed by the population.

Introduction

Vehicle exhaust, on-road re-suspended dust owing to vehicles, industrial fumes, construction dust, waste burning, residential cooking and heating, and some seasonal sources such as agricultural field residue burning and dust are all contributing to urban air pollution [1]. An increase in urban and industrial areas significantly contributes to deteriorating urban air quality, particularly in developing countries like India. Vehicular emission is a significant cause of the degradation of air quality. It

Please cite this article as: Muthulakshmi YR, Mathivanan S, Sindhumol MR. A study to access and estimation of air pollution using a multivariate statistical model in Chennai, India. Journal of Air Pollution and Health. 2023;8(1): 87-102.

Copyright © 2023 Tehran University of Medical Sciences. Published by Tehran University of Medical Sciences.
This work is licensed under a Creative Commons Attribution-NonCommercial 4.0 International license (https://creativecommons.org/licenses/by-nc/4.0/). Noncommercial uses of the work are permitted, provided the original work is properly cited.

includes Air Pollutants (APs) like Particulate Matter (PM), Oxides of Nitrogen, carbon monoxide, Oxides of Sulfur, hydrocarbons, Suspended Particulate Matter (SPM), and lead [2]. Most remarkably, the re-suspension of road dust due to rubber wheels and brake wear also generates large amounts of PM_{10} [3]. An insufficient change in the physical, chemical, or biological characteristics of air that impedes life and may cause health problems is called air pollution [4]. Air Pollution, in particular, irritates the eyes, lungs, nose, and throat. It also causes respiratory problems and aggravates pre-existing conditions like asthma and emphysema. The risk of cardiovascular disease escalates when humans are constantly exposed to air pollution. The harmful health effects of air contamination depend on the pollutant source, the source's potency, and the potentially exposed individual's behavior [5]. Air pollution has been projected to cause over 4 million premature deaths each year, and levels of air pollution are still rising in certain places [6].

Ambient airborne Particulate Matter (PM), which occurs in various sizes and chemical and biological components, is a major scientific and policy problem [7]. PM is responsible for most of the illness burden related to air pollutants, with more than half relating to ambient inhalation exposures. Among the significant risk factors threatening human health globally concerning its disease burden, PM has recently been ranked fifth and thus first among environmental risks. The current levels of city air pollution need to be evaluated and managed to givethe residents a healthy urban air environment.Numerous studies on outdoor land plants or vegetation as interventions capable of protecting our health from ambient air pollution at various scales have been inspired by rapid urbanization and increased awareness of the effects of the natural environment on our health [8, 9]. In India, air pollution is the third leading cause of death among health risks, and as a result, life expectancy has decreased by 2.6 years. As a result, it has become increasingly important to control pollution and effectively educate people affecting air quality to maintain a healthy standard. Temperature is another parameter that will increase air pollution with temperature increases. Extreme heat and stagnant air during a heat wave increase particulate pollutants. Demographic factors such as population density, household size, and literacy rate also affect the air pollution standard [10]. Thus, investigating the assessment of air pollution exposure and its influencing factors will benefit community health and well-being. This information will inevitably improve personal responses to pollutants or a specific harmful agent [11]. Theseair pollutants of $PM_{2.5}$ and PM_{10} have been used in conjunction with GIS to analyze and visualize spatial and temporal impacts of air pollution in Chennai [12]. Spatial interpolation methods like Inverse Distance Weighting (IDW) have been extensively used to foresee the concentration of air pollution [13-15].

Study area

The state executive and legislative headquarters are principally housed in the Secretariat Buildings on the Fort St George complex in Chennai, which serves as the capital of Tamil Nadu. The Chennai Metropolitan Development Authority (CMDA) is the central agency in charge of planning and development in the Chennai Metropolitan Area, which spans 1,189 km^2 (459 sq mi) and includes parts of the Tiruvallur and Kanchipuram districts. Although it is the smallest of the state's districts, it has the highest population density. The city has an area of 426 km^2. Chennai is the 4th most populated city, the 6th most densely inhabited city in India, and the 31st biggest urban in the world.

The area of the city possesses the rank of 27 out of 640 cities in India. It is the 'Gateway to South India' and is well-connected globally. Chennai is northeast of Tamil Nadu, on the east shore, next to the Bay of Bengal. It lies between the 12°50'43.615"N and 13°13'49.196"N latitudes and 80°8'37.79"E and 80°19'52.827"E longitude (Fig. 1). It extends 25.6 km along the bay coast, from Thiruvanmiyur in the south to Thiruvottiyur in the north. It runs inwards in a robust semicircular shape. It limits the east with the Bay of Bengal and the other three sides with the districts of Kanchipuram and Thiruvallur (Fig. 1).

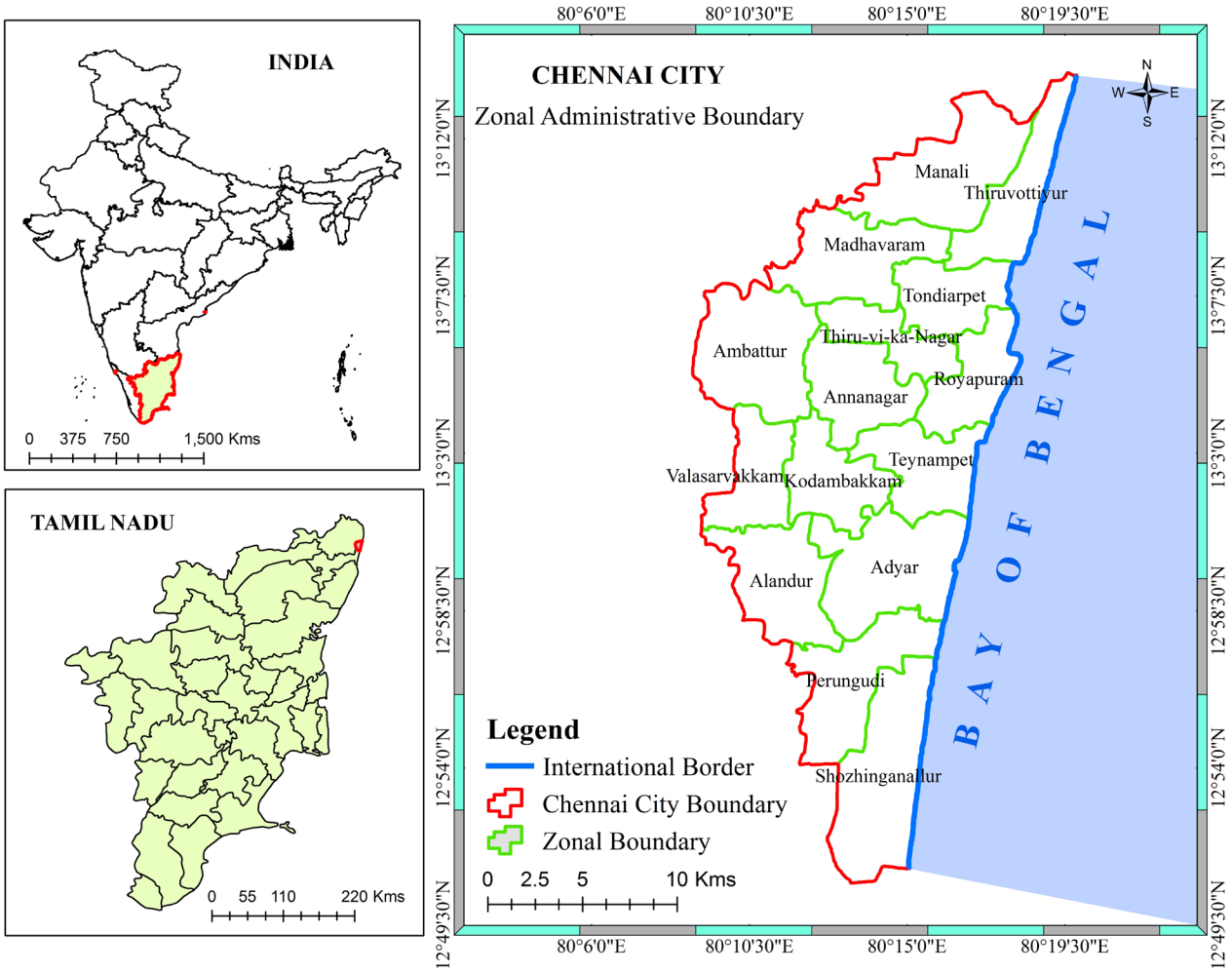

Fig. 1. Study area–Chennai city

Materials and methods

For finding the Land Surface Temperature (LST) of the study region, Landsat 8 Operational Land Imagers (OLI) and Thermal Infrared Sensor (TIRS) images with 143 paths and 51 row has used. These images have been downloaded from USGS (United States Geological Survey), which contains 11 bands with different wavelengths. These satellite images have been utilized to estimate the LST and vegetation. Particulate Matter ($PM_{2.5}$ and PM_{10}) air pollution data has been gathered from the Central Pollution Control Board (CPCB) for 2021. Demographic data like population, literacy rate, Household, and population density from the census of India, Chennai for the year 2011.

The satellite photos were preprocessed by extracting images based on the research region using the ArcGIS 10.2 extract by mask tool. The research region and accompanying satellite pictures are obtained after preprocessing for data analysis. Only bands 10, 4, and 5 are used to calculate the Land Surface Temperature in this study (LST). Thermal Infrared Sensor (TIRS) band 10 has a wavelength of 10.60 to 11.19, red band 4 has a wavelength of 0.64 to 0.67, and Near Infrared (NIR) band 5 has a wavelength of 0.85 to 0.88. The land surface temperature of the research region was determined using the following algorithm.

Calculation of top of atmospheric (TOA)

The introductory course of action for retrieving land surface temperature is estimating the spectral radiance of TOA.

$$\text{TOA (L)} = M_L * Q_{Cal} + A_L - O_i \quad (1)$$

Where ML signifies the precise band's multiplicative rescaling factor, Q_{cal} signifies the Quantized and calibrated standard product pixel values (DN), AL signifiesthe precise band's Additive rescaling factor, and O_i is the band correction from Table 1 [16].

Calculation of Brightness Temperature (TB)

The next step is transforming spectral reflectivity to TB using metadata's constant values. The reflectance was converted to brightness temperature using the equation below.

$$TTB = \frac{K_2}{In\left[\left(\frac{K_1}{L}\right)+1\right]} - 273.15 \quad (2)$$

Where K_1 and K_2 signify the specific band's thermal conversion constants, L signifies the Top of the atmosphere. In order to achieve the outcome value in Celsius, the radiant temperature is adjusted by summing the absolute zero (-273.15 0 C).

Calculation of land surface emissivity (LSE)

Since the LSE is a proportionality factor that scales blackbody radiance (Planck's law) to forecast emitted radiance, and it is the competence of transporting thermal energy across the surface into the atmosphere, it is necessary to know the LSE factor in order to compute the LST [17]. As a result, the emissivity is computed using the equation below.

$$\varepsilon = \varepsilon_v P_v + \varepsilon_s(1 - P_v) + d\varepsilon \quad (3)$$

Where $\varepsilon_v$signifies the emissivity of the vegetative of the region and $\varepsilon_s$signifies the emissivity of the soil, $P_v$signifies the proportion of vegetation of the region [18]. Following a research., the ultimate emissivity for the Landsat 8 image is specified by the equation given below [19].

$$\varepsilon = 0.004\ Pv + 0.989, \quad (4)$$

Where 0.004 signifies the standard deviation of 49 soil spectra, 0.989 signifies the average emissivity of the region's soil (0.97) and the region's vegetation's emissivity (0.99).

Table 1. Metadata for the Landsat 8

Constant	Factor	Band	Value
M_L	Band's rescaling feature	10	0.000342
A_L	Band's rescaling feature	10	0.1
K_1	Thermal constant value	10	1321.08
K_2	Thermal constant value	10	777.89
O_i	Correction	10	0.29

Calculation of vegetation and its share

The share of vegetation of a region (P_v) is estimated based on the following given equation [20].

$$P_v = \left(\frac{NDVI - NDVI_{min}}{NDVI_{max} - NDVI_{min}}\right)^2 \quad (5)$$

With the use of Landsat visible (band 4) and NIR (band 5) data, the following equation is used to determine the Normalized Difference Vegetation Index (NDVI). When identifying the LST, the amount of vegetation present is crucial [21].

$$NDVI = \frac{NIR - Red}{NIR + Red} \quad (6)$$

Calculation of land surface temperature (LST)

The concludingprocedure for calculating the LST is based on the following equation [22].

$$LST = \frac{TB}{\left\{1 + \left[\frac{\lambda TB}{\rho}\right] In\ \varepsilon_\lambda\right\}} ℃ \quad (7)$$

Where λ signifies the wavelength of emitted radiance by Landsat 8, which is 10.8 (given by NASA), ε_λ signifies the emissivity of the land surface, ρ is given by the equation given below,

$$\rho = h\frac{c}{\sigma} = 14388\ \mu m\ K \quad (8)$$

Where h signifies Planck's constant (6.626 X10^{-34} Js) , σ signifies the Boltzmann constant (1.38 x 10^{-23} J/K), and c signifies the velocity of light (2.988 x 10^8 m/s) [20]. The land Surface Temperature for the study region has been done for March 2021.

Statistical model

SPSS was used to develop a statistical model using multiple linear regression (statistical package for the social science).

$$Y = \alpha + \beta_1 x_1 + \beta_2 x_2 + \beta_3 x_3 \quad (9)$$

Where Y signifies the dependent variable, α signifies the intercept, $\beta_{1,2,3}$……. are regression coefficients of the independent variables, $x_{1,\ 2,\ 3}$ ….. are independent variables which would be the predictor of the dependent variable.

A supervised signature extraction with the maximum likelihood algorithm was employed to classify the digital Land use Land cover mapping for 2021. An extensive field survey was conducted throughout the research area utilizing Global Positioning System (GPS) equipment before the preprocessing and classification of satellite pictures began. This survey was conducted to acquire accurate locational point data for each Land Use Land Cover class in the categorization method, establish training sites, and generate signatures. The NRSC (National

Remote Sensing Centre) categorization system was used to classify land use/land cover (agriculture, built-up, wetlands, and wasteland). Using the picture interpretation element (such as tone, texture, shape, pattern, and association) and Arc-GIS software, the Indian Remote Sensing Satellite (IRS) data were visually and digitally interpreted. Before the theme maps were finalized, adequate field checks were performed.

Results and discussion

Distribution of particulate matter

Spatio-temporal distribution of air pollutant $PM_{2.5}$ for Chennai city has shown in Figure 2. Spatially northern parts of Chennai have high pollution of $PM_{2.5}$ as compared to the southern part. Wednesday and Thursday show the maximum $PM_{2.5}$, and Sunday records are low as compared to other days. Manali village has a high average of $PM_{2.5}$, followed by Kodungiyur and Arumbakkam, whereas Manali has recorded a low, followed by Perugudi shown in Figure 3. Spatio-temporal distribution of air pollutant PM_{10} for Chennai city has shown in Figure 3. Spatially northern parts of Chennai have high pollution of PM_{10} as compared to the southern part. Wednesday and Thursday show the maximum PM_{10}, and Sunday records are low as compared to other days. Manali village has a high average of PM_{10}, followed by Manali and Arumbakkam, whereas Velachery has a recorded low, followed by Perugudi and Royapuram, showed in Figure 5. Particulate matter ($PM_{2.5}$ and PM_{10}) is below the standard value prescribed by the Central pollution control board given in Table 2. Similarly, some resaearchers have reported that $PM_{2.5}$ has increased to 10 units from the normal period to the vacation period, whereas PM_{10} has increased to 22 units during the same period in Latin America Megacity [23].

Population and density

Chennai is one of the largest cities in South India, with a population of 72,53,531. The city's population increased from 17,49,000 (1966) to 72,53,531 (2011), and its area increased from 128.83 km^2 in 1961 to 426 km^2 in 2011, with the population density increasing from 128.83 to 17027 during the same period. Being an important commercial centre of the state, Chennai's population has experienced rapid population growth.

Table 2. National Ambient Air Quality Standards

S. No	Pollutant	Concentration in air ($\mu g/m^3$)
1	PM_{10}	100
2	$PM_{2.5}$	60

Source: CPCB, 2019

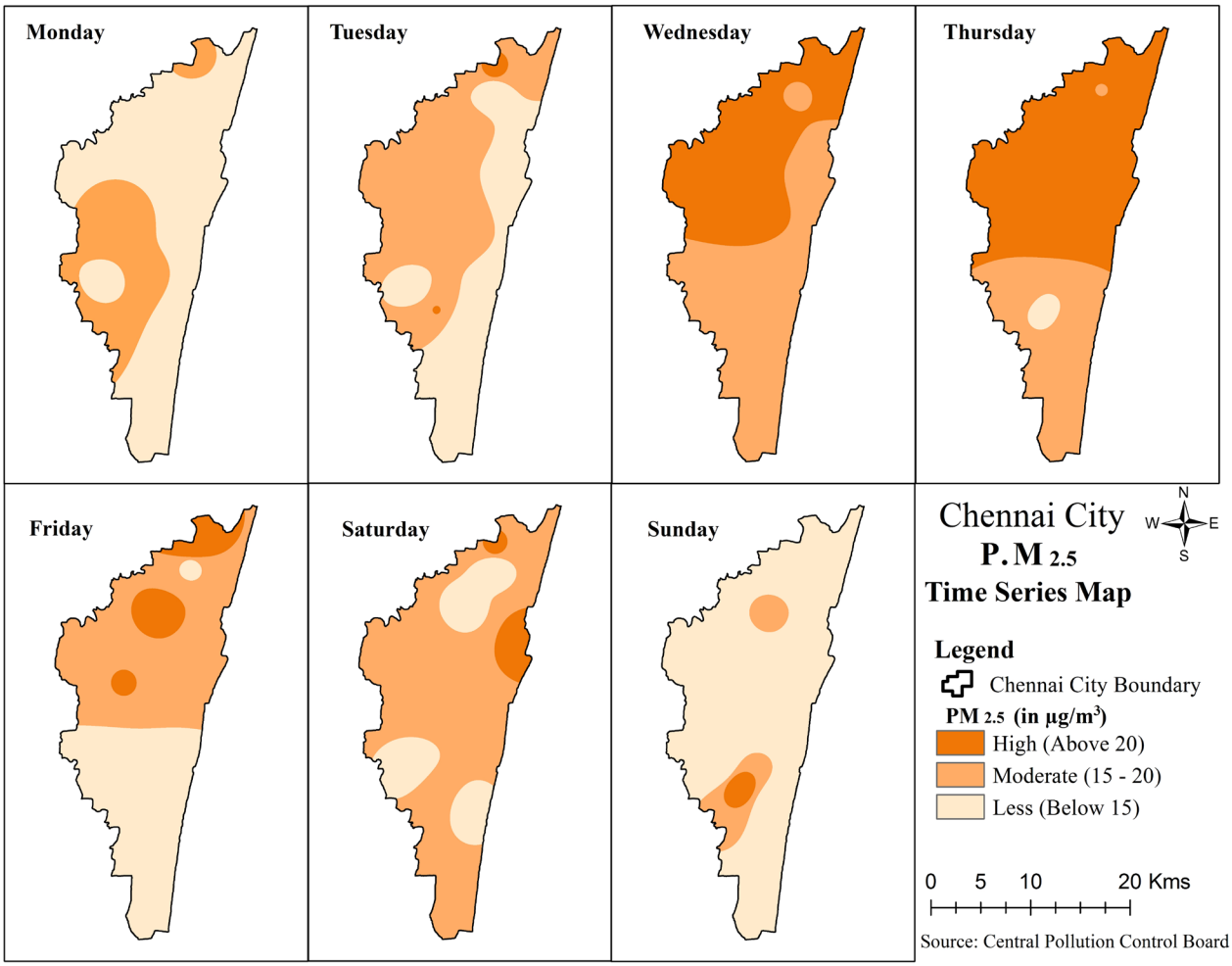

Fig. 2. Spatio-temporal distribution of $PM_{2.5}$- 2021

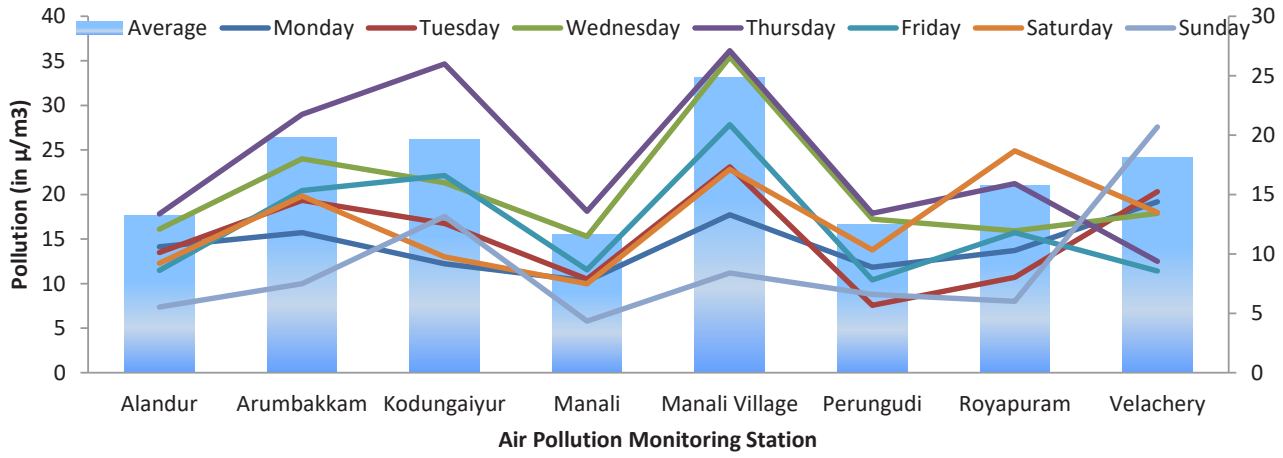

Fig. 3. Distribution of $PM_{2.5}$ – 2021

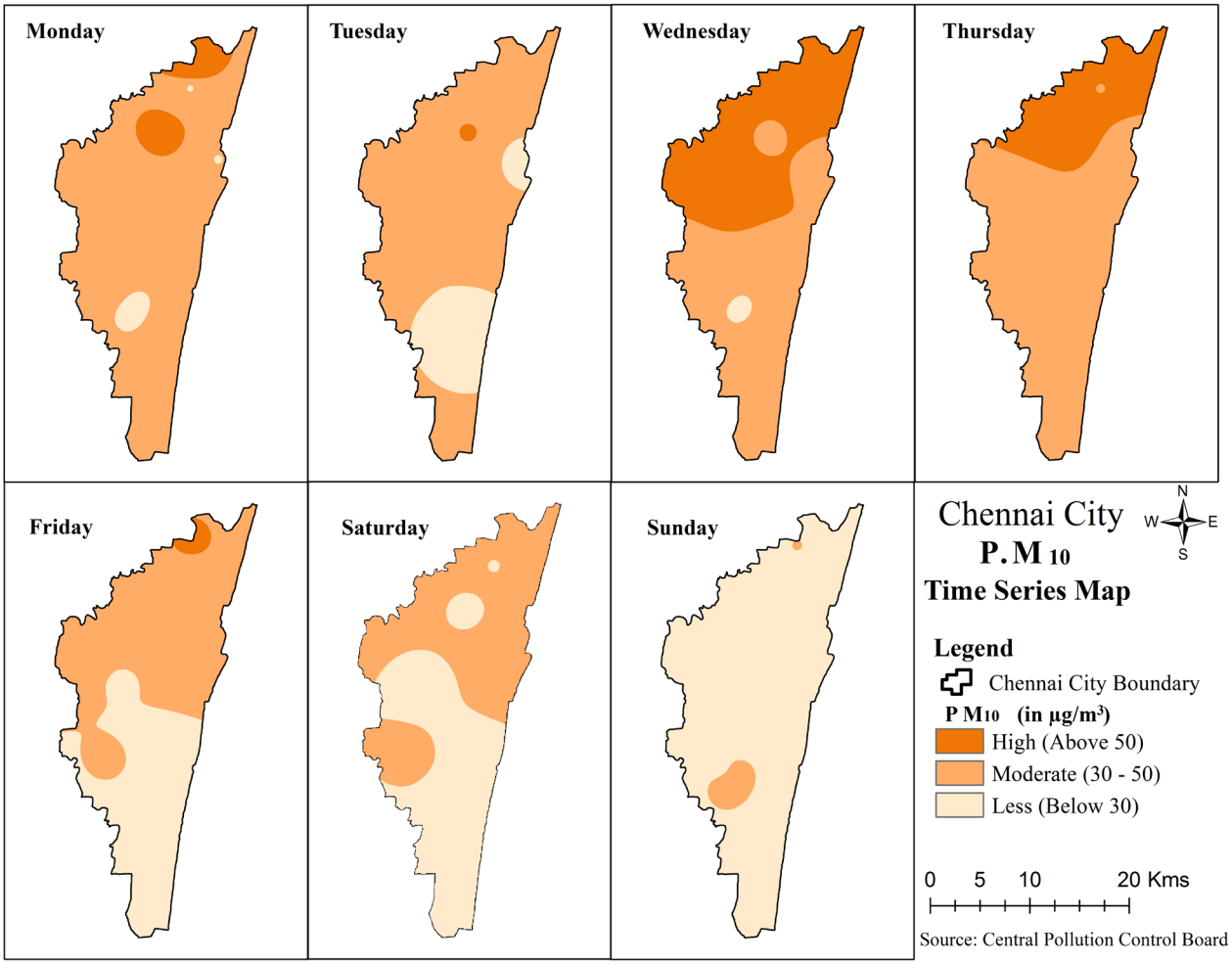

Fig. 4. Spatial and Temporal Distribution of PM_{10} - 2021

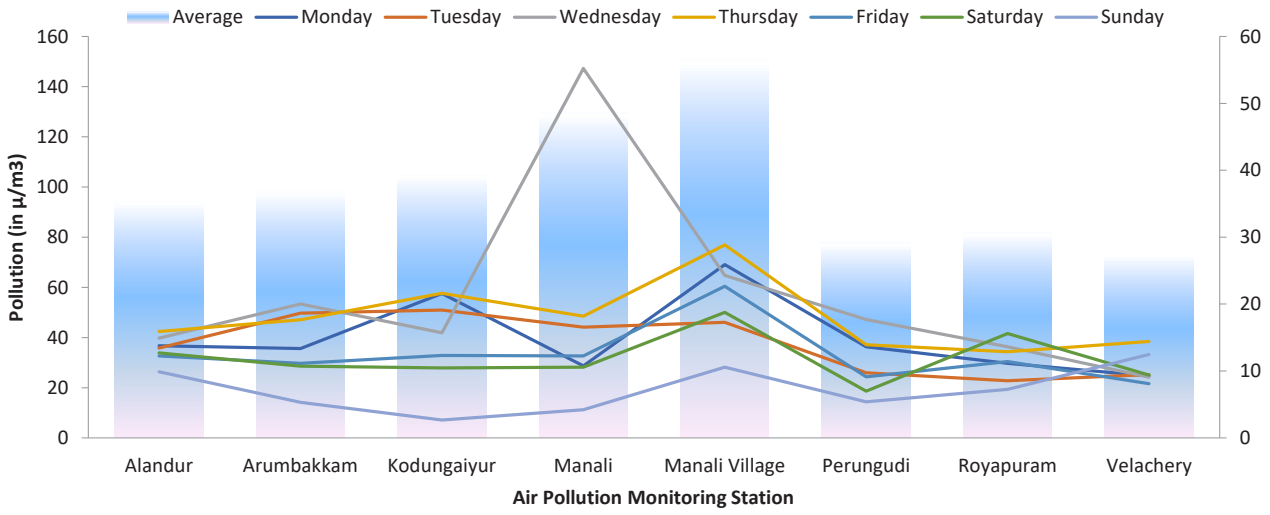

Fig. 5. Distribution of PM_{10} – 2021

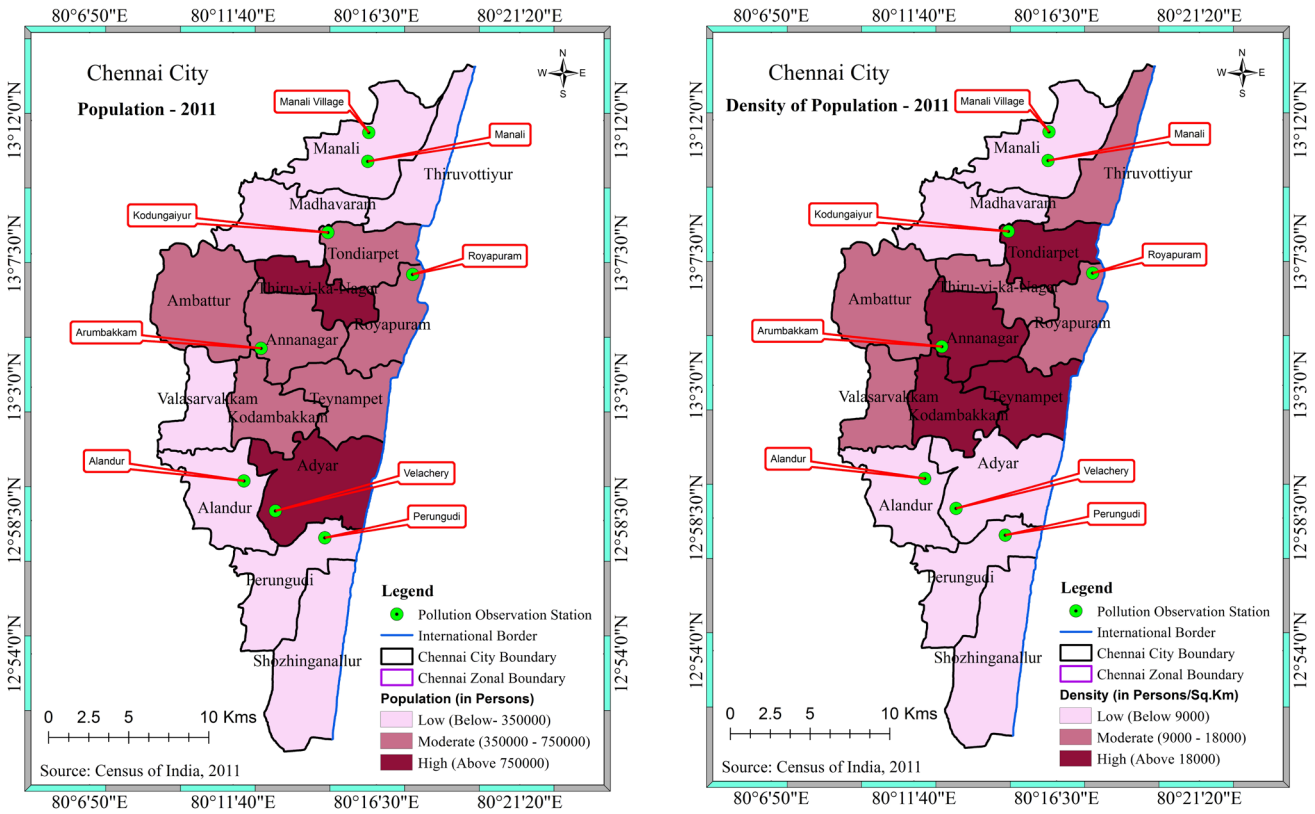

Fig. 6. Population and density of population

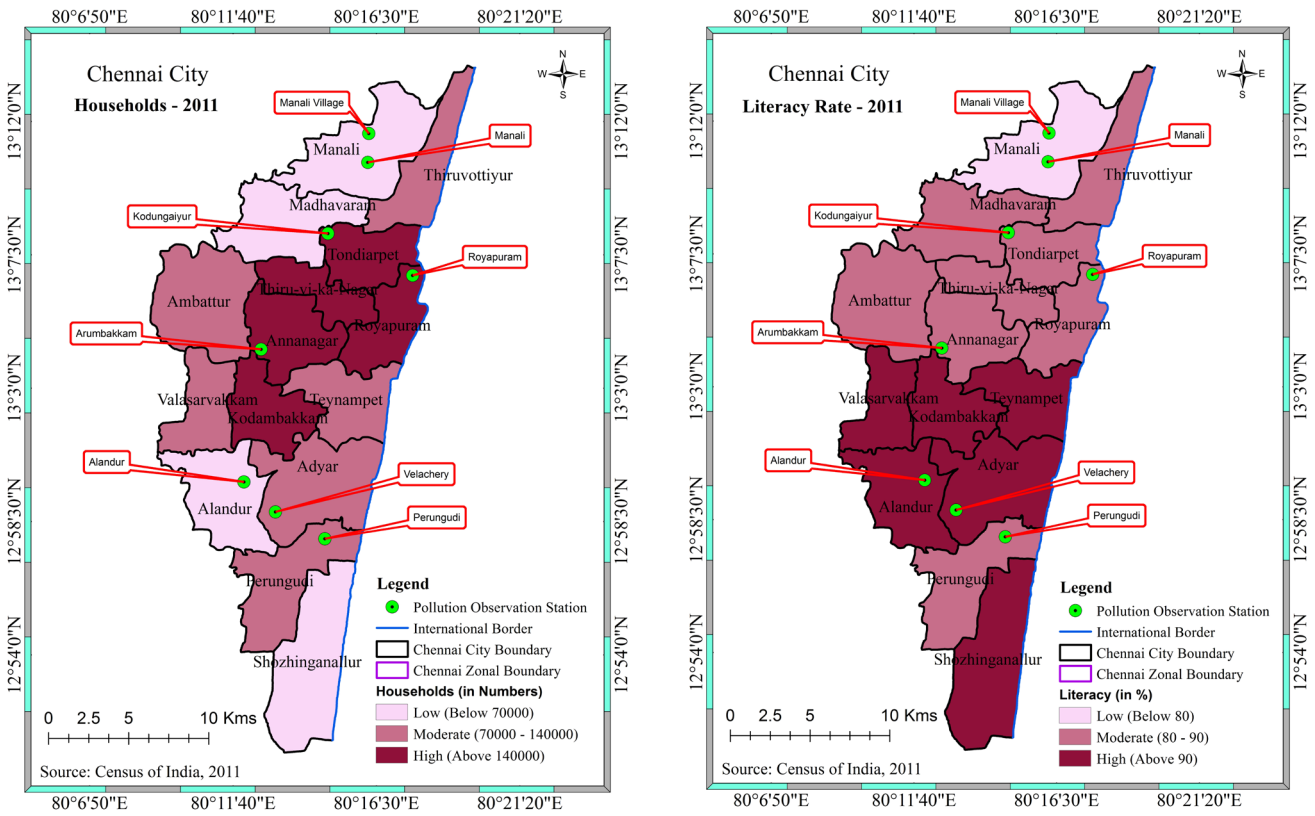

Fig. 7. Household and literacy rate

Chennai has become an important destination for trade and tourism in recent years. Due to its economic viability and available infrastructure, the city was referred to with enormous potential for industrial growth. According to the 2011 Census for Chennai, the population density is 26,553 people per km^2. Around 175 km^2 of the area is urban, though no rural area exists. Moreover, Anna Nagar, Tondairpet, Kodambakkam, and Teynampet zones had very high population density and female population density compared to Chennai city zones (Fig. 6). Researchers in a study reported that the population in urban area significantly impacts the air quality in China [24].

Households

According to the 2011 census, the Chennai district has 1.1 million families, with 51% in rented houses. Household is also very high in Thiru vi ka Nagar zone when comparing other zones in Chennai city followed by Royapuram, Kodambakkam and anna nagar zone. The lowest household population is in Sholinganallur and Manali zone, in the south and north extreme, respectively.

Literacy Rate

The mean literacy ratio in 2001 was 85.33 %, and 90.33 % in 2011. It is expressed much higher than the national mean of 79.5 %. Out of 3,776,276 literates, 1,968,079 were males (93.7%), while 1,808,197 were females (86.64%) in the Chennai district. Adyar, Kodambakkam, and Teynampet zones had very high female literacy rates when comparing other zones in Chennai city (Fig. 7).

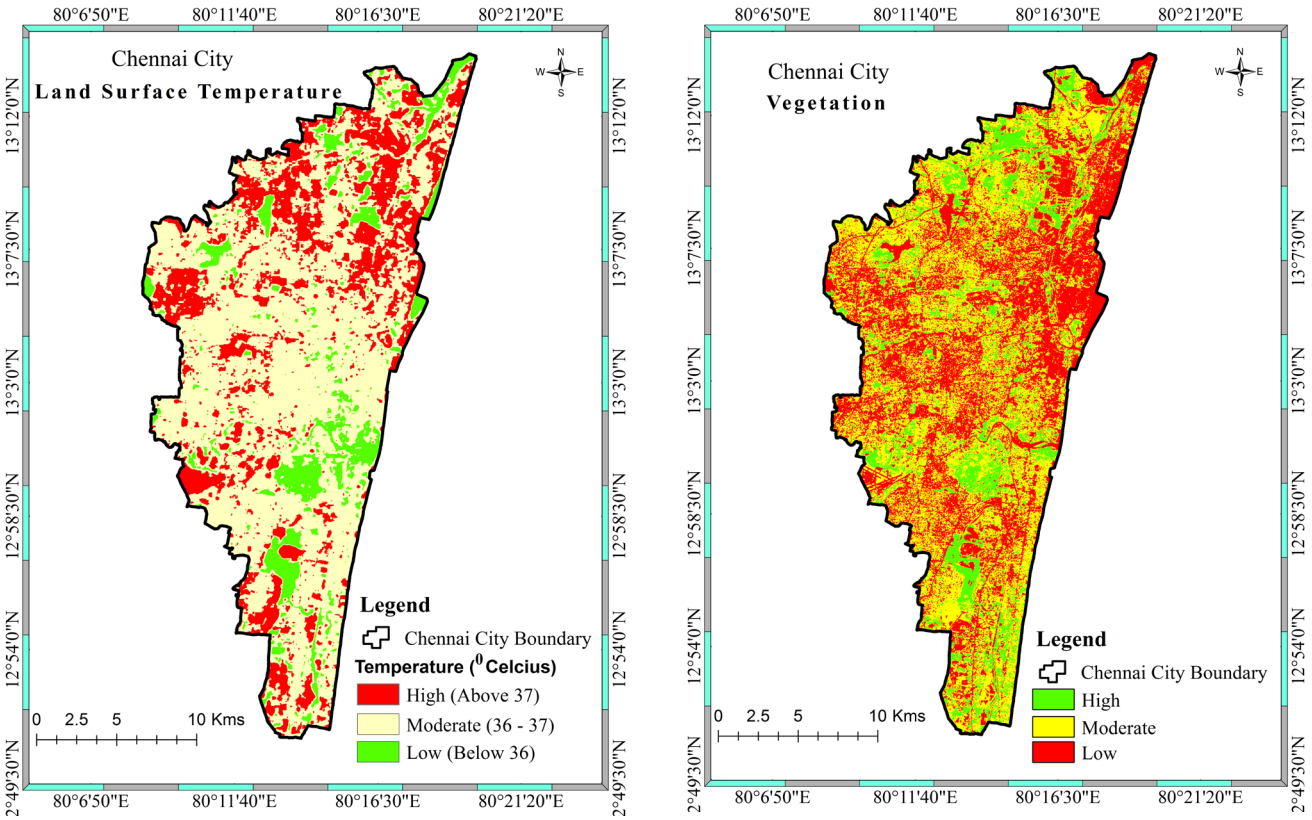

Fig. 8. Land surface temperature and vegetation - 2021

Land surface temperature (LST)

The land surface temperature has been identified using band 4, band 5 and band 10 of the Landsat image, a satellite image from the United State Geological Survey (USGS). Chennai city is located in a tropical region that receives maximum solar radiation, which triggers the land surface temperature, which will be regulated due to various reasons such as vegetation and water body. The Chennai region has been classified into three categories based on high, moderate and low land surface temperature. High LST is a region above 370C; moderate LST regions are between 360 C to 370 C; low LST is a region below 360 C. High LST occupies 108 sq. km (23%), moderate LST occupies 275 km^2 (24 %). Low LST occupies 44 sq. km (10 %) (Fig. 8). Similarly, some researchers have reported that the temperature in urban area significantly impacts the air quality in China [24].

Vegetation

The NDVI is a dimensionless index that reflects the variation in vegetation cover's visible and near-infrared reflectance and can be used to assess the density of green on a piece of Land. High vegetation in Chennai city occupies 39 km^2, 13% of the total area. Moderate vegetation occupies 195 km^2, which is 45% of the total geographical area of Chennai city. Low vegetation occupies 173 km^2, 40% of the total geographical area. Vegetation is maximum in the northern part and southern parts of Chennai (Fig. 8). Researchers has reported that the vegetation in the urban areasignificantly impacts the air quality in China [24].

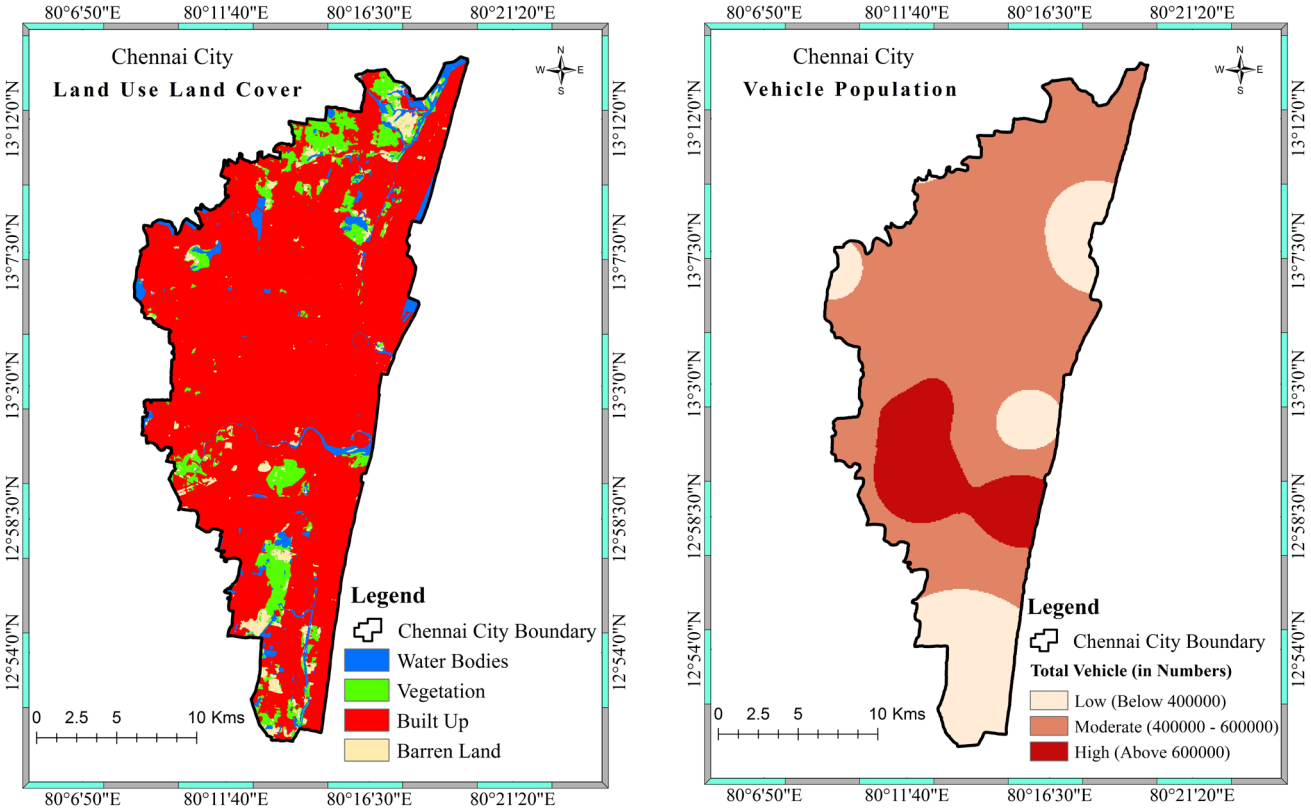

Fig. 9. Land use land cover and vehicle population-2021

Land use land cover (LULC)

LULC for Chennai has performed for 2021 with type 1 classification based on National Remote Sensing Corporation (NRSC). LULC classification of vegetation, built-up, water body and Barren Land has been demarcated. Vegetation features cover 34 km^2, which occupies 8% of the total area; built features are covered the maximum area of Chennai city with 357 sq. km, which is 83% of the total Chennai area. The water body covers 21 km^2 with 5% of the total area. Finally, the Barren land feature covers 14 km^2, which is 3.5% of the total area of Chennai city. Chennai city has three rivers: the Kosasthalaiyar river, with a total length of 136 km; the Coum river, with a total length of 64 km; and the Adyar river, which runs 42 km (Fig. 9).Similarly, researchers have reported that the buildup area has significantly impacted the air quality in China [24].

Vehicle population

Overall, Chennai the vehicle population is moderate level. In the Adyar, Alandur, Kodambakkam, and Valassaravakkam regions, the vehicle population is high, whereas, in Shozhinganallur and Tondiarpet, the vehicle population is less shown in Fig. 9.

Prediction model

The model performed based on multiple regression shows that the model predicting the responsible factor for $PM_{2.5}$ is significant with a correlation of 0.769, which is high. It reveals that the dependent variable is 76.9% predicting the air pollution for $PM_{2.5}$. Similarly, the model predicting the responsible factor for PM_{10} is significant, with a correlation of 0.854, which is high. It reveals that the dependent variable is 85.4% predicting the air pollution for PM_{10} shown in Table 3. Researchers has studied that automobile exhaust gas is discharged into the air, causing severe air pollution in Beijing, China [25].

The parameters such as LST and Vegetation has not significant in both pollutants ($PM_{2.5}$ and PM_{10}), revealing that neither LST nor Vegetation is not determining the air pollution in Chennai city. Literacy rate and Land use, land cover, and vegetation show negative values on both pollutants, which means air pollution and literacy rate, LULC and vegetation are inversely proportional. In contrast, households, population density, and vehicle population are directly proportional to air pollution, particularly $PM_{2.5}$ and PM_{10}. Vehicle population has more responsible for particulate matter, followed by density, households and population shown in Table 4.

Table 3. Model summary

Model	R	R^2	Sig. F Change
$PM_{2.5}$	.769[a]	.448	.000
PM_{10}	.854[a]	.729	.000

Table 4. Coefficient of regression

Parameters	$PM_{2.5}$		PM_{10}	
	B	Sig.	B	Sig.
(Constant)	18.237	0.000	55.476	0.000
Households	1.128	0.000	5.074	0.000
Densityof Population	1.573	0.000	3.910	0.000
Literacy Rate	-1.434	0.000	-7.281	0.000
Population	0.611	0.000	0.617	0.030
LST	0.186	0.151	0.126	0.669
LULC	-0.232	0.013	-0.512	0.016
Vegetation	-0.065	0.475	-0.095	0.648
Vehicle Population	14.000	0.001	22.000	0.005

The prediction model for $PM_{2.5}$ is:

$PM_{2.5}$=18.23 +1.12*households+1.57*Density of population-1.43*literacy rate+0.61 *Population -0.23 * LULC +14.00*Vehicle Population

The prediction model for PM_{10} is:

PM_{10}=55.47 +5.07*households + 3.91 *Density of population-7.28*literacy rate+0.61*Population -0.51* LULC+22.00*Vehicle Population

Conclusion

The study reveals that the particulate matter is below the standard value prescribed by the Central pollution control board. The highest air pollution in Chennai city is primarily responsible for vehicle population and industries. Wednesday and Thursday recorded maximum pollution in the study area, whereas Sunday was very low compared to other days. Regression shows that the vehicle populationis responsible for air pollution, followed by the population.Regression also reveals that vehicle population is highly responsible for PM_{10}, followed by $PM_{2.5}$.

Financial supports

The study has been funded by RUSA 2.0 "Research, Innovation and Quality Improvement" Data Analytics for Real-Time Monitoring and Prediction of Pollution in Chennai. Studies on Social and Behavioral Sciences and Linguistics (Theme-3).

Competing interests

The authors have declared no conflict of interest

Authors' contributions

Dr Yuvaraj R M: Conceptualization, Methodology,

Data curation, analysis, preparation of Map and Original draft preparation, M. Sakthivel and & M. R. Sindhumol: Data collection, Reviewing and Editing,

Acknowledgements

This study was carried out as part of the project funded by RUSA 2.0 "Research, Innovation and Quality Improvement" Data Analytics for Real-Time Monitoring and Prediction of Pollution in Chennai. Studies on Social and Behavioral Sciences and Linguistics (Theme - 3) in the Department of Geography, University of Madras. We thank the Central Pollution Control Board and State Pollution Control Board for providing the monitoring data.

Ethical considerations

Ethical issues (Including plagiarism, Informed Consent, misconduct, data fabrication and/or falsification, double publication and/or submission, redundancy, etc) have been completely ob-served by the authors).

References

1. Johnson TM, Guttikunda S, Wells GJ, Artaxo P, Bond TC, Russell AG, et al. Tools for improving air quality management: A review of top-down source apportionment techniques and their application in developing countries. Available from: http://hdl.handle.net/10986/17488

2. Goyal P, Krishna TR. Various methods of emission estimation of vehicular traffic in Delhi. Transportation Research Part D: Transport and Environment. 1998 Sep 1;3(5):309-17. Available from: http://dx.doi.org/10.1016/s1361-9209(98)00009-1

3. Cole MA, Neumayer E. Examining the impact of demographic factors on air pollution. Population and Environment. 2004 Sep 1:5-21. Available from: http://dx.doi.org/10.1023/b:poen.0000039950.85422.eb

4. Gore RW, Deshpande DS. An approach for classification of health risks based on air quality levels. In2017 1st International Conference on Intelligent Systems and Information Management (ICISIM) 2017 Oct 5 (pp. 58-61). IEEE. Available from: https://doi.org/10.1016/j.scitotenv.2021.148605

5. Litchfield I, Dockery D, Ayres J. Health effects of air pollution. Environmental Medicine [Internet]. 2010 Jul 30;141–52. Available from: http://dx.doi.org/10.1201/b13390-16

6. Shaddick G, Thomas ML, Mudu P, Ruggeri G, Gumy S. Half the world's population are exposed to increasing air pollution. NPJ Climate and Atmospheric Science. 2020 Jun 17;3(1):23. Available from: http://dx.doi.org/10.1038/s41612-020-0124-2

7. Ali MU, Liu G, Yousaf B, Ullah H, Abbas Q, Munir MA. A systematic review on global pollution status of particulate matter-associated potential toxic elements and health perspectives in urban environment. Environmental geochemistry and health. 2019 Jun 15;41:1131-62. Available from: http://dx.doi.org/10.1007/s10653-018-0203-z

8. Xu X, Xia J, Gao Y, Zheng W. Additional focus on particulate matter wash-off events from leaves is required: A review of studies of urban plants used to reduce airborne particulate matter pollution. Urban Forestry & Urban Greening. 2020 Feb 1;48:126559. Available from: http://dx.doi.org/10.1016/j.ufug.2019.126559

9. Diener A, Mudu P. How can vegetation protect us from air pollution? A critical review on green spaces' mitigation abilities for air-borne particles from a public health perspective-with implications for urban planning. Science of the Total Environment. 2021 Nov 20;796:148605.

10. Cole MA, Neumayer E. Examining the

impact of demographic factors on air pollution. Population and Environment. 2004 Sep 1:5-21. Available from: http://dx.doi.org/10.1023/b:poen.0000039950.85422.eb

11. Zou B, Peng F, Wan N, Mamady K, Wilson GJ. Spatial cluster detection of air pollution exposure inequities across the United States. PLoS One. 2014 Mar 19;9(3):e91917. Available from: http://dx.doi.org/10.1371/journal.pone.0091917.

12. Ilić I, Vuković M, Štrbac N, Urošević S. Applying GIS to Control Transportation Air Pollutants. Polish Journal of Environmental Studies. 2014 Sep 1;23(5). Available from: https://doi.org/10.18485/ecologica.2022.29.106.17

13. Syafei AD, Fujiwara A, Zhang J. A comparative study on NO concentration interpolation in Sena Baya city. Proceedings of the Eastern Asia Society for Transportation9. 2013:1-3. Available from: https://doi.org/10.1016/j.proenv.2015.07.061

14. Li L, Gong J, Zhou J. Spatial interpolation of fine particulate matter concentrations using the shortest wind-field path distance. PloS one. 2014 May 5;9(5):e96111. Available from: https://doi.org/10.1371/journal.pone.0096111.

15. Halek F, Kavousi-Rahim A. GIS assessment of the PM_{10}, $PM_{2.5}$ and PM1.0 concentrations in urban area of Tehran in warm and cold seasons. International Archives of the Photogrammetry, Remote Sensing & Spatial Information Sciences. 2014 Nov 15. Available from: http://dx.doi.org/10.5194/isprsarchives-xl-2-w3-141-2014

16. Barsi JA, Schott JR, Hook SJ, Raqueno NG, Markham BL, Radocinski RG. Landsat-8 thermal infrared sensor (TIRS) vicarious radiometric calibration. Remote Sensing. 2014 Nov 21;6(11):11607-26. Available from: http://dx.doi.org/10.3390/rs61111607.

17. J Jiménez-Muñoz JC, Sobrino JA, Gillespie A, Sabol D, Gustafson WT. Improved land surface emissivities over agricultural areas using ASTER NDVI. Remote Sensing of Environment. 2006 Aug 30;103(4):474-87. Available from: http://dx.doi.org/10.1016/j.rse.2006.04.012.

18. Carlson TN, Ripley DA. On the relation between NDVI, fractional vegetation cover, and leaf area index. Remote sensing of Environment. 1997 Dec 1;62(3):241-52. Available from: http://dx.doi.org/10.1016/s0034-4257(97)00104-1.

19. Sobrino JA, Jiménez-Muñoz JC, Paolini L. Land surface temperature retrieval from LANDSAT TM 5. Remote Sensing of environment. 2004 Apr 30;90(4):434-40. Available from: http://dx.doi.org/10.1016/j.rse.2004.02.003.

20. Weng Q, Lu D, Schubring J. Estimation of land surface temperature–vegetation abundance relationship for urban heat island studies. Remote sensing of Environment. 2004 Feb 29;89(4):467-83. Available from: http://dx.doi.org/10.1016/j.rse.2003.11.005.

21. Wang F, Qin Z, Song C, Tu L, Karnieli A, Zhao S. An improved mono-window algorithm for land surface temperature retrieval from Landsat 8 thermal infrared sensor data. Remote sensing. 2015 Apr 10;7(4):4268-89. Available from: http://dx.doi.org/10.3390/rs70404268.

22. Stathopoulou M, Cartalis C. Daytime urban heat islands from Landsat ETM+ and Corine land cover data: An application to major cities in Greece. Solar Energy. 2007 Mar 1;81(3):358-68. Available from: http://dx.doi.org/10.1016/j.solener.2006.06.014

23. Fredy Alejandro GL, Marco Andres GL, Nestor Yezid RR. Spatial-temporal assessment and mapping of the air quality and noise pollution in a sub-area local environment inside the center of a Latin American Megacity: Universidad Nacional de Colombia-Bogotá Campus. Asian Journal of Atmospheric Environment. 2018;12(3):232-43. Available from: http://dx.doi.org/10.5572/ajae.2018.12.3.232.

24. Zhang X, Gong Z. Spatiotemporal characteristics of urban air quality in China

and geographic detection of their determinants. Journal of Geographical Sciences. 2018 May;28:563-78. Available from: http://dx.doi.org/10.1007/s11442-018-1491-z

25. Chen P. Visualization of real-time monitoring datagraphic of urban environmental quality. Eurasip Journal on Image and Video Processing. 2019 Dec;2019(1):1-9. Available from: http://dx.doi.org/10.1186/s13640-019-0443-6.

Journal of Air Pollution and Health (Winter 2023); 8(1): 103-116

Review Article

Available online at http://japh.tums.ac.ir

House environmental conditions with the event of acute respiratory infection (ARI) in toddlers in Indonesian: A meta-analysis

Muhammad Addin Rizaldi

Department of Environmental Health, Faculty of Public Health, Airlangga University, East Java, Indonesia

ARTICLE INFORMATION

Article Chronology:
Received 05 October 2022
Revised 16 January 2023
Accepted 01 March 2023
Published 29 March 2023

Keywords:
Humidity; Ventilation; Acute respiratory infection (ARI); Toddler

CORRESPONDING AUTHOR:

muhammad.addin.rizaldi-2021@fkm.unair.ac.id
Tel: (+62 31) 5920948
Fax: (+62 31) 5920948

ABSTRACT

Acute Respiratory Infection (ARI) is an infection that attacks the lower or upper respiratory tract and has the potential to be transmitted to other people. It depends on the causative pathogen and home environmental factors which affect it. The study analyzes the relationship between home environmental conditions, including ventilation, humidity, floors, residential density, and smoking habits, with the incidence of Acute Respiratory Infection (ARI) in Toddlers in Indonesia by conducting a meta-analysis of data from various research articles. The method in this study is a meta-analysis by finding the effect size value using JASP software. Articles performed a meta-analysis of 25 articles. The results of the meta-analysis found that the variable density of residential has 1,135 times larger, 1,665 times greater ventilation, 1.568 times greater, and the floor conditions 1,309 times larger, as well as the habit sapped. The conclusion from the results of this study shows that the condition of the home environment that has the most influence is the humidity of the house, and the one with the lowest risk is residential density. Suggestions for controlling risk, providing community education, and assistance for healthy homes.

Review

Acute Respiratory Infection (ARI) is an infection that attacks the lower or upper respiratory tract and has the potential to be transmitted to other people so that it can cause an expansion of the disease ranging from asymptomatic to severe, the spread of the disease depends on the pathogen, environmental factors and host factors. However, ARI is also often defined as an acute respiratory tract disease caused by infectious agents transmitted from human to human [1]. Bacteria are the main cause of respiratory tract infections, whereas the bacteria that causes Streptococci pneumonia is the most common cause of pneumonia. However, most acute respiratory infections are caused by viruses or a mixture of viruses and bacteria. Acute respiratory infections have the potential to become endemic or even pandemic and may pose a public health risk [2].

Please cite this article as: Rizaldi MA. House environmental conditions with the event of acute respiratory infection (ARI) in toddlers in Indonesian: A meta-analysis. Journal of Air Pollution and Health. 2023;8(1): 103-116.

Copyright © 2023 Tehran University of Medical Sciences. Published by Tehran University of Medical Sciences.
This work is licensed under a Creative Commons Attribution-NonCommercial 4.0 International license (https://creativecommons.org/licenses/by-nc/4.0/). Noncommercial uses of the work are permitted, provided the original work is properly cited.

Acute Respiratory Tract Infection (ARI) causes the largest single infectious death in children worldwide. Data from World Health Organization (WHO) states that around 808,694 children under five died from ARI in 2017, accounting for around 15% of deaths of children under five. ARI is most common in South Asia and sub-Saharan Africa [3]. Based on what has been explained by the World Health Organization (WHO), Acute Respiratory Infection (ARI) is the main cause of morbidity and mortality due to infectious diseases in the world. Nearly 4 million people die from this infection yearly, of which lower respiratory tract infections cause nearly 98% of these deaths. Deaths from respiratory infections are usually at higher risk for infants, young children, and the elderly, especially those in low- and middle-income countries. ARI is one of the main causes of consultation or treatment in health care facilities, especially children's services [2].

The result from Indonesia Basic Health Research (Riskesdas) in 2013 showed that the incidence of ARI was 25%, while the highest occurred in the age group 1-4 years, namely 25.8%, 2014 ARI cases in toddlers were recorded at 657,490 cases or equivalent to 29.4% [4]. Data from the Indonesian Health Profile in 2019 shows an increase in the number of ARI cases in children under five, whereas, in 2019, 52.9% of ARI cases were found [5]. The mortality rate caused by ARI in children under five is 0.12% [6]. The research results showed that most ARI patients were found in the 12-60 month age group [7]. Based on the Indonesia Health Post in 2021, the scope of discovery of acute respiratory infection (ARI) cases still does not meet the target, meaning that many cases still have not been found. In 2021 the mortality rate due to pneumonia in toddlers was 0,16%. The mortality rate due to pneumonia in the infant group is almost double that in a group of children aged 1-4 years [8].

World Health Organization divides several factors that influence the occurrence of ARI. One of the causes is environmental conditions such as air pollution, household density, humidity, cleanliness, season, and temperature [9]. The incidence of ARI is influenced by environmental conditions, namely air pollution and home ventilation. Based on the results of research conducted in Padang, West Sumatra, that place of residence influences the incidence of ARI [7]. Another study stated that one of the environmental factors that affect the incidence of ARI is residential density [10]. Occupancy density is not a single factor that can affect the occurrence of ARI based on the results of research conducted in Mimika Papua showing that house ventilation has a significant relationship with respiratory tract infections in infants [11].

Physical components home environment is an important factor in impacting the health status of the house's occupants. Health requirements are needed because they are used for housing construction, which greatly influences the improvement of health status. Several factors that influence ARI to include nutritional status, exclusive breastfeeding, completeness of immunization, gender, ventilation, lighting, humidity, floors, walls, roofs, residential density, cooking fuel, smoking family members, mother's education, mot and her's occupation, and family income (Ministry of Health, Indonesia 2009). Research in Muna Regency shows that the condition of the home environment has a significant relationship with respiratory tract infections in infants [12].

This study aims to analyze the relationship between home environmental conditions, including ventilation, humidity, floors, and residential density, with the incidence of Acute Respiratory Infection (ARI) in Toddlers in Indonesia by conducting a meta-analysis of data from various research articles. Using the Meta-analysis method, researchers can combine a smaller study and make it a larger study so as to show the effect. In addition, meta-analysis can

improve the accuracy of the results.

Methods

The type of research that will be conducted is a meta-analysis study, a systematic study accompanied by statistical techniques to calculate several research results regarding the quality of home ventilation with ARI in toddlers. The study's literature searched was limited to only those who conducted research in Indonesia from 2017 to 2021.

The meta-analysis method has the advantage of being objective compared to other study methods and can estimate the effect size quantitatively and its significance. However, it is difficult to use this study to conclude because the combined studies were of different quality, there was publication bias, and the limitations of the data collected. So the meta-analysis research must apply several selections in the selected journal articles.

The data is then compiled and analyzed to be used as a solution to the problems carried out by the Meta-Analysis. The Fig. 1 is an image of a literature scattering diagram.

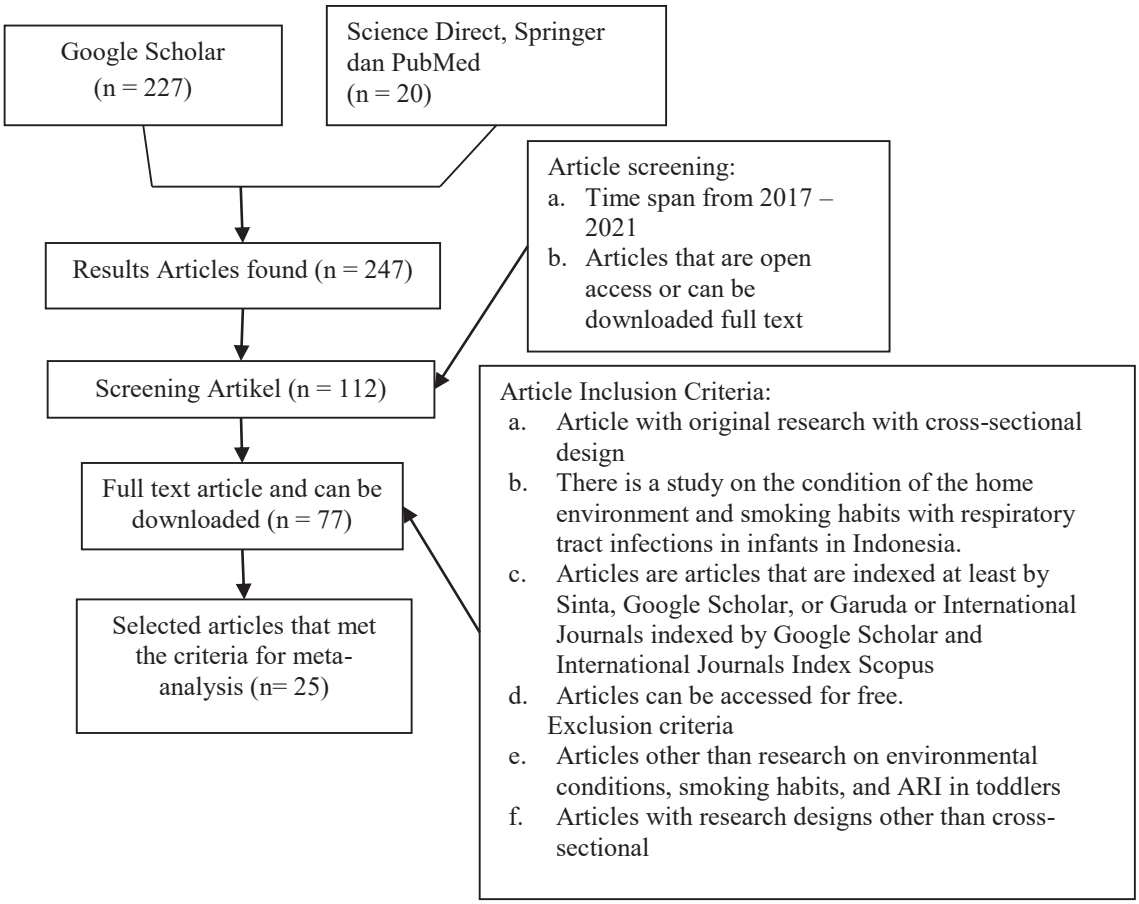

Fig. 1. An image of a literature scattering diagram

The articles that have been obtained are then carried out by a meta-analysis, with 25 research articles obtained. The analysis was carried out to obtain the pooled odds ratio estimate using the Mentel–Haenszel method for the fixed effect analysis model and the DerSimonian–land method for the random-effects model analysis. Meanwhile, if the variation between the variables is heterogeneous or the p-value of heterogeneity is smaller than 0.05, the analysis model used is the random-effects model. The meta-analysis calculates the Prevalence Ratio (PR) value as follows:

1. If the PR value>1 and the confidence interval range is not more than 1, the variable has a risk factor between House Environmental Conditions with respiratory tract infections in infants.

2. If the PR value<1 and the range of confidence intervals exceeds 1, this variable is a protective factor between the condition of house environmental conditions with respiratory tract infections in infants.

3. If the PR value=1 and the confidence interval range is not more than 1, then the variable has no significant relationship.

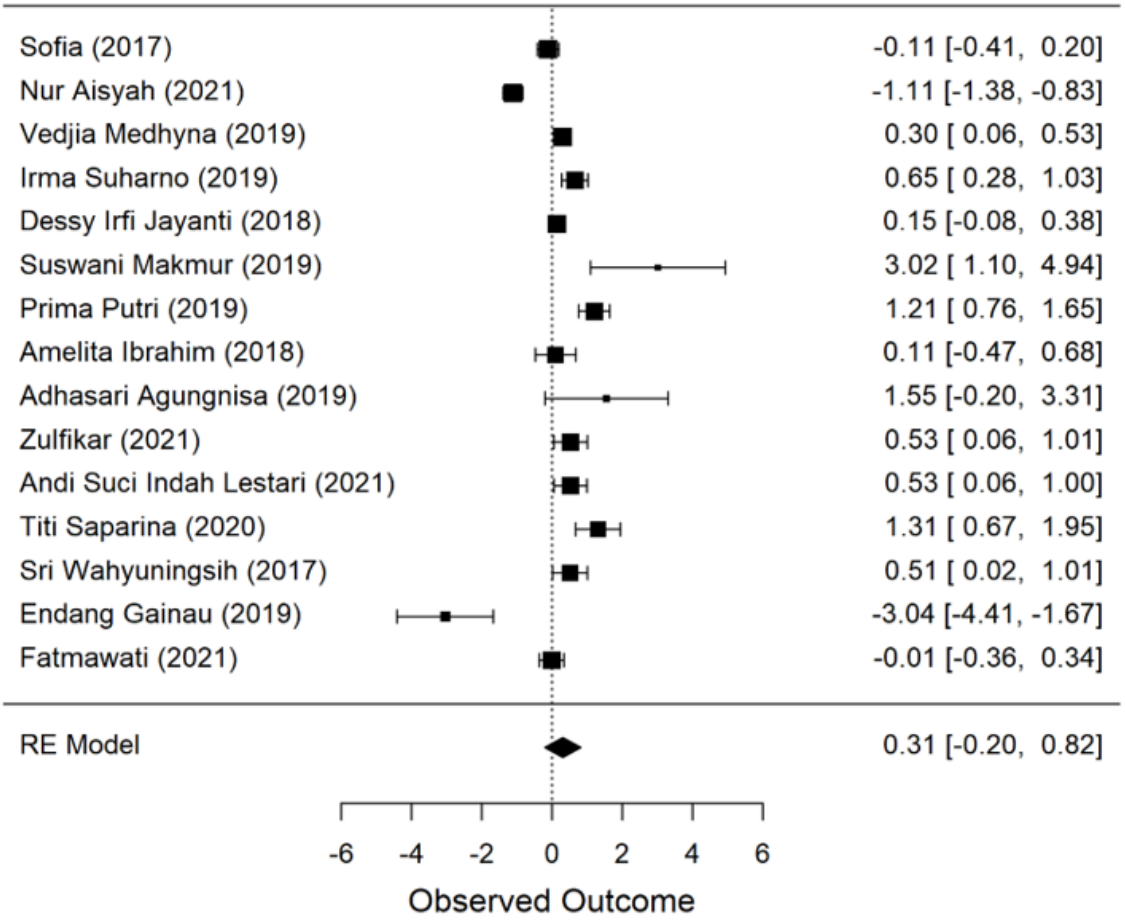

a) Accuracy density variable with ARI incidence in Toddlers

Fig. 2. An image of the result of Forest plot diagram about house environmental conditions (ventilation, occupancy density, humidity, lighting) with respiratory tract infections in infants

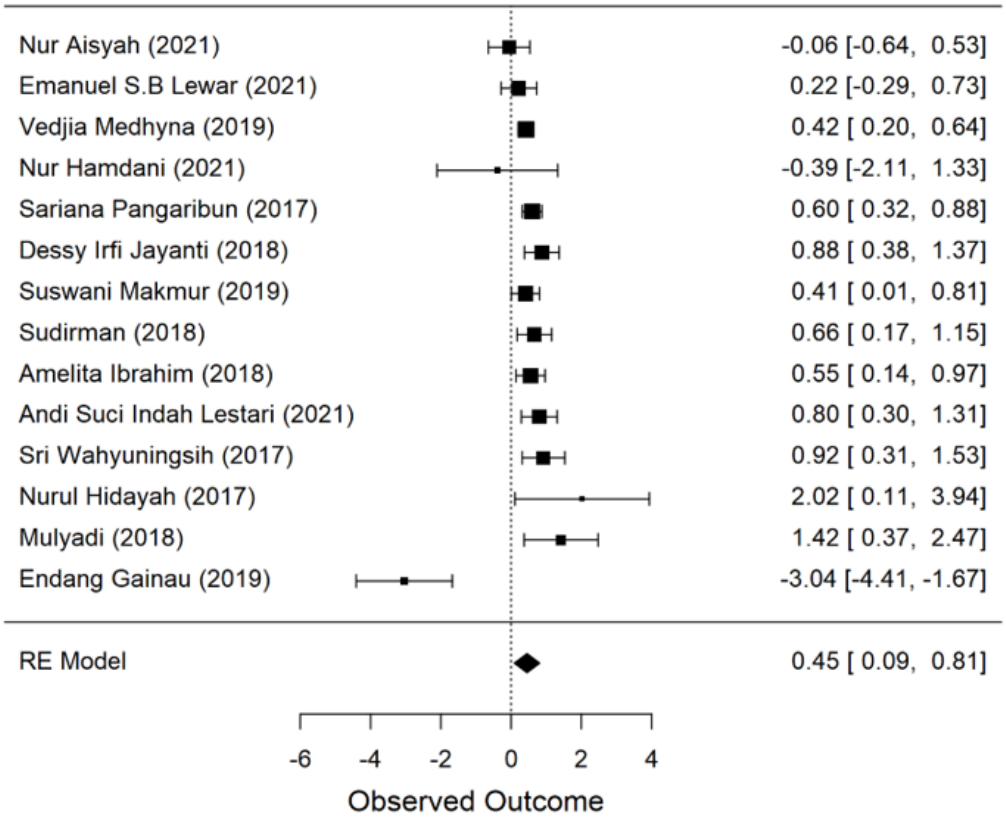

b) Variable Quality of Ventilation with Incidence of ARI in Toddlers

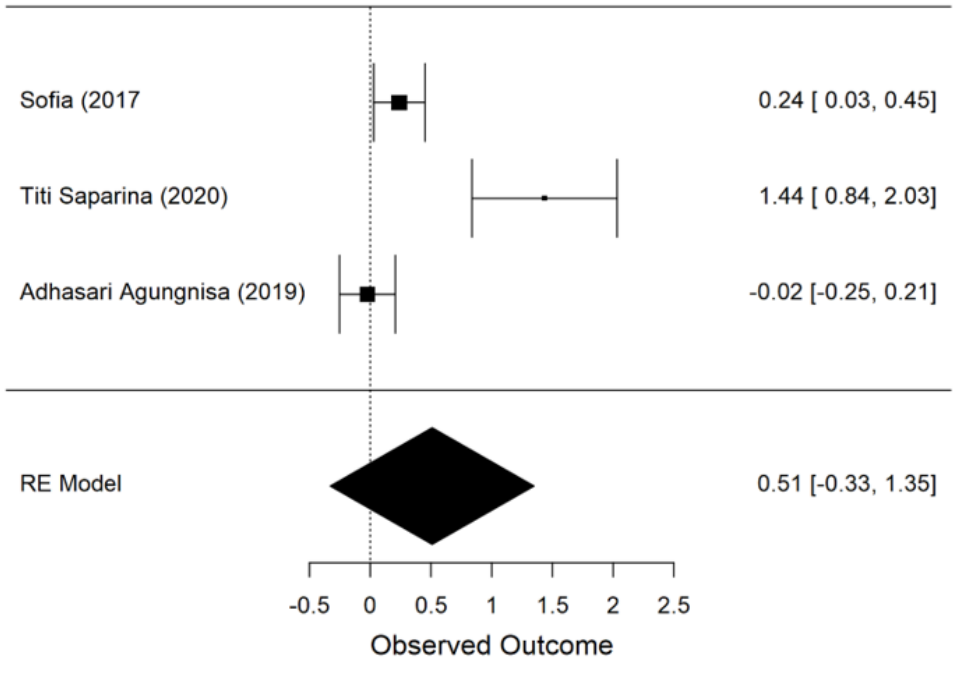

c) Variables of Humidity with the Incidence of ARI in Toddlers

Fig. 2. An image of the result of Forest plot diagram about house environmental conditions (ventilation, occupancy density, humidity, lighting) with respiratory tract infections in infants

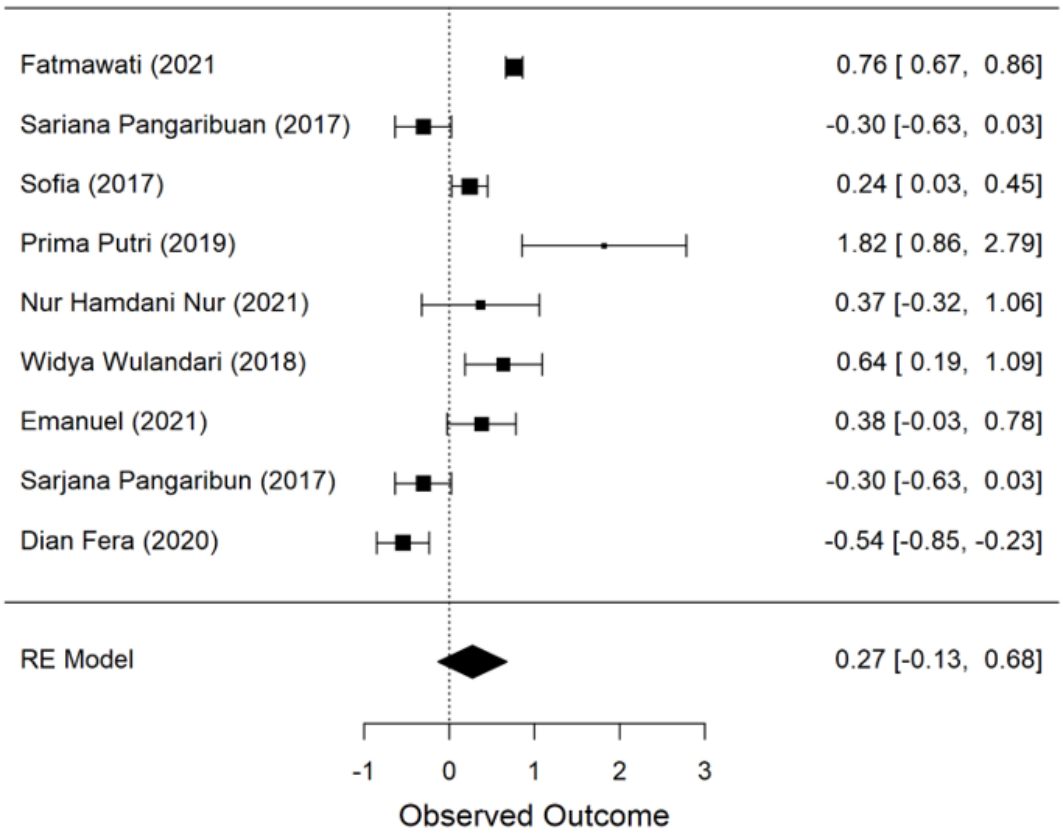

d) Floor Quality Variable with ISPA Incidence in Toddlers

Fig. 2. An image of the result of Forest plot diagram about house environmental conditions (ventilation, occupancy density, humidity, lighting) with respiratory tract infections in infants

Relationship of home environmental conditions (ventilation, occupancy density, humidity, lighting) with respiratory tract infections in infants

a. Meta-Analysis of the Relationship between Occupancy Density and the incidence of ARI in Infants

The p-value in the heterogeneity test is smaller than the value of or less than 0.05, namely p=<0.001, which means that some of these studies have heterogeneous data, so the analysis uses a random-effects model. The results of the forest plot in Fig. 2a shows that the value of pooled PR = $e^{0.31}$ = 1.138 (95% CI -0.20 – 0.82).

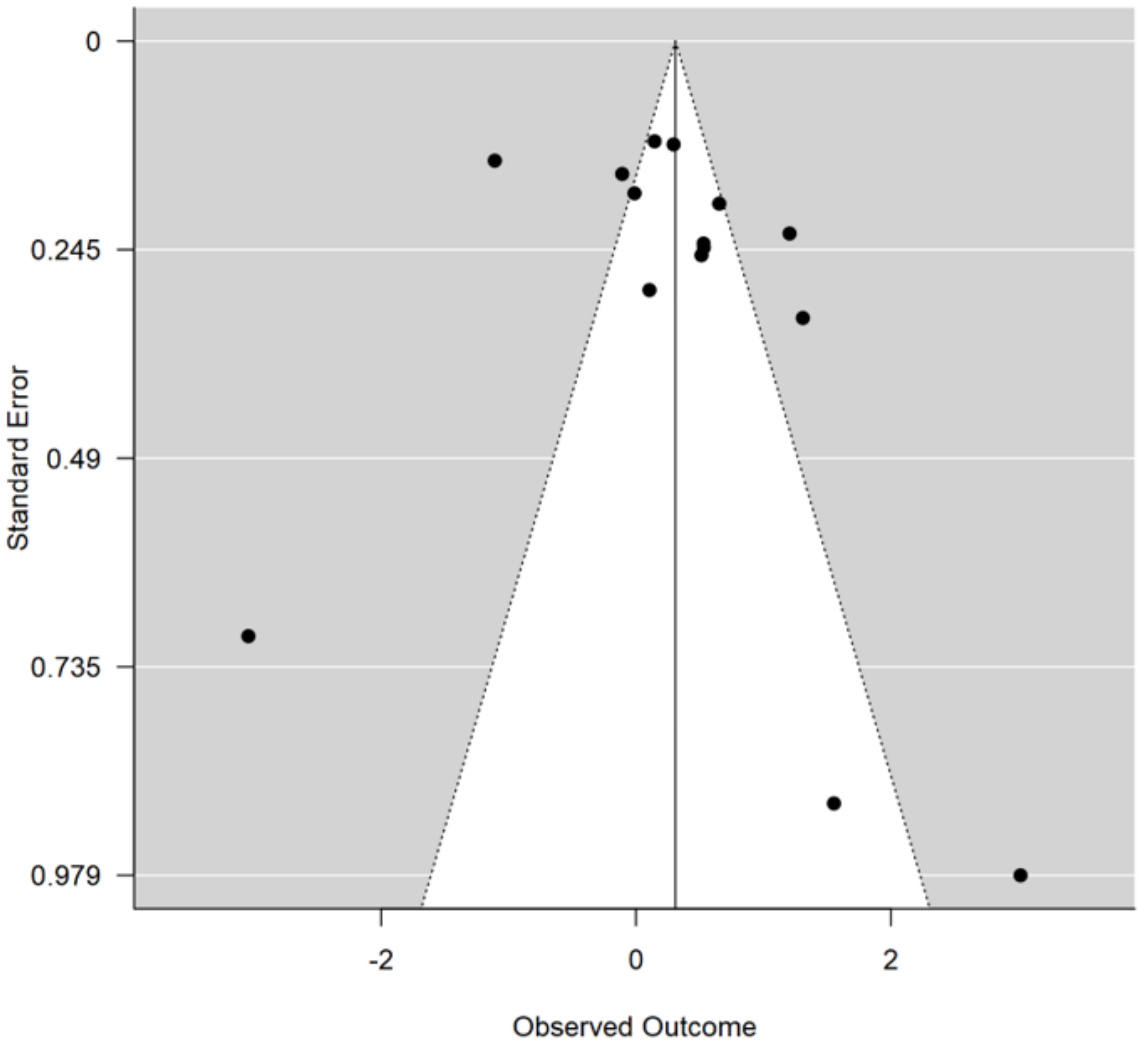

Fig. 3. An Image of the Funnel plot diagram occupancy density with the incidence of ARI in infants

Based on Fig. 3, it can be seen that several points come out of the triangle area, which means that there are indications of publication bias.

The p-value in Egger's test is greater than or more than 0.05, namely the p-value = 0.234, meaning there is no indication of publication bias.

The condition of the home environment, in this case, the density of housing that does not meet the requirements, has a risk of 1,138 times greater for with respiratory tract infections in infants compared to the condition of the density of housing that meets the requirements with a CI value of 95% and does not exceed the number 1 so that the difference between the two groups is a statistically significant risk. From the results of the meta-analysis in this study, poor ventilation can affect the incidence of ARI in infants by 1.138 times greater than good ventilation. This is in line with research that has been conducted, which shows that occupancy density has a significant relationship between ventilation quality and the incidence of ARI in toddlers [13].

This research is also in line with the results of research conducted in the coastal area of Kore village, where the research showed a relationship between settlement density and the incidence of ARI in toddlers [14]. In contrast, several studies conducted in Sorong, Papua, did not show a relationship between occupancy density and the incidence of ARI. The p-value was 0.519 or more

which means there was no relationship. A study conducted in Bangladesh showed that the risk of hospitalization for ARI in children increased in children who lived with high occupancy densities, with a 3.6 times greater chance of having an infection compared to children who lived with low occupancy densities (COR 3.61, 95% CI 2.29–5.74) [15]. Based on research conducted in Nagas Raya Regency showed that occupancy density related to the events of acute respiratory infections with p-value<0.05 (0.006) and occupancy density of 1,845 times the chance of causing ARI in toddlers (PR 95% CI 1,184 -2,876) [16]. Other studies also showed the same results, where the density of occupancy has a relationship that follows the incidence of ARI with p-value<0.05 (p-value = 0.001) and 14.35 times can cause the risk of ARI in children under five (OR CI 95% 2.69-17.04) [17]. Another study conducted in Donggala showed that occupancy density had a significant relationship with respiratory tract infections in infants with a p-value<0.05 (p-value=0.003) [18].

b. Meta-analysis Relationship of ventilation quality with respiratory tract infections in infants The p-value is less than 0.05, meaning the p-value is <0.001 or less than 0.05, so it can be concluded that the air quality data with the incidence of ARI is heterogeneous. When the data is heterogeneous, the analysis uses a random-effects model. The results from the forest plot in Fig. 2b show that the Pooled PR=e=1.568 (95% CI 0.09–0.81).

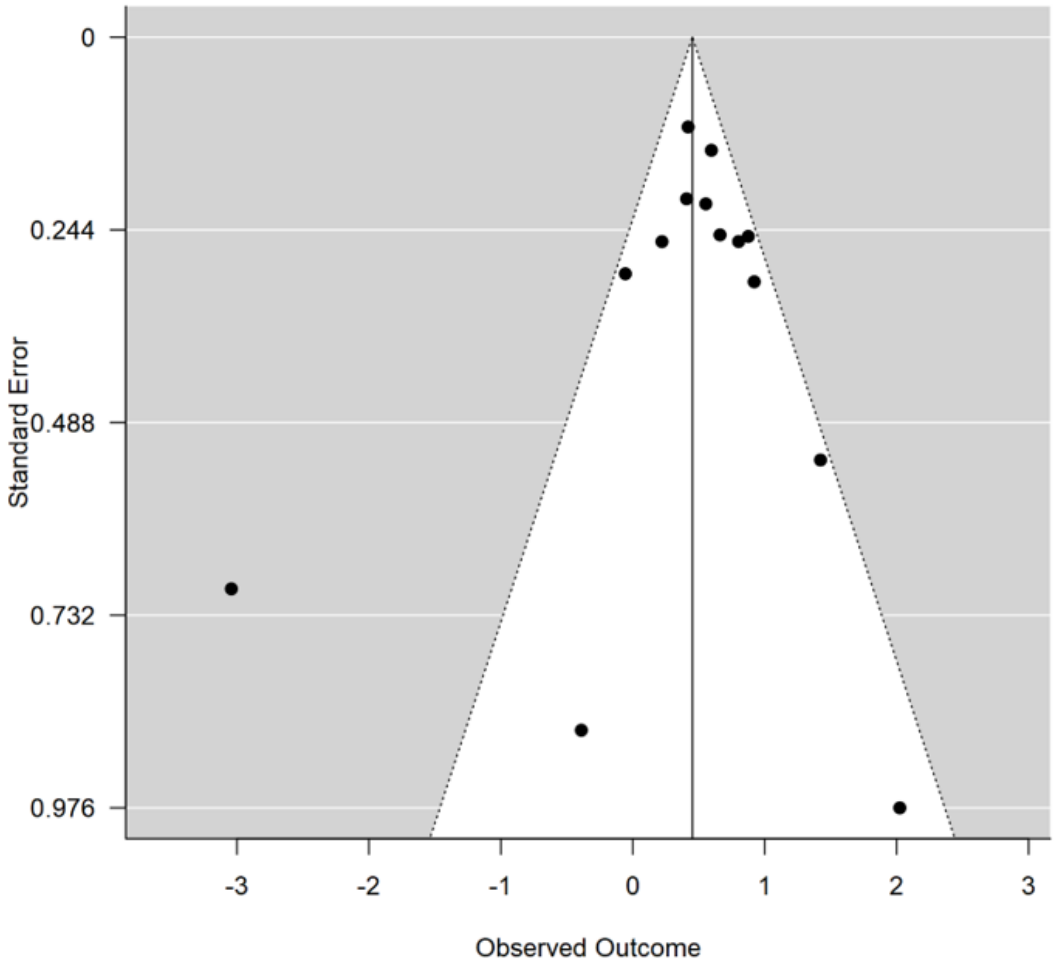

Fig. 4. An image of Funnel plot diagram of ventilation quality with respiratory tract in infants

Based on the picture above, it can be seen that there are points outside the triangle, which means that there is an indication of publication bias on the ventilation variable with the incidence of ARI.

The p-value value is less than 0.05, which means that there is an indication of publication bias on the natal variable with the incidence of ARI in toddlers.

The risk of ARI occurrence in infants with inadequate ventilation is 1.568 times greater than that of infants with adequate ventilation with a 95% CI value and a confidence interval of not more than 1, so the quality of ventilation has a significant relationship. Home ventilation is one of the factors that can affect the development of bacteria and viruses in the house, so it can potentially increase the incidence of ARI in toddlers. This is to the results of the meta-analysis that has been carried out that poor ventilation quality in the house can cause a 1,568 times greater risk of ARI in children under five.

Based on the results of research on Sapuli Island, South Sulawesi, that poor household ventilation is associated with ARI in toddlers, where the results of the study show a P-Value of 0.002 (<0.05) [19]. In line with the research above, the research conducted in Sibolga showed that there was a significant relationship between the quality of home ventilation and the incidence of ARI in toddlers where the P-Value value was 0.019 or less than 0.05, with a PR value of 1.208 which means that toddlers living in houses with ventilation that do not meet the requirements have a 1,208 times greater risk of getting ARI [20]. Another study conducted in Jakarta showed the same results, namely that home ventilation is related to the incidence of ARI in infants; it can be seen that the p-value is 0.000 (<0.05) with a PR value of 5.193, meaning that ventilation is a risk factor for respiratory tract infections in infants [21]. Another study showed that ventilation that did not meet the requirements had a significant relationship with respiratory tract infections in infants with a p-value of 0.000 (<0.05) [22].

In Africa, fossil fuels are still widely used for cooking, heating, and lighting equipment, but this is not accompanied by proper ventilation. Poor ventilation can increase the risk of ARI occurrence. In Ethiopia, a study conducted showed that those who live in houses that do not have windows significantly affect the incidence of ARI (Maor 4.03, 95% CI 1.74-9.35) [23, 24]. Another study conducted in Indonesia showed that ventilation had a significant relationship (p-value<0.05) with the incidence of respiratory infections, namely pneumonia in infants with P-Value = 0.000 [25]. So it can be concluded that home ventilation is a risk factor for the incidence of ARI in infants and toddlers who live in homes whose ventilation does not meet the requirements have a risk of getting ARI and a risk of admission to the hospital.

c. Meta-analysis of the relationship between house humidity and with respiratory tract infections in infants

The results of the forest plot in Fig. 2c shows that the value of pooled PR=$e^{0.51}$ =1.665 (95% CI-0.33–1.35). In the humidity variable with ARI, the publication is not biased because, in this variable, the meta-analysis data is not more than 10.

The humidity of the house that does not meet the requirements has a 1.665 times greater risk of ARI in children under five compared to the humidity of the house that meets the

requirements. The results of the forest plot test above shows that the 95% CI value is more than 1, meaning that the humidity variable is a protective factor in this study. This means that the house's humidity can reduce the risk of ARI in toddlers.

Humidity in the house can affect the humidity of the floor of the house. Research conducted in Bilang Muko explained that moist floors are related to the incidence of ARI in toddlers [26]. Research on house humidity with the incidence of ARI in Toddlers has a significant relationship with respiratory tract infections in infants with a p-value value of 0.039 or less than (0.05) with a PR value=1.3 which means that house humidity that does not meet the requirements has a risk 1.3 times more likely to cause ARI in Toddlers [26]. The results of the study showed that the average heat index could also affect the severity of respiratory diseases, and high heat temperatures in the house can affect the humidity in the house [27]. Humidity in the home environment has a 5-fold risk of causing ARI in toddlers (OR=5.00; CI 95% 0,79-31,51) [17]. Unqualified home humidity can cause the risk of ARI in Toddlers. Research conducted in Lampung Tengah, Indonesia, shows that flatness has a significant relationship (p-value<0.05) with the incidence of ARI in toddlers (p-value 0.001) [28].

d. Meta-Analysis of the relationship between house floor conditions and the incidence of ARI in Toddlers

In the heterogeneity test, it can be seen that the p-value value is less than 0.05 or no more than, which means that the variable data on floor quality with the incidence of ARI is heterogeneous, so it must use a random effect model analysis.

In the Forest plot test in Fig. 2d, the value of Pooled PR= $e^{0.27}$ =1.309 (95% CI -0.13–0.68), which means that the quality of the floor of the house does not meet the requirements has a risk of 1.309 times greater influence with respiratory tract infections in infants compared with the quality of the floor that meets the requirements. In this case, the 95% CI value is not more than one, so the quality of the floor of the house with the incidence of ARI has a significant relationship. There is no publication bias on this variable because the data that did the meta-analysis were not more than 10.

This study shows that floors that do not meet the requirements have a risk of developing ARI in toddlers. This is in line with research conducted in Jakarta that the condition of the floor of the house has a significant relationship with respiratory tract infections in infants, where the p-value value is 0.019 or less than 0.05 with a PR value of 1.665 which means that the floor condition has a risk of 1.665 more. Causes the incidence of ARI in Toddlers [21].

This study is also in line with research conducted in Sibolga that the condition of the floor of the house is associated with respiratory tract infections in infants with a p-value of 0.013 or less than 0.05 with a PR value of 1.33 which means that it has a relationship of 1.33 times greater than good floor conditions [20]. Research conducted in Bilang Muko also shows that the quality of the floor of the house has a relationship with respiratory tract infections in infants with a p-value value of 0.014 or less than 0.05 with a PR value of 1.9 meaning that poor floor conditions cause 1,9 times greater incidence of ARI in children under five. Poor house floors cause dusty and damp floors,

increasing the risk of ARI [26].

Toilet facilities, cooking gas, and taking intestinal parasite drugs are slightly related to ARI. Meanwhile, ARI has a significant relationship with (p-value<0.20) age, gender, stunting, economic conditions, living environment conditions, maternal age in childbirth, level of education, and Body Mass Index (BMI) of the mother [29]. The study showed that home environmental factors have a significant relationship with the incidence of ARI, so it can be concluded that home environmental factors such as house floors, ventilation, and others have a relationship in causing ARI.

So that the variable of home environmental conditions with the highest risk of causing the incidence of ARI in toddlers is air humidity, the results of the meta-analysis of house humidity with the incidence of ARI in toddlers have a 1.665 greater risk of causing the incidence of ARI. House humidity has a Pooled PR value greater than several other variables, namely occupancy density, ventilation, and house floors. However, in a meta-analysis, house humidity is also a protective factor in the incidence of ARI. This is because the 95% CI value exceeds 1, which means it is a protective factor.

Conclusion

Based on the results of the meta-analysis, the highest risk factor for environmental conditions with respiratory tract infections in infants is the house humidity variable with a value of PR = $e^{0.51}$ =1.665 (95% CI-0.33-1.35). In contrast, the lowest variable is environmental conditions. House with respiratory tract infections in infants is the variable density of occupancy with a value of PR = $e^{0.31}$ =1.138 (95% CI-0.20–0.82).

Efforts that can be made to minimize the incidence of ARI are to control the risk of ARI, namely by not smoking in the house, keeping the house from being humid, and making good home ventilation so that it can minimize the occurrence of ARI in toddlers, for policyholders to conduct a healthy home survey and help the underprivileged in maintaining a healthy home environment, as well as providing education about the dangers of smoking in the house by family members.

Financial supports

No external funding was received or used for this research study.

Competing interests

The authors declare that they have no competing interests.

Acknowledgements

We want to thank the Department of Environmental Health and the Master Program in Environmental Health, Faculty of Public Health, Airlangga University, which facilitated writing scientific articles for international journals. And we would like to thank the lecturers of the Master's Program in Environmental Health Universitas Airlangga who guided and corrected this scientific article we have compiled.

Ethical considerations

"Ethical issues (Including plagiarism, Informed Consent, misconduct, data fabrication and/or falsification, double publication and/or submission, redundancy,

etc.) have been completely ob-served by the authors."

References

1. Masriadi H. Epidemiologi penyakit menular. Depok: Rajawali Pers. 2017:31-54.
2. World Health Organization. Severe acute respiratory infections treatment centre: practical manual to set up and manage a SARI treatment centre and a SARI screening facility in health care facilities. World Health Organization; 2020.
3. WHO. Pneumonia [Internet]. 2019. Available from: https://www.who.int/news-room/fact-sheets/detail/pneumonia
4. Kementrian Kesehatan Republik Indonesia. Laporan Riskesdas 2018 Nasional. pdf [Internet]. 2019. p. 674. Available from: http://repository.bkpk.kemkes.go.id/3514/1/Laporan Riskesdas 2018 Nasional.pdf
5. Ministry of Health R of I. Indonesia Health Profile 2019. Short Textbook of Preventive and Social Medicine. 2020.
6. Sofia S. Faktor Risiko Lingkungan dengan Kejadian ISPA pada Balita Di Wilayah Kerja Puskesmas Ingin Jaya Kabupaten Aceh Besar. AcTion: Aceh Nutrition Journal. 2017;2(1):43-50.
7. Maharani D, Yani FF, Lestari Y. Profil Balita Penderita Infeksi Saluran Nafas Akut Atas di Poliklinik Anak RSUP DR. M. Djamil Padang Tahun 2012-2013. Jurnal Kesehatan Andalas. 2017 Jul 20;6(1):152-7.
8. Kemenkes RI. Profil Kesehatan Indonesia 2020. Kementrian Kesehatan Republik Indonesia. https://pusdatin. kemkes. go. id/resources/download/pusdatin/profil-kesehatan-indonesia/Profil-Kesehatan-Indonesia-Tahun-2020. pdf. 2021 Apr.
9. World Health Organization. A Practical Manual To Organize And Manage ARI Treatment Centers And ARI Screening Facilities In Health Care Facilities. World Health Organization. 2020. 100 p
10. Syahidi MH, Gayatri D, Bantas K. Faktor-faktor yang Mempengaruhi Kejadian Infeksi Saluran Pernapasan Akut (ISPA) pada Anak Berumur 12-59 Bulan di Puskesmas Kelurahan Tebet Barat, Kecamatan Tebet, Jakarta Selatan, Tahun 2013. Jurnal Epidemiologi Kesehatan Indonesia. 2016 Dec 13;1(1).
11. Gainau E, Rantetampang AL, Pongtiku A, Mallongi A. Factors Influence of Acute Respiratory Infection Incidence to Child Under Five Years in Timika Jaya Health Primary Mimika District. Population. 2018 Nov;2018.
12. Titi Saparina L, Noviati SH. Hubungan Kondisi Lingkungan Dengan Kejadian Penyakit Ispa Pada Balita Di Kelurahan Wasolangka Wilayah Kerja Puskesmas Parigi Kabupaten Muna. Miracle Journal Of Public Health. 2020 Dec 30;3(2):133-41.
13. Agungnisa A. Physical Sanitation of the House that Influence the Incidence of ARI in Children under Five in Kalianget Timur Village. Jurnal Kesehatan Lingkungan. 2019 Feb 1;11(1):1-9.
14. Wahyuningsih S, Raodhah S, Basri S. Acute Respiratory Infection (ARI) in Toddlers in the Coastal Area of Kore Village, Sanggar District, Bima Regency. Hig J Kesehat Lingkung. 2017;3(2):97–105.
15. Islam M, Sultana ZZ, Iqbal A, Ali M, Hossain A. Effect of in-house crowding on childhood hospital admissions for acute respiratory infection: A matched case–control study in Bangladesh. Int J Infect Dis. 2021;105:639–45.
16. Fera D, Sriwahyuni S. The relationship

between home environmental conditions and the occurrence of acute respiratory infection (ARI) in toddlers in Nagan Raya Regency. J-Kesmas: Jurnal Fakultas Kesehatan Masyarakat (The Indonesian Journal of Public Health). 2020 Apr 21;7(1):38-43.

17. Hidayanti R, Yetti H, Putra AE. Risk factors for acute respiratory infection in children under five in Padang, Indonesia. Journal of Maternal and Child Health. 2019 Mar 1;4(2):62-9.

18. Krisnasari S, Aulia T, Syahadat DS, Marsellina M, Wandira BA. The Relationship of Environmental Factors and Nutritional Status and The Incidence of ARI of Toddler in the Working Area of Donggala Public Health Center. Journal of Health and Nutrition Research. 2022 May 31;1(1):43-8.

19. Mulyadi HS. Risk Factors at Home on Acute Respiratory Infection (ARI) Incidence in Children Under Five in Sapuli Island, South Sulawesi. EXECUTIVE EDITOR. 2018 Jun;9(6):210.

20. Pasaribu RK, Santosa H, Kumala S, Nurmaini N, Hasan D. Faktor-Faktor yang Berhubungan dengan Kejadian Infeksi Saluran Pernafasan Akut (ISPA) pada Balita Di Daerah Pesisir Kota Sibolga Tahun 2020. Syntax Idea. 2021 Jun 20;3(6):1442-54.

21. Aprillia Romauli EF, Handayani P, Nitami M, Handayani R. Hubungan Antara Kualitas Lingkungan Fisik Rumah Dengan Kejadian Ispa Pada Balita Di Wilayah Kerja Puskesmas Rawajati 2 Pancoran Jakarta Selatan. Forum Ilm [Internet]. 2021;18(2):138. Available from: https://ejurnal.esaunggul.ac.id/index.php/Formil/article/download/4297/3069

22. Senggunawu TP, Roga AU, Aspatria U. The relationship between physical sanitation of the house and the incidence of ARI in children under five in the working area of the Naioni Public Health Center in 2021. The relationship between physical sanitation of the house and the incidence of ARI in children under five in the working area of the Naioni Public Health Center in 2021. 2022 Apr 25;99(1):12-.

23. Gordon SB, Bruce NG, Grigg J, Hibberd PL, Kurmi OP, Lam KB, Mortimer K, Asante KP, Balakrishnan K, Balmes J, Bar-Zeev N. Respiratory risks from household air pollution in low and middle income countries. The Lancet Respiratory Medicine. 2014 Oct 1;2(10):823-60.

24. Hassen S, Getachew M, Eneyew B, Keleb A, Ademas A, Berihun G, et al. Determinants of acute respiratory infection (ARI) among under-five children in rural areas of Legambo District, South Wollo Zone, Ethiopia: A matched case–control study. Int J Infect Dis [Internet]. 2020;96:688–95. Available from: https://doi.org/10.1016/j.ijid.2020.05.012

25. Yuliniar U, Wijayanti Y, Indriyanti DR. An Analysis Factors Affecting the Cases of Pneumonia in Toddlers at Public Health Center (Puskesmas) Pati I. Public Health Perspective Journal. 2021 Sep 13;6(3).

26. Safrizal S. Hubungan ventilasi, lantai, dinding, dan atap dengan kejadian ISPA pada balita di Blang Muko. InProsiding Seminar Nasional IKAKESMADA "Peran Tenaga Kesehatan dalam Pelaksanaan SDGs 2017 (Vol. 1, No. 1, pp. 41-48).

27. Fishe J, Zheng Y, Lyu T, Bian J, Hu H. Environmental effects on acute exacerbations of respiratory diseases: A real-world big data study. Science of The Total Environment. 2022 Feb 1;806:150352.

28. Putri RA. Hubungan Kondisi Rumah Dengan Kejadian Ispa Di Desa Kotagajah Kecamatan Kotagajah Kabupaten Lampung Tengah. Ruwa Jurai: Jurnal Kesehatan

Lingkungan. 2021 Jul 13;13(2):75-80.
29. Imran MI, Inshafi MU, Sheikh R, Chowdhury MA, Uddin MJ. Risk factors for acute respiratory infection in children younger than five years in Bangladesh. Public health. 2019 Aug 1;173:112-9.